PN-ABF-779

Research Report Series 01

# Upland Rice Simulation and Its Use in Multicriteria Optimization

Evangelyn C. Alocilja
Joe T. Ritchie

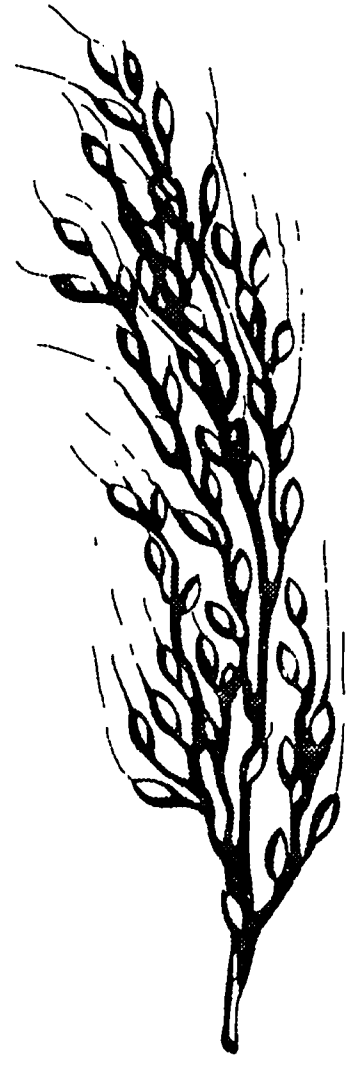

April 1988

Published for distribution by the IBSNAT Project:
University of Hawaii
and
Michigan State University

International Benchmark Sites Network for Agrotechnology Transfer

Published for distribution by the IBSNAT Project:

University of Hawaii
College of Tropical Agriculture & Human Resources
Department of Agronomy and Soil Science
Honolulu, Hawaii 96822

and

Michigan State University
Homer Nowlin Chair,
Department of Crop and Soil Sciences, and
Department of Electrical Engineering and Systems Science
East Lansing, Michigan 48824

IBSNAT, the International Benchmark Sites Network for Agrotechnology Transfer, is a a group consisting of the contractor (the University of Hawaii) and several collaborators. Together they have created a prototype network of national, regional, and international agricultural research centers for the purpose of developing, validating, and using a scientific method for the effective transfer of agrotechnology among and within countries in the tropics and subtropics.

Support for this work was provided by the IBSNAT Project, a program of the U.S. Agency for International Development implemented by the University of Hawaii, under Contract No. AID/DAN-4054-A-00-7081-00. All reported opinions, conclusions, and recommendations are those of the authors and not those of the funding agency or the United States government.

This publication was part of a Ph.D. dissertation by Evangelyn C. Alocilja in the Department of Electrical Engineering and Systems Science, Michigan State University, East Lansing, Michigan.

IBSNAT Research Report Series 01—02/88 (250)

# Upland Rice Simulation and Its Use in Multicriteria Optimization

Evangelyn C. Alocilja
*Department of Electrical Engineering and Systems Science, MSU*

Joe T. Ritchie
*Department of Crop and Soil Science, MSU*

**IBSNAT Research Report Series 01**
April 1988

## ACKNOWLEDGMENT

We wish to express our sincere gratitude to several people and organizations which made this research and publication possible. First, to Dr. Herman E. Koenig who provided technical guidance and enthusiastic support to the research. The encouragement and helpful suggestions by Dr. Robert O. Barr, Dr. Thomas J. Manetsch, and Dr. R. Lal Tummala to improve the scope of the study from a systems science perspective have been very valuable. Farm economic applications have been broadened by the kind suggestions of Dr. J.B. Dent of the Edinburgh School of Agriculture.

The writing tips offered by Sharlene Rhines made the writing of the manuscript easier. The editorial management by Sharon Balas and the cover artwork by Victoria Pecsok are highly appreciated.

The weather and experimental data from the International Rice Research Institute (IRRI), Philippines, have been tremendously helpful in the validation of the CERES-Rice simulation model and the Simulation-Multicriteria Optimization Technique (SMOT).

Finally, we wish to thank the International Benchmark Sites Network for Agrotechnology Transfer (IBSNAT) for the financial support in the conduct and publication of this research.

## PREFACE

Agriculture is a risky business with much of the risk associated with uncertainties in weather. Farmers who subsist in these environments learn from years of costly trial and error to minimize risk by sacrificing high yields for stable and sustainable food supplies. But low yields do not always need to be a product of stable farming systems.

One of the great challenges of agricultural research is to discover ways to increase production without compromising stability and sustainability. The challenge is to supplement trial-and-error development with faster, cheaper, and more reliable ways to integrate new crops, products, or practices into existing farming systems to make them more productive in a non-disruptive manner.

In response to this challenge, the United States Agency for International Development established the International Benchmark Sites Network for Agrotechnology Transfer (IBSNAT) Project in 1982 to add systems analyses and crop simulations to its arsenal of weapons to combat the war against hunger. Based at the University of Hawaii, IBSNAT has mobilized an international group of systems scientists to bring to bear on the problem of risk and uncertainty in agriculture, the powerful new tools of information science and computer technology. This report is an example of how these tools can be used to increase farm income under situations of risk and uncertainty.

**ABSTRACT**

Low-yielding rice-growing countries can benefit from the agrotechnology developed and made available through experimental stations and from high-yielding countries. However, the conventional method of agrotechnology transfer may be costly and time-consuming, and the farmers' perception of risk within the context of the economic environment in which they function is sometimes a major barrier to adapting high-yielding technologies.

The CERES-Rice simulation model reported here is a computer software package designed to aid in the initial selection of new varieties and management practices in various soil types and climatic environments of the tropics and subtropics. Varieties and management practices which look promising in the context of the simulation are the principal technologies to be tried in the field. This procedure is expected to reduce dramatically the cost and time required in agrotechnology transfer.

The extent to which farmers are willing to adapt high-yielding technologies depend upon the economic environment of the farm and their perception of risk in this environment. The costs of fertilizer, chemicals, and other inputs required to support high-yielding technologies are not only a financial barrier to the farmers, they greatly amplify the real and perceived levels of risk. A crop failure not only results in a loss of current food supply, it incumbers any future profits of the farmer to pay for lost input resources. A method for assessing profit/risk trade-offs and designing the production system in conformity with these trade-offs is required. This need is translated quantitatively into the simulation-multicriteria optimization technique (SMOT). SMOT is a computer software package that uses the Monte Carlo procedure to explore the space of feasible production technologies and generate those that are noninferior in the Pareto optimal sense. From the set of Pareto optimal solutions, the min-max optimization is used to identify the technologies that provide the best compromise between profit and a limited class of weather-related risk, when both profit and risk are equally weighted.

As a decision support system, SMOT represents a significant step toward the development of a tool for quantifying some of the profit/risk issues that are of practical use to rice production advisers, researchers, and policymakers in the economic analysis of rice farms.

## TABLE OF CONTENTS

CHAPTER I INTRODUCTION AND NEEDS ANALYSIS 1

CHAPTER II OBJECTIVES AND SCOPE OF RESEARCH 3

Objectives 3
Scope 3

CHAPTER III SYSTEM IDENTIFICATION 5

The Exogenous Input Variables 6
The Controllable Input Variables 6
The Output Variables 6
The System Parameters 7
Performance Criteria 8
The Multicriteria Optimization 8
Pareto Optimization 9
Min-max Optimization 10

CHAPTER IV THE AGRONOMY OF UPLAND-RICE PRODUCTION 11

The Effect of Temperature on Rice Growth 12
Rice Phenology 12
Germination 12
Seedling Emergence 13
Juvenile Stage 14
Panicle Initiation 14
Heading 15
Grain Filling 15
The Influence of Solar Radiation on Plant Growth 16
Photosynthesis 16
Carbohydrate Partitioning 17
Grain Yield 18
Soil-Water Conditions and Water Losses 18
The Importance of Nitrogen Fertilization 20

CHAPTER V THE ANALYTICAL STRUCTURE OF THE CERES-RICE SIMULATION MODEL 23

Sowing Stage (ISTAGE 7) 27
Germination Stage (ISTAGE 8) 27
Emergence Stage (ISTAGE 9) 28
Juvenile Stage (ISTAGE 1) 30
Panicle Initiation Stage (ISTAGE 2) 34

Heading Stage (ISTAGE 3) 35
Beginning of Grain Filling Stage (ISTAGE 4) 37
End of Grain Filling Stage (ISTAGE 5) 39
Physiological Maturity Stage (ISTAGE 6) 41

CHAPTER VI THE ANALYTICAL STRUCTURE OF THE MULTICRITERIA OPTIMIZATION PROCEDURE 42

The Monte Carlo Search Method 43
Pareto Optimization 43
Min-max Optimization 45
Function Minimization 46
The Analytical Representation of the Objective Functions 47
The Economic Scenario of the Rice Farm 48

CHAPTER VII THE ALGORITHM OF THE SIMULATION-MULTICRITERIA OPTIMIZATION TECHNIQUE 50

CHAPTER VIII DISCUSSION OF RESULTS 54

The CERES-Rice Simulation Model 54
The Simulation-Multicriteria Optimization Technique (SMOT) 70

CHAPTER IX CONCLUSION 86

CHAPTER X OTHER POSSIBLE APPLICATIONS OF SMOT 88

Objective Function Pairs 88
Production Constraints 91

LITERATURE CITED 93

# CHAPTER I. INTRODUCTION AND NEEDS ANALYSIS

While there is food surplus in some regions of the world, serious food deficiency, leading to malnutrition and starvation, is a grim reality in many others. Unfortunately, these food-deficient regions are not economically able to gain access to the food surplus. To eliminate the destructive effect of food deficiency, the concerned countries must find ways and means to increase food production to keep pace with population growth.

Food supply is a direct function of many factors, among which are weather and soil environments, market system, government policies and programs, agrotechnology, and the farmer's objective of profit and production stability. As much as 95 percent of the world's food supply is provided by the plant system (Michigan State University Agricultural Experiment Station 1981). Specifically, for more than a third of the world's population, rice is a primary staple in the diet and critical to survival (Barker, Herdt, and Rose 1985). De Datta (1981) reported that in 1976-1978, rice was harvested from about 143.5 million ha, from Asia (accounting for 90 percent of the total), Africa, South and Central America, Australia, and part of the United States. Rice, grown as a flooded wetland or dryland crop, has received considerable attention -- political, economic, and through research -- from all over the world. But in many of the Asian, African, and Latin American rice-growing countries today, rice production does not meet the food needs of their populations, making the daily food supply unreliable and consequently driving the cost of subsistence proportionately higher relative to income. Particularly for upland-rice agriculture, the regional average grain yield is very low: from 0.5 to 1.5 t $ha^{-1}$ in Asia, about 0.5 t $ha^{-1}$ in Africa, and from 1 to 4 t $ha^{-1}$ in Latin America (De Datta 1975). However, under experimental conditions, yields are reported to be from 5.4 to 7.2 t $ha^{-1}$.

In order to increase rice production, the low-yielding countries will have to do one or both of two things: increase the area devoted to production and/or increase the frequency and intensity of cultivation. At the present rate of population growth, agricultural land is being continuously reduced in favor of urbanization, so increasing production by increasing land area is at best only a partial and short-term solution. Hence, increased rice productivity must come from increases in output per unit area, per unit input, and per unit time through

high-yielding, science-based technologies tailored to the unique combination of soil, climatic, biological, economic, and cultural conditions of the local area (Wortman and Cummings 1978; Swaminathan 1975; Ruttan 1982). However, the generation of technology is a complex process. Plant agriculture is a complex system. It is characterized by unique properties and nonlinear functions (Baker and Curry 1976). It is a system which requires natural resources as part of the inputs, imposing their stochastic behavior on the transformation process from input to output (Amir, Shamir, and Broughton 1978). The development of science-based technologies is evolutionary in nature and requires a long-term investment (Sahal 1980). Agricultural research techniques are costly, time-consuming, site-specific and, by their nature, trial-and-error undertakings. In many of the food-deficient countries, an increasing uncertainty exists as to whether the current agricultural research methods are adequate to meet the food requirements of the growing population and to provide for the management skills necessary to sustain food production.

Thus, the complex circumstances surrounding the rice-production system, particularly in narrowing the yield gap of upland-rice agriculture, require the development of a methodology that will hasten the evaluation of appropriate transferable agrotechnologies. Varietal and field management practices should be taken from the high-yielding to the low-yielding rice-growing countries, or from sites of origin to other locations, at low cost, minimum failure rate, and shortest waiting time. Such a methodology can be embodied in a computer software program that simulates a rice-production system for a chosen variety or management practices and considers the stochastic factors of the production environment.

Increased yield per hectare, however, is not in itself a sufficient goal. Rather than simply striving for maximum yield, agricultural production is increasingly dependent on the degree to which cost-effective technology is employed (Avery 1985) and the farmer's vulnerability to the uncertainties of environmental factors is reduced. A procedure is needed for designing and managing the production system so returns are maximized and production risks minimized under highly uncertain enviromental conditions. This need translates into an analytical, multicriteria, resource-allocation optimization procedure through which trade-offs between two conflicting objectives -- maximum profit and minimum risk -- can be evaluated. To the authors' knowledge, this is the first time that a multicriteria optimization technique of the type presented here has been applied to agriculture production in general and to upland-rice production in particular.

# CHAPTER II. OBJECTIVES AND SCOPE OF RESEARCH

## Objectives

The general objective of this research is to develop a computer software package as a decision support system for use by farmers, agricultural extension workers, researchers, and government policymakers in the design and management of the rice-production system.

The specific objectives of the research are: (1) to develop a practical, interactive, and flexible computer software for simulating an upland rice-production system as a tool in the effective transfer of agrotechnologies among and within countries in the tropics and subtropics from their sites of origin to new locations and (2) based on this simulation, to develop a simulation-multicriteria optimization technique (SMOT) software as an analytical tool in evaluating profit and a limited class of weather-related production risk, subject to constraints in resources, environment, and relevant food production policies.

## Scope

The rice simulation software is developed for upland conditions in the tropical and subtropical environments. The software is designed primarily to predict:

1. the phenological development or duration of growth stages as influenced by plant genetics, weather, and soil factors;
2. biomass production and partitioning; and
3. the effect of soil-water deficit and nitrogen deficiency on the photosynthesis and photosynthate partitioning in the plant system.

The simulation software provides the foundation for SMOT. SMOT is designed as a decision support system for upland-rice production where profit and production risk are quantitatively evaluated subject to the simultaneous constraints in resources, environment, and production policies. Through the use of SMOT, alternative production strategies can be identified based on the level of profit and risk as well as on the capability of the farmer to finance the operation.

As with all software packages, SMOT has its limitations. Diseases and insect pests, for example, which are highly variable with respect to location, are important considerations in rice production. Conceptually, the simulation model has been bifurcated into (1) a plant system without the destructive effect of pests and (2) one with the influence of pests. The first system, devoid of the effect of pests, is considered here. The incorporation of pest models will come in the future. In the work reported here, it is assumed that pests are controlled to the extent that they have no economic effect and that the cost of this control can be represented as a fixed cost in the optimization technique.

As structured, the simulation software assumes that:

1. The production field has no bund.
2. Method of planting is by direct-seeding.
3. Fertilizer application is basal.
4. Except for nitrogen, all nutrients required for plant growth are nonlimiting.
5. There are no highly problematic soil conditions, such as high salinity and acidity, heavy compaction, or trace element deficiencies.
6. The effects of typhoons are negligible.

As structured, SMOT assumes further that the market situation, including the price of grain and input costs, are constant over the period of the optimization. The optimization procedure, however, can be repeated as often as desired for alternative prices and costs.

For the present application, capital is assumed as a constraint, while labor is abundant. This assumption is based on the fact that the majority of rice production is an activity among highly populated, low-income developing countries. Consequently, it is assumed that harvesting is done manually and the cost of the harvest is on a per weight basis. Harvesting mechanization, however, can be implemented by SMOT.

The present applications of SMOT also assume that the unavoidable by-products of rice production, such as nitrate leaching, runoff, and pesticide pollution, have negligible impact on the environment. However, where necessary, these by-products can be analytically incorporated as constraints on the inputs to the simulation and/or optimization processes of SMOT.

## CHAPTER III. SYSTEM INDENTIFICATION

The rice-production system is governed by the input-process-output relationship, as a function of time, t. The input vectors fall into two classes: (1) the exogenous input variables, which are uncontrollable and may be stochastic in nature, and (2) the controllable input variables, which are deterministic in nature. The vector of exogenous input variables is represented analytically as $\bar{e}(t)$ and the vector of controllable input variables as $\bar{u}(t)$. The vector of state variables is denoted by $\bar{x}(t)$. The vector $\bar{x}(t)$ describes the internal as well as the external behavior of the plant system. The system parameters are the coefficients in the analytical equations which define the analytical structure of the system.

The output vectors also fall into two classes: (1) the desired output variables, represented as $\bar{y}(t)$, and (2) the undesired, unavoidable by-products which are generated when the system produces the desired outputs. The performance criteria are defined in order to evaluate whether the desired outputs are acceptable.

The rate of change of the state variables at time t ($\dot{\bar{x}}(t)$), as well as the output variables at time t ($\bar{y}(t)$), depend on the inputs $\bar{u}(t)$ and $\bar{e}(t)$, the state of the system, $\bar{x}(t)$, and time, t. This relationship is expressed by the vector functions $\bar{g}$ and $\bar{h}$ in a state-space representation as follows:

$$\dot{\bar{x}}(t) = \bar{g}[\bar{x}(t), \bar{u}(t), \bar{e}(t), t]$$

$$\bar{y}(t) = \bar{h}[\bar{x}(t), \bar{u}(t), \bar{e}(t), t]$$

The rice-production system forms a class of system characterized technically as stochastic, continuous-time, with memory, nonlinear, time-varying, and dynamic. The system is stochastic because the weather variables can only be described probabilistically, that is, they cannot be described exactly for all time. It is also continuous-time because the environmental-biological interactions in the plant system occur continuously during the growth process. The system has memory because the output of the system at a given time $t_1$ depends not only on the input applied at $t_1$ but also on the input applied before $t_1$ (Swisher 1976). The nonlinearity of the system is related to the fact that the relaxed system, or zero initial condition of the system, can only be described sufficiently with nonlinear

relationships. In this case, the principle of superposition (Swisher 1976) will not hold true, that is,

$$L\{a_1u_1(t) + a_2u_2(t)\} \neq a_1L\{u_1(t)\} + a_2L\{u_2(t)\}$$

for any two inputs $u_1(t)$ and $u_2(t)$ as functions of time t, and any constant scalars $a_1$ and $a_2$.

The state of the plant system during its growth varies with time, hence the system is time-varying. The rice-production system is also a dynamic system because the two conditions describing a dynamic system are properties of the rice-production system. The two conditions are (Swisher 1976):

1. A real output $\bar{y}(t)$ exists for all $t > t_0$ given a real input $\bar{u}(t)$ for all t, where $t_0$ is initial time.
2. Outputs do not depend on inputs $\bar{u}(\tau)$ for $\tau > t$.

Because of the second condition, the rice-production system is also considered causal, that is, the output of the system at time t does not depend on the input at times after time t.

**The Exogenous Input Variables**

The major contribution of the exogenous input variables makes rice production seasonal, geographically dispersed, and uncertain. These exogenous variables are grouped into two categories, namely, physical and socioeconomic. The physical exogenous input variables are solar radiation, daylength variations, air temperature, and rainfall. The socioeconomic exogenous input variables are product prices, input costs, and marketing costs.

**The Controllable Input Variables**

The controllable input variables in the rice production system are classified into the following: manpower (such as the farmers and hired workers); budget allocation; material flow inputs (such as seeds, fertilizers, water, pesticides); capital facilities (such as irrigation system, storage or barns, farm animals, tractors, threshers, and land); and cultural management practices (such as sowing or planting date, plant density, sowing depth, amount and frequency of fertilizer application, amount of irrigation, and type of pest control).

**The Output Variables**

Rice production involves the transformation of inputs into desirable outputs, such as grain yield and straw. However, unavoidable, undesirable by-products result from the process, such as pesticide pollution, nitrate leaching, runoff, and,

sometimes, the buildup of insect populations. These by-products degrade the environment and, while there is no apparent cost to the farmers at the moment, future generations will pay for the damage if it is not dealt with now.

**The System Parameters**

The system parameters determine the functional relationship in the input-process-output and define the structure of the system. They are classified into two categories: (1) the system design parameters, which are manageable, and (2) the natural system parameters, which are unmanageable. The system design parameters depend upon the technologies used and how these technologies are organized into a production system. The design parameters for rice production are grouped into (a) genetic-dependent and (b) labor- or mechanization-dependent. The genetic-dependent parameters, which describe the variety, are: (1) the time required for the plant to develop from seedling stage to floral initiation, (2) the rate of photoinduction, (3) optimum photoperiod, (4) the time required to complete grain filling, (5) the plant's conversion efficiency from sunlight to carbohydrates, and (6) tillering characteristic.

The labor- or mechanization-dependent variables are: (1) method of land preparation, (2) method of fertilizer application, (3) method of pesticide control, (4) irrigation method, and (5) method of harvesting.

The natural system parameters are: (1) the latitude of the production area and (2) the properties and initial conditions of the soil profile, such as soil nutrition and toxicities, water saturation properties, landscape hydrology, textural profile of the soil, and the topographic position of the field.

The system parameters are affected directly or indirectly by socioeconomic and institutional factors, such as availability of farm inputs, access to credit and markets, inflation and interest rates, local and international market situation, consumers' demands, consumers' nutritional requirements, customs reflecting preferences of consumers for certain varieties and of farmers for farm practices, production policies by the government (price support, production input subsidies, government-supported storage facilities, etc.), form of government or political system (socialism, capitalism, communism, etc.), the needs of the rice industry, and the availability of agrotechnologies from research institutions.

The exogenous input variables, the system parameters, and the socioeconomic and institutional factors determine the type of agriculture in any particular environment.

## Performance Criteria

The criteria by which the performance of the rice-production system is evaluated are: (1) the farmer's profit and (2) weather-related production risk. These two criteria conflict in the sense that production strategies that generate higher profit are usually very risky operations. Thus, the evaluation procedure will exercise trade-offs to identify simultaneously the best acceptable values of the two objective functions. The evaluation process is embodied in SMOT.

## The Multicriteria Optimization

Optimization is an analytical procedure or a mathematical programming technique used to find the optimum solution that would maximize or minimize an objective function subject to defined equality or inequality constraints. The optimization techniques were developed in response to such questions as "Are we making the most effective use of our scarce resources?" or "Are we taking risks within acceptable limits?" (Bazaraa and Shetty 1979). The recent growth of fast computing facilities aided the use of these techniques. Problem optimization can either be linear or nonlinear programming. Within the class of nonlinear programming is another classification according to the number of objective functions: the single criterion and the multicriteria or vector optimization problem. The class of problem to be dealt with here is a nonlinear, multicriteria optimization problem because of the nonlinearity of the system, the nonlinearity of some of the constraint functions, and the nonlinearity of the objective functions. In a multicriteria optimization problem, the objective functions form a vector of criteria (Osyczka 1984). The formulation requires a definition of the objectives to be maximized or minimized, the decision variables that must be optimized, and the constraint functions surrounding the problem.

Multicriteria optimization has had its applications in engineering fields. It is an analytical procedure used to find the "optimum" solution which would give acceptable values or trade-offs for all the objective functions to be considered simultaneously. The goal of the multicriteria optimization is to help decision makers make the right decision in conflicting situations (Osyczka 1984). Recently, multicriteria or multiobjective decision making has gained popularity and applications in management science because of the realization that a decision has more than one dimension that affects successive actions or decisions. For example, Shapiro (1984) argued that the assumption that a firm is interested only in profit is an oversimplification. He presented research results indicating that management decides on the allocation of scarce resources with reference to several, sometimes conflicting,

goals, such as profit, market share, balanced business portfolio, long-range growth rate, and risk, in the strategic (long-term) sense, as well as employment level, management-labor relations, and product quality, in the tactical (short-term) sense. Also nonfinancial demands exist which need to be addressed, including such issues as equal employment opportunities, pollution control, product safety, and work safety.

SMOT uses the Pareto optimization and min-max optimization techniques. The Monte Carlo search method, which assigns random numbers to generate new and random points, is employed to search the space of feasible solution.

*Pareto Optimization*

The concept of Pareto optimization was originated in 1896 by Vilfredo Pareto who began a study of efficient solution theory as applied to welfare economics (French et al. 1983). French et al. indicated that Pareto's study provided the earliest recognition of the difficulty of reducing decision problems to forms involving a single objective. However, its application to engineering and management science did not gain momentum until the early 1970s, when the idea of multiobjective or multicriteria decision making became formalized. The original version of Pareto optimality theory was quoted by Cirillo (1979) as follows:

*There are, as we have noted, two problems to be resolved in obtaining the maximum well-being for a collectivity. Given certain rules of distribution, we can investigate what positions, following these rules, will give the greatest well-being to the members of the collectivity. Let us consider any particular position and let us suppose that a very small move is made compatible with the relations involved. If in doing so the well-being of all the individuals is increased, it is evident that the new position is more advantageous for each one of them, vice-versa, it is less so if the well-being of all the individuals is diminished. The well-being of some may remain the same without these conclusions being affected. But, if on the other hand, this small move increases the well-being of certain individuals and diminishes that of others, it can no longer be said that it is advantageous to the community as a whole to make such a move. We are, hence, led to define a position of maximum ophelimity as one where it is impossible to make a small change of any sort such that the ophelimities of all individuals with the exception of those that remain constant, are either all increased or all diminished.*

In short, Pareto optimality states that an optimum position is reached when it is not possible to increase the utility of

some consumers without diminishing that of others (Cirillo 1979).

*Min-max Optimization*

Min-max optimization procedure was developed by Osyczka (1984). It uses the information of the separately attainable minima of the objective functions. These minima can be obtained by solving the optimization problems for each criterion separately. Then the values of the objective functions are compared to these minima through their relative deviations. The min-max optimum is that solution which gives the smallest values of the relative increments of all the objective functions.

The detailed analytical structures of both the Pareto and min-max optimization procedures are presented in chapter VI.

## CHAPTER IV. THE AGRONOMY OF UPLAND-RICE PRODUCTION

The topical presentation of this chapter follows the subject division of the CERES (Crop Estimation through Resource and Environment Synthesis) crop models.

Upland-rice agriculture is rice production on flat and sloping fields with no bunds, where land preparation and seeding take place under dry conditions (De Datta 1975). Primarily a tropical or subtropical crop, rice (*Oryza sativa L.*) is grown from 53°N to 35°S latitude, and from sea level or below to elevations of about 2000 m (Yoshida 1981).

The growth cycle of a rice plant takes about 3 to 6 months depending on the climate of the production area and on the genetic characteristics of the variety with regards to photosensitivity and thermosensitivity (Tanaka, Kawano, and Yamaguchi 1966; Yoshida 1981). Because of the weather factors, especially temperature and daylength, and genetic interactions in the plant system, the growth duration is highly site and season specific.

During the growth cycle, the plant completes several stages, generally classified as the vegetative, reproductive, and ripening stages. The vegetative stage can be further subdivided into germination, emergence, juvenile, and floral or panicle initiation, and the reproductive and ripening stages can be subdivided into heading, grain filling, and physiological maturity. The duration of the vegetative stage varies among varieties and largely determines the growth duration of the plant (International Rice Research Institute (IRRI) 1964; Yoshida 1981). The duration of the vegetative stage is said to have a minimum and maximum limit (IRRI 1964). The minimum limit, which is relatively constant for a variety, is known as the basic vegetative phase, and the duration between the minimum and maximum limits is known as the photoperiod sensitive phase. The duration of the photoperiod sensitive phase varies with the daylength or photoperiod. The photoperiod, which is a function of the latitude of the production area, is the hourly interval between sunrise and sunset.

The vegetative stage is characterized by active tillering, increase in plant height, leaf emergence, and increase in the leaf area (Yoshida 1981). The reproductive and ripening stages are characterized by panicle and grain growth.

## The Effect of Temperature on Rice Growth

An optimum temperature for different physiological processes has been observed (Yoshida 1981). This optimum temperature varies with variety. The optimal temperature appears to shift from high to low as growth advances from the vegetative to the reproductive and ripening stages (IRRI 1972; Yoshida 1981). Within the critical high and low temperatures, high temperatures are required for active growth at early stages, while low temperatures favor spikelet production during the reproductive stage (Yoshida 1981). However, extremely high or low temperatures are not favorable to plant growth. Yoshida (1981) reported that a high percentage of spikelet sterility occurred when temperatures exceeded 35°C at anthesis and lasted for more than one hour. Injury to rice occurred when the daily mean temperature dropped below 20°C. Low temperatures, such as 12°C, induced 100 percent sterility when they lasted for six days. Other injuries due to cold temperatures were failure to germinate, delayed seedling emergence, stunting, leaf discoloration, panicle tip degeneration, incomplete panicle exsertion, delayed flowering, and irregular maturity.

Crop duration is directly related to temperature and modeled as thermal time or degree-days (Yoshida 1981). It is calculated as follows:

$$\text{Degree-days} = \Sigma\ (\text{daily mean temperature} - \text{threshold temperature})$$

Rice has been observed to have a threshold temperature of 8°C. Yoshida (1981) indicates that the concept of thermal time or degree-days assumes that the growth or development of a plant is linearly related to temperature or the total amount of heat to which it is exposed. However, he cautions that this concept should be handled carefully because there are some physiological and biochemical processes in the plant which are not linearly dependent on temperature. He demonstrated the presence of the "idling effect" of high temperatures, suggesting that a "ceiling temperature" existed.

## Rice Phenology

Phenology is concerned with the duration of the growth stages of the plant. As mentioned in the earlier section, the growth stages are germination, emergence, juvenile, panicle initiation, heading, grain filling, and physiological maturity.

### *Germination*

The concept of thermal time was applied to the germination study by Livingston and Haasis (1933) in order to determine the thermal time requirement for complete germination in rice seeds.

The result showed that it took about 45 degree-days to germinate healthy rice seeds between 15°C and 37°C. At the incubation temperature of 42°C, only about 8 percent germinated in 10 days and no germination was observed in a period of six days at 45°C.

At germination, the coleoptile emerges and the first leaf follows (Yoshida 1981). A study by Yoshida (1973) indicated that temperature affected the rate of leaf emergence. At 22°C one leaf emerged every 5.4 days, while a leaf emerged every 3.5 days at 31°C. The concept of thermal time was applied on the above study. The temperature ranges were converted to degree-days using a threshold temperature of 8°C. A graph of degree-days versus number of leaves per culm (or stem) showed that the relationship was linear and that the slope, number of leaves per degree-day, was 0.012. The inverse of the slope is 83.3 degree-days per leaf. The 83.3 is also known as the phyllocron interval. However, phytotron studies to determine the phyllocron interval for some rice varieties conducted at Duke University during the period 1983-1984 (unpublished results) showed an average value of 90 degree-days per leaf. Most varieties develop 10 to 22 leaves on the main culm (Yoshida 1973, 1981).

Roots develop immediately after germination. Root growth is observed to be regulated by both varietal characteristics and root environment. A study on rice growth under controlled environments by Yoshida (1973) showed that at the very early stage of plant growth, root to shoot ratio was about 0.21, decreasing exponentially as the plant weight increased, and stabilizing at about 0.10 as the plant weighed 1 g or more. Root weight was not markedly affected by temperature, at least between 22°C and 31°C. However, water stress was found to increase root growth relative to shoot growth (IRRI 1974).

*Seedling Emergence*

Seedling emergence is the time when the tip of a seedling emerges from the soil surface and so starts the growth process in the field (Yoshida 1981). Thus, the time required for emergence is a function of the sowing depth.

Up to this point, plant growth is supported by the nutrients in the endosperm, often known as the seed reserve (Yoshida 1973; IRRI 1973). The concept of thermal time was applied on the seedling growth experiment by Yoshida (1973) in order to evaluate growth rate at this stage of plant development. The result showed that growth was linearly related to thermal time up to 120 degree-days, with a slope of 0.00008265 g dry weight per plant per degree-day.

*Juvenile Stage*

Juvenile stage is characterized by root growth, leaf emergence, leaf growth, and tillering.

During the initial stages of seedling growth (first and second week after sowing), growth of the coleoptile and subsequent leaves is largely dependent on the seed reserve (Yoshida 1973, 1981). Photosynthesis takes over carbohydrate production after the second week of growth. Yoshida (1973, 1981) reported that between 22°C and 31°C, photosynthesis was responsible for about 30 percent of growth during the first week, 84 percent during the second week, and 100 percent thereafter. Yoshida also indicated that during the first week after sowing and until the middle growth stages, growth rate increased almost linearly with increasing temperatures.

Studies (IRRI 1968) have shown that tillering is initiated when the total nitrogen uptake becomes greater than 10 mg per plant or the dry weight is greater than 300 mg per plant, demonstrating that tillering initiation depends on the size of the main tiller. The tiller number was observed to increase when the nitrogen content of the leaf blade was higher than 2 percent, but tillering stopped when nitrogen content dropped below 2 percent. Tillering ability is known to be a varietal character, that is, high-tillering varieties tiller more actively than low-tillering ones. Tillering increase by a plant population follows a curvilinear shape, increasing monotonically until the maximum tiller number stage. Tiller number decreases after the heading stage. High temperatures encourage tillering (IRRI 1972).

Leaf area development of a rice variety is highly related to its tillering capacity at conventional plant spacing (Yoshida and Parao 1972). A high-tillering variety tends to have a vigorous vegetative growth.

*Panicle Initiation*

Since rice is a short-day crop, rice initiates panicle primordia in response to short photoperiods (Yoshida 1981). The duration of this stage varies with the degree of photosensitivity of the variety. Depending on the daylength condition of the production area, the duration could be at its shortest or longest. The daylength at which the duration from sowing to flowering is a minimum is called the optimum photoperiod (Yoshida 1981; IRRI 1966). The optimum photoperiod of most varieties is observed to be from 9 to 10 hours (Yoshida 1981; IRRI 1969). The critical photoperiod is the longest photoperiod at which the plant will flower; flowering will not occur beyond the critical photoperiod (Yoshida 1981; IRRI 1966).

The critical photoperiod of most varieties ranges from 12 to 14 hours (Yoshida 1981; IRRI 1969). Short photoperiods decrease the growth period of the plants. Photosensitivity is a varietal character, that is, the critical and optimum photoperiod differs among varieties. The growth of a variety that is less sensitive to photoperiod does not fluctuate as much as a highly sensitive variety under various daylength conditions (Tanaka, Kawano, and Yamaguchi 1966).

It is usually during the panicle initiation stage that the plant reaches the maximum tiller number (Yoshida 1981). There is a period before the maximum tiller stage when the tiller number becomes numerically equal to the panicle number at maturity.

*Heading*

Yoshida (1981) defines heading as the time when 50 percent of the panicles have exserted. From his experience, heading in the field is completed in 10 to 14 days.

As the rice plant grows, the leaf area index (LAI) increases. LAI is the sum of the leaf area of all the leaves divided by the ground area where the leaves have been collected. Studies by Yoshida (1981) show that LAI increases curvilinearly with time and reaches a maximum at around heading. After heading, LAI decreases as the lower leaves senesce. The same studies demonstrate that a rice crop can attain maximum LAI values of 10 or more at heading time, with a LAI value of 5 or 6 at maximum crop photosynthesis.

Tiller number also starts to decrease during the heading stage. The nonbearing tillers and weak-bearing tillers are killed as a result of shading and senescence (IRRI 1964). The number of tillers and the number of panicles become equal at harvest.

*Grain Filling*

Grain filling is characterized by increase in grain size and weight, resulting in the increase in panicle weight. It is also characterized by changes in grain color and senescence of leaves (Yoshida 1981). The process of grain growth is quantified by the increase in dry weight and the decrease in water content. Yoshida observed that the rate of grain growth was faster and the grain-filling period was shorter at higher temperatures. Grain growth was initially slow, then entered a linear phase where the growth rate was fast, and then slowed down toward maturity.

During the grain-filling period, some of the assimilates

from the other plant organs are translocated to the grains. Studies have shown that about 5 percent of the assimilates absorbed by the plant during the panicle development, and from 30 to 50 percent of the assimilates absorbed after flowering, are translocated to the grains (IRRI 1964). The duration of grain filling, that is, the time required to reach maximum weight, varies with the variety.

**The Influence of Solar Radiation on Plant Growth**

Aside from temperature, solar radiation influences rice yield by directly affecting the physiological processes involved in grain production. Photosynthesis in green leaves uses solar energy in wavelengths from 0.4 to 0.7 $\mu$m, often referred to as the photosynthetically active radiation (PAR) (Yoshida 1981). The ratio of PAR to total solar radiation is close to 0.50 in both the tropics and the temperate regions. This ratio represents a weighted mean between the fractions for direct radiation and diffuse sky radiation. The solar radiation requirement of a rice crop differs from one growth stage to another with the greatest effect on grain yield during the reproductive and ripening stages (Yoshida 1981).

**Photosynthesis**

Photosynthesis is a process by which solar energy is captured and converted into chemical energy and stored in the form of carbohydrates (Yoshida 1981). It supplies organic substances which are used as building blocks in the process of plant growth and as energy sources for respiration (IRRI 1965). About 80 to 90 percent of the dry matter of green plants is derived from photosynthesis; the rest (minerals) come from the soil (Yoshida 1981). The photosynthetic activity occurs in the leaves which intercept the incident solar radiation. Thus, a rice plant with more surface leaf area is likely to intercept more solar energy than a rice plant with less surface leaf area. Yoshida (1981) outlined the factors that determine crop photosynthesis in the field. These factors were: incident solar radiation, photosynthetic rate per unit leaf area, leaf area index (LAI), and leaf orientation. The photosynthetic rate per unit leaf area is controlled by varietal characters and nitrogen nutrition at a given stage (IRRI 1968).

The leaf area index (LAI) is estimated from one surface of the leaf blade. It is a function of (a) tiller number per unit field area, (b) leaf number per tiller, and (c) average leaf size (IRRI 1964). An active tillering variety tends to have a large LAI. Environmental and genetic factors influence leaf size. Studies have shown that LAI increases with increase in the dry weight of the leaves (IRRI 1964). But, while photosynthesis increases with increase in LAI, the

photosynthetic activity by one plant is not linearly proportional to the total photosynthetic activity of a plant community because of the effect of mutual shading. The fully exposed leaves receive more light than they are able to utilize, while the leaves further down receive less sunlight than they need (IRRI 1964). The degree of mutual shading is expressed by the light transmission ratio (LTR) (IRRI 1964). LTR is the light intensity at the ground level of the plant population (I) divided by the light intensity at the top of the population ($I_o$). This ratio is expressed as the negative exponential function of the product between LAI and the extinction coefficient K. The result of the relationship is written as follows:

$$LTR = \frac{I}{I_o} = e^{-(K \cdot LAI)}$$

K measures leaf orientation. The optimum K value increases with the decrease in LAI (Tanaka, Kawano, and Yamaguchi 1966).

Studies indicate that the LAI values necessary to intercept 95 percent of the incident light in rice canopies range from 4 to 8. A large LAI and K values imply long, wide leaves, while short leaves have smaller LAI and K values (Tanaka, Kawano, and Yamaguchi 1966). In many studies, the concept of mutual shading explains why tiller number, plant weight, LAI, and grain yield decrease when the surrounding plants increase in leafiness (IRRI 1964).

## Carbohydrate Partitioning

The distribution of assimilates or carbohydrates into the different plant organs varies with the growth stages and environmental conditions (Suzuki 1983). Generally, the organs actively developing at the time of growth get a large proportion of the carbohydrates, such as sugars and starch (IRRI 1964). Suzuki (1983) indicated that the ratio of distribution to roots and blades was high in the early growth stages, then a higher distribution to the stem and leaf sheath was evident during the middle growth stages, and finally, after heading, the distribution to the panicle was predominant. A research study (IRRI 1964) showed that, during the early growth stage and until panicle development, about 50 percent of the carbohydrates assimilated became part of the cell walls and was not translocated; however, only 10 percent was retained after flowering. Yoshida (1981) reported that carbohydrates began to accumulate sharply about two weeks before heading and reached a maximum concentration in the plant's vegetative parts, mainly in the leaf sheath and culm, at heading. The concentration began to decrease as ripening proceeded and rose slightly again near

maturity. Another study (IRRI 1970) on the distribution of carbohydrates revealed that, 10 days before flowering, about 18 percent went to the leaf, 22 percent to the sheath and culm, 55 percent to the panicle, and about 5 percent was lost by respiration and senescence. Carbohydrates lost from the vegetative parts during grain filling and not used for respiration are translocated to the grains (IRRI 1964).

**Grain Yield**

Rice yield generally is reported as rough rice at 14 percent moisture content (IRRI 1964; Yoshida 1981). Grain yield is a function of panicle number $m^{-2}$, spikelet or grain number per panicle, percent filled spikelets, and grain weight. The product of panicle number $m^{-2}$ and number of spikelets or grains per panicle is the number of spikelets or grains $m^{-2}$. The relationship is written as follows (Yoshida 1981):

$$\text{Grain yield (t ha}^{-1}) = \text{Spikelet No. m}^{-2} \cdot \text{\% filled Spikelets} \cdot \text{1000-grain weight (g)} \cdot 10^{-5}$$

The equation above shows that grain yield is directly related to spikelet or grain number. In most conditions, the 1000-grain weight of rice is relatively constant and a very stable varietal character (IRRI 1967; Murayama 1979; Yoshida 1981). The constant 1000-grain weight of a given variety does not mean, however, that individual grains have the same weight per grain. The percent filled-spikelet is also observed to be about 85 percent over a wide range of grain number (IRRI 1971, 1972) although it has been observed to decrease to 60 percent when grain number is very large. At the wider spacing, grain yield is directly related to the panicle number, that is, the larger the panicle number, the larger is grain yield (Yoshida and Parao 1972).

**Soil-Water Conditions and Water Losses**

The soil conditions of upland rice are diverse. De Datta and Feuer (1975) reported that soil texture varied from sand to clay; pH, from 3 to 10; organic matter content from 1 to 50 percent; salt content from almost 0 to 1 percent; nutrient availability from acute deficiency to oversupply.

Soil texture affects particularly the moisture status of upland rice soils. A clayey textural profile with a medium texture on the surface horizon is suggested as the most favorable for rice cultivation (De Datta and Feuer 1975). Yoshida (1975) indicates that the soil texture determines the capillary ascent of water in soils. Water moves upward at a slow rate but for a longer distance in a fine soil compared to a

rapid capillary action for a short distance in a coarse soil. For an illustration, he reported Kramer's work in 1969 which showed that with a water table 60 cm deep, water moved upward at 5 mm $day^{-1}$ in a coarse-textured soil but only at 2 mm $day^{-1}$ in a fine-textured soil.

Different soils vary in their water storage capacities. Yoshida (1975) defined the water storage capacity as the water readily available to plants (in the range between the field capacity and permanent wilting point), measured in mm of water per unit depth of soil. He demonstrated that the storage capacity ranged from 4.3 to 8.6 mm per 30 cm in fine sand to 77.0 mm per 30 cm in a clay. As a result, plants growing in soils that had low storage capacities exhausted the readily available water and suffered from drought much sooner than plants growing in soils with high storage capacities. Yoshida further indicated that the extent to which groundwater could supply the needed moisture to the root zones was primarily determined by the depth of the water table and the soil texture. A higher water table would supply more moisture to the root zones than a lower water table.

A major difference between upland-rice soils and lowland-rice soils is the soil-water regime. Unlike lowland-rice soils, Ponnamperuma (1975) explains, upland-rice soils are not submerged or saturated with water for a long period of time during the growing season. He indicates, however, that the rice plant is physiologically, morphologically, and anatomically adapted to submerged, anaerobic soils. So, under upland conditions, the rice plant has to adjust to a dry, aerobic soil conditions. Ponnamperuma (1975) further illustrates that nutrients are delivered by mass flow and diffusion, the delivery rate decreasing with moisture content. So, the low soil moisture content in upland soils reduces the potential supply of nutrients to the roots. Thus, moisture stress is a primary limiting factor on the growth and yield of upland rice (Ponnamperuma 1975; IRRI 1974). This observation was supported by Chang and Vergara (1975) who reported that, under severe water stress, rice yield was poor despite heavy fertilization and effective weed control. Ponnamperuma adds that unlike submerged soils, upland soils are not able to adjust their pH levels to the favorable range of 6.5 to 7.0, a condition which could result in manganese and aluminum toxicities in strongly acid soils, and iron deficiency in alkaline soils. Finally, Ponnamperuma suggests that upland rice does best on the lower members of the toposequence of slightly acid soils, discouraging the use of sodic, calcareous, and saline soils, acid sulfate soils, and soils low in organic matter.

Consistent with Ponnamperuma's findings, Yoshida (1975) observed that nitrogen became the major limiting factor for

yield if adequate water was provided either through rainfall or irrigation.

Water stress is brought about through many processes. One is by transpiration. Transpiration is the amount (g) of water lost from plant surfaces per g of dry matter or carbohydrate produced. It is needed for plant growth. Yoshida (1975) reported that the transpiration ratio was generally from 250 to 350 g $g^{-1}$, implying that dry matter production was proportional to the amount of water transpired by the plant.

Aside from transpiration, water is lost through evaporation, surface runoff, percolation, and seepage. Evaporation is the loss of water from free water surfaces (Yoshida 1981). The combined water losses due to evaporation and transpiration are called evapotranspiration. The potential evapotranspiration, which is the amount of water lost through transpiration by a vegetation that completely covers a ground that is never water deficient, represents the maximum possible evaporative loss from a vegetative-covered surface. Yoshida presented several methods of calculating the potential evapotranspiration. These methods are the Penman equation, the Thornwaite method, and the van Bavel method. The procedure proposed by Priestly and Taylor (1972) is the method used in the CERES crop models.

Yoshida (1981) further defines percolation, seepage, and runoff. Percolation, which occurs in a vertical direction, is largely affected by the topography, soil characteristics, and depth of the water table. Seepage is the water lost through the horizontal movement of water in a levee as determined by the slope and roughness of the soil surface in upland fields. Generally, percolation and seepage are taken as a measure of the water-retaining capacity of the field. Surface runoff or overland flow occurs when rainfall intensity exceeds the surface storage capacity and the percolation-plus-seepage rate or infiltration rate.

Water stress severely affects shoot growth more than root growth, while tillering is least affected (IRRI 1974).

The analytical relationship of the soil-water balance and the water losses by evapotranspiration, surface runoff, percolation, and seepage are presented and discussed by Ritchie (1985).

**The Importance of Nitrogen Fertilization**

As plants grow, they absorb nitrogen from the soil to support photosynthesis. Studies have shown that photosynthesis and respiration, and correspondingly grain yield, increase with

increasing levels of nitrogen, especially in fields short of the element (IRRI 1964). This absorption will deplete the amount of nitrogen in the soil (IRRI 1963). In order to maintain high leaf photosynthetic activity for assimilating a large amount of carbohydrates and to supply more nitrogenous compounds to grains during the ripening stage, Murayama (1979) indicated that additional nitrogen must be supplied from the soil to the plant. He reported that high-yielding rice plants had high nitrogen concentration throughout their growth cycle. The straw of ordinary varieties contained 0.5 to 0.6 percent nitrogen at maturity, while the high-yielding varieties contained 0.7 to 1.0 percent. For a high yielding plant, he reported that the optimum nitrogen concentration in the leaf blade was from 2.3 to 4.0 percent at the early panicle formation stage and from 2.2 to 3.3 percent at the heading stage. He further added that from 50 to 60 percent of total plant nitrogen in high-yielding plants with high nitrogen concentration had been absorbed by the early panicle formation, from 70 to 80 percent by heading, and finally, from 20 to 30 percent of nitrogen was absorbed during the ripening stage.

Nitrogen compounds are mobile in the plant. They are constantly translocated from old organs to new ones (IRRI 1963). During the ripening stage, about 70 percent of the nitrogen absorbed by the straw is translocated to the grain (Yoshida 1981). Nitrogen content of the grain does not fluctuate.

Patnaik and Rao (1979) outlined the many sources of nitrogen that could be applied to regulate nitrogen nutrition in the soil. Soil organic matter is one good source and the process of supplying nitrogen from this source to the plant is through mineralization by biochemical or microbial means. Another source of nitrogen is organic and green manures. Organic and green manures are crop residues, such as straw or well-rotten compost, incorporated into the soil. Chemical fertilizers, such as urea, ammonium sulfate, and ammonium phosphate to name a few, have been identified as the major sources of nitrogen. Choice of the form depends on availability and on the condition of the soil. The incorporation of fertilizer nitrogen into the reduced subsurface layer during land preparation is one method of application. This method has been observed to minimize losses resulting from runoff, volatilization, leaching, and denitrification. The recommended amount of application is between 40 and 50 kg N $ha^{-1}$ with a maximum of 60 kg N $ha^{-1}$ during the wet season, and between 80 and 100 kg N $ha^{-1}$ with a maximum of 120 kg N $ha^{-1}$ during the dry season.

Without nitrogen fertilization in soils unable to meet the nitrogen requirements of the plant, the plant suffers a nitrogen deficiency. Nitrogen deficiency eventually results in low

yield. However, higher nitrogen application does not always bring about higher yields. Many studies have shown that when plants grow taller and actively tiller, the field becomes crowded with leaves, especially at high nitrogen levels, resulting in serious mutual shading and sometimes lodging. This event could cause an imbalance between photosynthesis and respiration in the later stages of growth and reduce the effectiveness of the nitrogen applied (IRRI 1963). Thus, the nitrogen effect tends to decrease with increase in growth duration (Tanaka, Kawano, and Yamaguchi 1966).

The nitrogen transformation processes under upland conditions, such as nitrogen mineralization, denitrification, and nitrate leaching, follow those outlined for the CERES-Wheat model by Godwin and Vlek (1985).

## CHAPTER V. THE ANALYTICAL STRUCTURE OF THE CERES-RICE SIMULATION MODEL

In adapting the rice-production system to a digital computer, the state-space description has to be transformed into a discrete-time system so that the problem can be solved recursively by using difference equations. In discrete-time system representation, the rice-production system is described in the following state-space equation:

$$\bar{x}(kT+T) = \bar{g}[\bar{x}(kT), \bar{u}(kT), \bar{e}(kT), kT]$$

$$\bar{y}(kT) = \bar{h}[\bar{x}(kT), \bar{u}(kT), \bar{e}(kT), kT]$$

where the variable k is the discrete time and takes on positive integer values exclusively, while the variable T is the sampling period or interval. The functions $\bar{g}$ and $\bar{h}$ are vector valued and nonlinear; $\bar{y}(kT)$ is the output vector at discrete time k; $\bar{u}(kT)$ is the controllable input vector at discrete time k; $\bar{e}(kT)$ is the exogenous input vector at discrete time k; and, $\bar{x}(kT)$ is the state vector at discrete time k.

The sampling interval T is 1 day, that is, the value of the variables is a sequence of numbers spaced at 24-hour intervals. Replacing T with 1 simplifies the state-space equation into the following:

$$\bar{x}(k+1) = \bar{g}[\bar{x}(k), \bar{u}(k), \bar{e}(k), k]$$

$$\bar{y}(k) = \bar{h}[\bar{x}(k), \bar{u}(k), \bar{e}(k), k]$$

The vector components of $\bar{u}(k)$ are the day of the year for sowing (ISOW); number of plants $m^{-2}$ (PLANTS); depth of sowing (SDEPTH, cm); day of the year (JFDAY) and amount of nitrogen fertilizer (AFERT, kg N $ha^{-1}$), depth of fertilizer application (DFERT, cm), and type (IFTYPE) of fertilizer; day of the year (JDAY) and amount of irrigation (AIRR, mm).

The vector components of $\bar{e}(k)$ are the solar radiation at time k (SOLRAD(k), MJ $m^{-2}$); maximum air temperature at time k (TEMPMX(k), $^{o}$C); minimum air temperature at time k (TEMPMN(k), $^{o}$C); and rainfall at time k (RAIN(k), mm $day^{-1}$).

The controllable input variables or signals are of the

Kronecker delta sequence, that is,

$$u(k) = \delta(k) = \begin{cases} 1, & \text{for } k = 0 \\ 0, & \text{for } k \neq 0 \end{cases}$$

while the exogenous input signals or variables are of the Kronecker-delta-like sequences, that is,

$$u(k) = \delta(k-p) = \begin{cases} 1, & \text{for } k = p \\ 0, & \text{for all other values of } k \end{cases}$$

where p is any fixed integer (Cadzow 1973). The sequence $\delta(k-p)$ is equal to the sequence $\delta(k)$ shifted p discrete-time units to the right since k will take only positive integer values.

The vector $\bar{y}(k)$ has two components: grain yield (YIELD, t $ha^{-1}$) and plant straw (PSTRAW, g $m^{-2}$).

The natural system parameters are the latitude of the production area (LAT) and parameters related to the soil properties and soil water balance. The number (NLAYR) and depth of the soil layers ($DLAYR_\lambda$, $\lambda = 1,\ldots,NLAYR$), and the lower limit of plant extractable soil water of the soil layer ($LL_\lambda$) are soil-related parameters which will be mentioned in the discussion. However, there are other parameters related to the soil, water, and nitrogen fertilization which are needed for the numerical estimation of the water-related and nitrogen-related stress factors. These parameters are outlined by Ritchie (1985), Godwin and Vlek (1985), and Ritchie et al. (1986).

The system design parameters are the genetic coefficients of the variety. These coefficients are: P1 (duration, in degree-days, from emergence to end of juvenile stage), P2R (rate of photo-induction, in degree-days per hour), P2O (optimum photoperiod, in hours), P5 (duration, in degree-days, required for grain filling), G1 (conversion efficiency from intercepted photosynthetically active radiation (PAR) to dry matter production, g $MJ^{-1}$), and TR, a unitless tillering factor.

The input-process-output relationship in the rice-production system is best related to the phenological stages and growth patterns of the plant. The phenological stages describe the duration of each growth stage in the life cycle of the rice plant. Growth pertains to the production and distribution of carbohydrates to the various plant parts resulting in plant growth. Unless otherwise stated, the unit of production area is $m^2$, the unit of carbohydrate production and plant growth is g $m^{-2}$, and the unit of leaf area expansion is in $m^2$ leaf area per $m^2$ of land area occupied by the plants ($m^2$ $m^{-2}$).

As in other CERES crop models, the phenological stages are numbered one through nine, with the active, above-ground stages numbered one through five. This numerical sequencing is based on carbohydrate partitioning which varies according to stages. The phenological stages are identified as follows: sowing (ISTAGE 7), germination (ISTAGE 8), emergence (ISTAGE 9), juvenile (ISTAGE 1), panicle initiation (ISTAGE 2), heading (ISTAGE 3), beginning of grain filling (ISTAGE 4), end of grain filling (ISTAGE 5), and physiological maturity (ISTAGE 6).

As mentioned in chapter IV, the duration of each phenological stage makes use of the concept of thermal time or degree-days at time k (DTT(k)). DTT(k) is the difference between the mean temperature (TEMPM(k)) and temperature threshold (TBASE) of 1 day, hence the unit degree-day. TEMPM(k) at time k is the average of TEMPMX(k) and TEMPMN(k) at time k. However, this estimation process is valid only when TEMPMN(K) is greater than TBASE and TEMPMX(k) is less than 33°C. That is,

$$\mathrm{TEMPM}(k) = \frac{\mathrm{TEMPMX}(k) + \mathrm{TEMPMN}(k)}{2}$$

$$\mathrm{DTT}(k) = \mathrm{TEMPM}(k) - \mathrm{TBASE}, \quad \mathrm{TEMPMN}(k) > \mathrm{TBASE};\ \mathrm{TEMPMX}(k) < 33^{\circ}\mathrm{C}$$

Otherwise, DTT(k) is estimated by dividing a 24-hour day into eight three-hourly sections, calculating a temperature correction factor for each section (TMFAC), interpolating the air temperature for that section (TTMP), and then calculating the appropriate thermal time at time k. That is,

$$\mathrm{TMFAC}(k)_i = 0.931 + 0.114i - 0.0703i^2 + 0.0053i^3, \quad i = 1,\ldots,8$$

$$\mathrm{TTMP}(k)_i = \mathrm{TEMPMN}(k) + \mathrm{TMFAC}(k)_i \cdot (\mathrm{TEMPMX}(k) - \mathrm{TEMPMN}(k)),$$

$$i = 1, \ldots, 8$$

$$\mathrm{DTT}(k) = \begin{cases} \dfrac{1}{8} \displaystyle\sum_{i=1}^{8} (\mathrm{TTMP}(k)_i - \mathrm{TBASE}), & \mathrm{TBASE} \le \mathrm{TTMP}(k)_i \le 33^{\circ}\mathrm{C} \\[2ex] \dfrac{(33 - \mathrm{TBASE})}{8} \displaystyle\sum_{i=1}^{8} [1 - (\mathrm{TTMP}(k)_i - 33)/9], & 33^{\circ}\mathrm{C} < \mathrm{TTMP}(k)_i < 42^{\circ}\mathrm{C} \\[2ex] 0, \text{ otherwise.} & \end{cases}$$

The production and distribution of carbohydrates are

affected at each phenological stage by temperature, water, and nitrogen stresses. So these stress factors have to be estimated quantitatively.

A temperature-related stress factor at time k (PRFT(k)), taking on real values in the closed interval between 0 and 1, affects carbohydrate production. PRFT(k) is calculated from TEMPMN(k) and TEMPMX(k) weighted accordingly, with optimum at 26°C mean temperature.

$$PRFT(k) = 1 - 0.0025 \cdot [(0.25 \cdot TEMPMN(k) + 0.75 \cdot TEMPMX(k)) - 26]^2,$$

$$PRFT(k) \in [0,1]$$

Another temperature-related stress factor at time k is SLFT(k). SLFT(k) takes on real values in the closed interval between 0 and 1 and affects leaf senescence due to temperatures below 6°C.

$$SLFT(k) = \begin{cases} 1, & TEMPM(k) > 6^{\circ}C \text{ and } TEMPMN(k) > 0^{\circ}C \\ 1 - \dfrac{6 - TEMPM(k)}{6}, & 0^{\circ} \le TEMPM(k) \le 6^{\circ}C \\ 0, & TEMPM(k) < 0^{\circ}C \text{ or } TEMPMN(k) < 0^{\circ}C \end{cases}$$

The water-related stress factors at time k are SWDF1(k) and SWDF2(k), while the nitrogen-related stress factors at time k are NDEF1(k) and NDEF2(k). These factors take on real values in the closed interval between 0 and 1. SWDF1(k) and NDEF1(k) are the water stress and nitrogen stress factors, respectively, affecting carbohydrate production, while SWDF2(k) and NDEF2(k) are the water stress and nitrogen stress factors, respectively, affecting leaf expansion. The analytical relationships of the soil-water balance and nitrogen transformation and uptake leading to the quantification of these stress factors are presented by Jones et al. (1986).

Plant competition for sunlight, nutrients, and water becomes a factor in plant growth when plant population is dense, so a population density factor affecting the actual carbohydrate production (POPFAC), which takes on real values in the closed interval between 0 and 1, is also calculated.

$$POPFAC = 0.94 + 0.0006 \cdot PLANTS, \quad POPFAC \in [0,1]$$

All the stress factors, PRFT(k), SLFT(k), SWDF1(k),

SWDF2(k), NDEF1(k), and NDEF2(k), and the population factor (POPFAC) are unitless.

**Sowing Stage (ISTAGE 7)**

Sowing stage is the point in time when seeds are sown in the ground and the discrete time k is set to zero and will be incremented by one hereafter, taking on a positive integer value exclusively for every simulation step.

The location of the seeds in the soil profile is determined from the sowing depth (SDEPTH) and the thickness (cm) of the soil layers (DLAYR). The soil-seed layer is indexed with $\lambda 0$. Its location in the soil profile (CUMDEP) is calculated as follows:

$$\text{CUMDEP} = \sum_{\lambda=1}^{\lambda 0} \text{DLAYR}_{\lambda}$$

At this time also, the vector components of $\bar{x}(0)$, the initial state of the system, is defined.

**Germination Stage (ISTAGE 8)**

Germination stage covers the period from sowing until germination. Germination will occur if all four conditions outlined below are satisfied:

1. $SW(k)_{\lambda 0} > LL_{\lambda 0}$, where $SW(k)_{\lambda 0}$ is the soil water content of the seed layer $\lambda 0$ at time k and $LL_{\lambda 0}$ is the lower limit of plant extractable soil water of that layer. Otherwise, the extractable soil water at the sowing depth at time k (SWSD(k)), calculated proportionately between $SW(k)_{\lambda 0}$ and $LL_{\lambda 0}$ and the soil water content and lower limit of plant extractable soil water of the next layer, $SW(k)_{\lambda 0+1}$ and $LL_{\lambda 0+1}$ respectively, has a value of 0.02 or greater. That is,

$$SWSD(k) = (SW(k)_{\lambda 0}-LL_{\lambda 0})\cdot 0.65 + (SW(k)_{\lambda 0+1}-LL_{\lambda 0+1})\cdot 0.35 \geq 0.02 \ .$$

2. The mean air temperature at time k is between 15°C and 42°C, that is,

$$15^{o}C \leq TEMPM(k) \leq 42^{o}C \ .$$

3. The accumulated degree-days from sowing time ($k_7$) until time k is 45 or more, that is,

$$\sum_{k_7}^{k} DTT(k) \geq 45 \ .$$

4. The duration of the seeds in the ground is ≤ 40 days.

If germination does not occur 40 days after sowing, crop failure is assumed.

If germination occurs, the initial rooting depth (RTDEP(k), cm) is equivalent to the sowing depth (SDEPTH), that is,

$$RTDEP(k) = SDEPTH .$$

**Emergence Stage (ISTAGE 9)**

Emergence stage covers the period from germination to emergence of the seedling from the soil surface. The duration, in degree-days, required from germination to emergence is P9. P9 is a linear function of the sowing depth (SDEPTH) with a slope of 7 degree-days per cm depth.

$$P9 = 7 \cdot SDEPTH$$

During the emergence stage, the seedling gets its food supply from the seed reserve. The potential carbohydrate production at time k (PCARB(k)) under optimum water, nitrogen, and temperature conditions is a linear function of the thermal time at time k (DTT(k)). That is, within the optimal high and low temperature range, growth is faster at higher temperatures than at lower temperatures. From chapter IV, the slope of potential dry matter or carbohydrate production is given as 0.00008265 g carbohydrate per plant per degree-day. At this stage, seedling growth is not affected by plant competition, so the total potential carbohydrate production is the product of a single plant's production and the plant population $m^{-2}$ (PLANTS).

$$PCARB(k) = 0.00008265 \cdot PLANTS \cdot DTT(k)$$

However, the actual carbohydrate production at time k (CARBO(k)) is not always equal to the potential production due to environmental constraints. The actual carbohydrate produced can be less than the potential due to reduction by the most limiting of either the temperature stress (PRFT(k)) or soil water deficit (SWDFl(k)).

$$CARBO(k) = PCARB(k) \cdot \min[PRFT(k), SWDFl(k)]$$

The carbohydrates produced during this stage are distributed between the leaves and roots in proportional fractions. The fraction going to the roots at time k (PFR(k)) is represented as the negative exponential function of the seedling weight at time k-1 (PLTWT(k-1)/PLANTS), where PLTWT(k-1) is the total plant weight $m^{-2}$ at time k-1.

$$PFR(k) = 0.21 \cdot e^{-(PLTWT(k-1)/PLANTS)}$$

The fraction of carbohydrates going to the leaves at time k (PFL(k)) is the remainder of the total. That is,

$$PFL(k) = 1 - PFR(k).$$

Root growth (GRORT(k)) and leaf growth at time k (GROLF(k)) are proportional to the amount of carbohydrates allocated to these parts at time k. That is,

$$GRORT(k) = CARBO(k) \cdot PFR(k)$$

$$GROLF(k) = CARBO(k) \cdot PFL(k).$$

The weight of the roots (RTWT(k)) and the leaves (LFWT(k)) at time k are the sum of their respective weights at time k-1 and growth at time k. That is,

$$RTWT(k) = RTWT(k-1) + GRORT(k)$$

$$LFWT(k) = LFWT(k-1) + GROLF(k)$$

During this stage, the increase in the rooting depth at time k is a linear function of the thermal time (DTT(k)) at time k with a slope of 0.15 cm per degree-day. So the rooting depth at time k (RTDEP(k)) is the sum of the rooting depth at time k-1 and the increase in the rooting depth at time k, that is,

$$RTDEP(k) = RTDEP(k-1) + 0.15 \cdot DTT(k)$$

The nitrogen content of the roots at time k (ROOTN(k)) is determined from the actual nitrogen concentration of the roots (RANC(k-1)), in g N $g^{-1}$ root, and total root weight (RTWT(k-1)) at time k-1.

$$ROOTN(k) = RANC(k-1) \cdot RTWT(k-1)$$

The nitrogen content of the stover at time k (STOVN(k)) is calculated from the total stover weight (STOVWT(k-1)) and the actual nitrogen concentration of the tops (TANC(k-1)), in g N $g^{-1}$ top weight, at time k-1.

$$STOVN(k) = STOVWT(k-1) \cdot TANC(k-1)$$

The leaves start to grow during this stage. Leaf emergence per plant at time k (TI(k)) is a linear function of the thermal time at time k (DTT(k)) with a slope equivalent to the phyllocron interval. The phyllocron interval used in the simulation model is 83 degree-days per leaf.

$$TI(k) = \frac{DTT(k)}{83}$$

The total number of fully expanded leaves from k = 0 to time k (CUMPH(k)) is the sum of the daily leaf emergence (TI(k)).

$$CUMPH(k) = \sum_{k=0}^{k} TI(k)$$

**Juvenile Stage (ISTAGE 1)**

Juvenile stage covers the period from emergence to the end of the basic vegetative phase. The duration, in degree-days, is the genetic coefficient P1.

The root length density for the soil layers at time k ($RLV(k)_\lambda$), in cm root per $cm^3$ soil, is first estimated at this stage. $RLV(k)_\lambda$ is initialized as a function of the plant population (PLANTS) and the thickness of the soil layer ($DLAYR_\lambda$). $\lambda$ is the soil layer index going from one through the total number of soil layers (NLAYR), $\lambda 0$ being the index for the seed layer. For each soil layer above the seed layer, RLV(k) is proportional to the plant population by a factor of 0.2 cm root per $cm^2$ soil per plant, that is,

$$RLV(k)_\lambda = \frac{0.2 \cdot PLANTS}{DLAYR_\lambda}, \qquad \lambda = 1, \ldots, \lambda 0-1$$

However, RLV(k) in the seed layer is reduced by a unitless fraction proportional to the difference between the cumulative depth of the seed layer (CUMDEP) and the rooting depth of the plants at time k (RTDEP(k)). That is,

$$RLV(k)_{\lambda 0} = \frac{0.2 \cdot PLANTS}{DLAYR_{\lambda 0}} \cdot \left(1 - \frac{CUMDEP - RTDEP(k)}{DLAYR_{\lambda 0}}\right)$$

RLV(k) is zero after the seed layer, that is,

$$RLV(k)_\lambda = 0, \qquad \lambda = \lambda 0+1, \ldots, NLAYR$$

When the seed reserve is still available for the plant to use, the potential carbohydrate production at time k (PCARB(k)) for each seedling is a logarithmic function of the thermal time at time k (DTT(k)) by a factor of 0.001 g carbohydrate per plant per degree-day. The total potential production is multiplied by the plant population $m^{-2}$ (PLANTS). That is,

$$PCARB(k) = 0.001 \cdot PLANTS \cdot \log(DTT(k)).$$

Then CARBO(k), PFR(k), PFL(k), ROOTN(k), and STOVN(k) are calculated as in ISTAGE 9.

When the seed reserve is used up, growth is supported by photosynthesis. Photosynthesis is the process where the plant converts the intercepted light at time k (SOLRAD(k)) into carbohydrates. The plant utilizes the photosynthetically active radiation (PAR(k)) which is 50 percent of solar radiation (SOLRAD(k)). Thus,

$$PAR(k) = 0.50 \cdot SOLRAD(k)$$

where PAR(k) has the unit MJ $m^{-2}$.

In chapter IV, the Light Transmission Ratio (LTR) was given as the negative exponential function of the product of the leaf area index (LAI(k)) and the extinction coefficient K. That is,

$$e^{-(K \cdot LAI(k))}$$

This means that the interception can be written as

$$1 - e^{-(K \cdot LAI(k))}$$

The intercepted light, in the form of PAR(k), is then converted into carbohydrates as influenced by the plant's genetic or varietal character for conversion efficiency, G1. Intuitively, G1 defines the erectness or droopiness of the leaves. When used in this equation, G1 has the unit g carbohydrate per MJ of intercepted PAR(k). Thus the equation is stated as follows:

$$PCARB(k) = G1 \cdot PAR(k) \cdot [1 - e^{-(K \cdot LAI(k-1))}]$$

where LAI(k-1) is the leaf area index at time k-1. K varies with LAI(k-1), thus,

$$K = \begin{cases} e^{-(LAI(k-1))} & LAI(k-1) \le 0.6 \\ 0.58 - 0.04 \cdot LAI(k-1), & 0.6 < LAI(k-1) \le 5.0 \\ 0.36 & LAI(k-1) > 5.0 \end{cases}$$

The actual carbohydrates produced at time k (CARBO(k)) can be less than the potential production due to shading (POPFAC), temperature stress (PRFT(k)), and the most limiting effect due to water (SWDF1(k)) and nitrogen (NDEF1(k)) stresses at time k. That is,

$$CARBO(k) = PCARB(k) \cdot POPFAC \cdot PRFT(k) \cdot \min[SWDF1(k), NDEF1(k)]$$

When photosynthesis takes over carbohydrate production completely, a very slow growth in the stem occurs. The distribution of carbohydrate to the plant parts then changes. The fraction going to the leaves at time k (PFL(k)) is now a linear function of thermal time at time k with a slope of 0.001 per degree-day.

$$PFL(k) = PFL(k-1) + 0.001 \cdot DTT(k), \quad PFL(k) \leq 0.84$$

PFL(k), however, is bounded on the right by 0.84. This condition ensures that a fraction of carbohydrates going to the leaves is at most 0.84, and allows for positive fractions going to the stem and roots, under a favorable growing day. The fraction going to the stem at time k (PFC(k)) is also a function of thermal time with a slope of 0.00002 per degree-day, that is,

$$PFC(k) = PFC(k-1) + 0.00002 \cdot DTT(k).$$

The fraction that goes to the roots (PFR(k)) is the remainder of the total, that is,

$$PFR(k) = 1 - PFL(k) - PFC(k).$$

However, during the presence of a water deficit (SWDF2(k)) or nitrogen deficiency (NDEF1(k)) at time k, the plants redistribute their carbohydrates or assimilates in favor of the roots, reducing PFL(k) by the most limiting factor of the two stresses. This redistribution is active until just before the beginning of grain filling.

Daily root growth (GRORT(k)) and leaf growth (GROLF(k)) are calculated, while root weight (RTWT(k)) and leaf weight (LFWT(k)) at time k are updated, as in ISTAGE 1. That is,

$$GRORT(k) = CARBO(k) \cdot PFR(k)$$

$$GROLF(k) = CARBO(k) \cdot PFL(k)$$

$$RTWT(k) = RTWT(k-1) + GRORT(k)$$

$$LFWT(k) = LFWT(k-1) + GROLF(k)$$

Daily stem growth (GROSTM(k)) at time k is proportional to the amount of carbohydrates distributed to the stem.

$$GROSTM(k) = CARBO \cdot PFC(k)$$

The stem weight at time k (STMWT(k)) is the sum of the weight at

time k-1 and growth at time k.

$$STMWT(k) = STMWT(k-1) + GROSTM(k)$$

The total stover weight (STOVWT(k)) is the sum of LFWT(k) and STMWT(k), that is,

$$STOVWT(k) = LFWT(k) + STMWT(k).$$

The juvenile stage is characterized by leaf expansion. When the seed reserve is used up, leaf area expansion at time k (PLAG(k)) is calculated. PLAG(k) is a function of leaf growth at time k (CARBO(k)·PFL(k)) and the number of leaves per plant emerging at time k (TI(k)). Leaf expansion is also a function of the plant's genetic characteristic for tillering (TR·G1), which is a varietal character to form tillers or new plants; thus, it is given the unit: number of plants. As indicated in chapter IV, a high value of (TR·G1) indicates that the plant has a high capacity for tillering (or forming new plants) and therefore bigger capacity for leaf expansion. The conversion factor is 0.037 $m^2$ leaf area expansion per leaf per g of leaf growth. Leaf expansion is, however, reduced by the most limiting of the three stress factors at time k: soil-water deficit (SWDF2(k)), nitrogen stress (NDEF2(k)), and low temperature (SLFT(k)). That is,

$$PLAG(k) = 0.037 \cdot TR \cdot G1 \cdot TI(k) \cdot CARBO(k) \cdot PFL(k) \cdot$$

$$\min[SWDF2(k), NDEF2(k), SLFT(k)].$$

Total leaf area at time k (PLA(k)) is the sum of the leaf area at time k-1 and leaf expansion at time k, that is,

$$PLA(k) = PLA(k-1) + PLAG(k).$$

In this situation, PLA(k) is numerically equal to the leaf area index at time k (LAI(k)). Thus,

$$LAI(k) = PLA(k).$$

Tillering is also a characteristic of the juvenile stage. The tiller number $m^{-2}$ at any time k (TILNO(k)) is the sum of the tiller number at time k-1 and the tillering growth at time k. The tillering growth at time k is a function of the number of leaves per plant emerging at time k (TI(k)), the fraction of carbohydrates going to the leaves at time k (PFL(k), unitless), the plant's genetic characteristic for tillering (TR·G1, number of plants), and a tillering-population factor (100/PLANTS, $m^{-2}$). The conversion factor is 32 tillers per leaf. Thus,

$$TILNO(k) = TILNO(k-1)+32 \cdot TI(k) \cdot PFL(k) \cdot TR \cdot G1 \cdot (100/PLANTS).$$

**Panicle Initiation Stage (ISTAGE 2)**

The panicle initiation stage covers the period from the end of the juvenile stage to panicle initiation.

The photoperiod or daylength at time k (HRLT(k), in hours) is determined from the daylength variation at time k (DLV(k)), which is a function of the solar declination at time k (DEC(k), in radians), the sine and cosine of the latitude of the production area (LAT), and the angle of the sun at civil twilight (in radians). The solar declination at time k (DEC(k)) is a sine function of the day of the year (JDATE), that is,

$$(1) \quad DEC(k) = 0.4093 \cdot \sin(0.0172 \cdot (JDATE-82.2)).$$

The daylength variation (DLV(k)) is calculated from the sine and cosine of both the latitude of the area (LAT) and the solar declination. DLV(k) is adjusted by the angle of the sun at civil twilight (0.1047). Thus,

$$(2) \quad DLV(k) = \frac{-\sin(LAT) \cdot \sin(DEC(k)) - 0.1047}{\cos(LAT) \cdot \cos(DEC(k))}$$

However, DLV(k) is bounded on the left by -0.87. Finally, the photoperiod is an arccosine function of the daylength variation, that is,

$$(3) \quad HRLT(k) = 7.639 \cdot \arccos(DLV(k)).$$

The rate of floral induction per degree-day at time k (RATEIN(k)) is a constant 1/136 if the photoperiod is less than or equal to the optimum photoperiod (P20). However, if the photoperiod at time k (HRLT(k)) is greater than P20, RATEIN(k) is slowed down and becomes a function of the photoperiod HRLT(k), the optimum photoperiod (P20), and the rate of photo-induction (P2R).

$$RATEIN(k) = \frac{1}{136 + P2R \cdot (HRLT(k) - P20))}$$

The panicle initiation stage is completed when the sum of the product of RATEIN(k) and DTT(k) from the beginning of this stage ($k_2$) until time k is 1.0. That is,

$$\sum_{k=k_2}^{k} RATEIN(k) \cdot DTT(k) = 1.0 .$$

The panicle initiation stage is characterized by root

growth, leaf emergence, leaf growth, stem growth, and tillering. The fraction going to the roots is set to 0.15. The fraction going to the leaves is decreasing, with a negative slope of 0.001 per degree-day, in favor of the stem. That is,

$$PFR(k) = 0.15$$

$$PFL(k) = PFL(k-1) - 0.001 \cdot DTT(k)$$

$$PFC(k) = 1 - PFR(k) - PFL(k)$$

As in ISTAGE 1, PFL(k) is adjusted in favor of PFR(k) whenever there is a water deficit or nitrogen deficiency.

Daily root growth (GRORT(k)), leaf growth (GROLF(k)), stem growth (GROSTM(k)), root weight (RTWT(k)), leaf weight (LFWT(k)), stem weight (STMWT(k)), and stover weight (STOVWT(k)) at time k are updated, as in ISTAGE 1. That is,

$$GRORT(k) = CARBO(k) \cdot PFR(k)$$

$$GROLF(k) = CARBO(k) \cdot PFL(k)$$

$$GROSTM(k) = CARBO \cdot PFC(k)$$

$$RTWT(k) = RTWT(k-1) + GRORT(k)$$

$$LFWT(k) = LFWT(k-1) + GROLF(k)$$

$$STMWT(k) = STMWT(k-1) + GROSTM(k)$$

$$STOVWT(k) = LFWT(k) + STMWT(k)$$

**Heading Stage (ISTAGE 3)**

The heading stage covers the period from the end of panicle initiation to heading where 50 percent of the panicles have exserted. The duration of this stage is P3. It is equivalent to 450 degree-days plus 15 percent of the accumulated degree-days from the beginning of the juvenile stage ($k_1$) until just before heading stage ($k_3$), that is,

$$P3 = 450 + 0.15 \cdot \sum_{k=k_1}^{k_3} DTT(k) \ .$$

The heading stage is characterized by root growth, leaf growth, emergence of last leaf, stem elongation, increase in plant height, panicle growth, and decline in tiller formation.

PFR(k) is set to 0.10 during this stage. PFL(k) is reduced linearly with thermal time by a slope of 0.0014 per degree-day, but bounded on the left by 0, while PFC(k) is increasing monotonically as a linear function of thermal time with a slope of 0.00072 per degree-day. That is,

$$PFR(k) = 0.10$$

$$PFL(k) = PFL(k-1) - 0.0014 \cdot DTT(k)$$

$$PFC(k) = PFC(k-1) + 0.00072 \cdot DTT(k)$$

Since panicle growth is also a characteristic of this stage, the fraction going to the panicles at time k (PFP(k)) is positive. The positive fraction is guaranteed because the rate of decrease from PFL(k) is greater than the rate of increase for PFC(k).

$$PFP(k) = 1 - PFR(k) - PFL(k) - PFC(k)$$

The panicle growth at time k (PAWT(k)) is proportional to the amount of carbohydrates allocated to it, that is,

$$PAWT(k) = CARBO(k) \cdot PFP(k)$$

The panicle weight at time k (PPAWT(k)) is the sum of the weight at time k-1 and growth at time k.

$$PPAWT(k) = PPAWT(k-1) + PAWT(k)$$

One panicle is allowed to grow as a linear function of thermal time with a slope of 0.00095 g per degree-day. This single panicle will be used to estimate the total number of panicles during harvest. Thus, the single panicle growth at time k (PNWT(k)) and the single panicle weight at time k (PERPAWT(k)) are estimated and updated as follows:

$$PNWT(k) = 0.00095 \cdot DTT(k)$$

$$PERPAWT(k) = PERPAWT(k-1) + PNWT(k)$$

As in ISTAGE 1, PFL(k) is adjusted in favor of PFR(k) whenever there is a water deficit or nitrogen deficiency.

Daily root growth (GRORT(k)), leaf growth (GROLF(k)), stem growth (GROSTM(k), root weight (RTWT(k)), leaf weight (LFWT(k)), stem weight (STMWT(k)), and stover weight (STOVWT(k)) at time k are updated, as in ISTAGE 2. That is,

$$GRORT(k) = CARBO(k) \cdot PFR(k)$$

$$GROLF(k) = CARBO(k) \cdot PFL(k)$$

$$GROSTM(k) = CARBO \cdot PFC(k)$$

$$RTWT(k) = RTWT(k-1) + GRORT(k)$$

$$LFWT(k) = LFWT(k-1) + GROLF(k)$$

$$STMWT(k) = STMWT(k-1) + GROSTM(k)$$

$$STOVWT(k) = LFWT(k) + STMWT(k)$$

The biomass at time k (BIOMAS(k)) is the sum of LFWT(k), STMWT(k), and PPAWT(k), while the total plant weight at time k (PLTWT(k)) is the sum of BIOMAS(k) and RTWT(k), that is,

$$BIOMAS(k) = LFWT(k) + STMWT(k) + PPAWT(k)$$

$$PLTWT(k) = BIOMAS(k) + RTWT(k)$$

At the end of the heading stage, the leaves stop to grow.

**Beginning of Grain Filling Stage (ISTAGE 4)**

The beginning of grain filling stage covers the period from the time when 50 percent of the panicles have exserted to the beginning of grain filling. The duration is 170 degree-days.

A temperature-related stress factor is modeled to affect the percentage of grain filling (FERTILE). When the mean temperature at time k (TEMPM(k)) is between 17°C and 35°C, FERTILE is a constant 85.3 percent; however, this percentage is reduced by shading effects due to plant population (PLANTS). That is,

$$FERTILE = 0.853 - 0.00028 \cdot PLANTS.$$

Otherwise, at extremely high or low temperatures, the percentage of grain filling is estimated as follows:

$$FERTILE = \begin{cases} 0.75-0.1 \cdot (TEMPM-35), & TEMPM > 35^{o}C \\ 0.75-0.1 \cdot (17-TEMPM), & TEMPM < 17^{o}C \end{cases}$$

PFR(k) is set to a fixed fraction of 0.10 during this stage. PFL(k) continues to decrease linearly with thermal time by a slope of 0.0006 per degree-day.

$$PFL(k) = PFL(k-1) - 0.0006 \cdot DTT(k)$$

During this growth stage, there is a possibility of

assimilate translocation from the leaves to the panicle. This event occurs when the value of PFL(k) becomes negative. The absolute value is added to the fraction allocated to the panicle. The negative value of PFL(k) causes a negative value of leaf growth and leaf expansion. This negative growth and negative leaf expansion represents leaf senescence. Although leaf senescence has occurred slightly during the previous growth stages as part of a natural process, it is during this stage that leaf senescence is clearly demonstrated, since leaves have stopped growing. Leaf senescence at time k (PLAG(k)), in $m^2$ leaf area senescence per $m^2$ of land area, is estimated to be influenced by the weight of leaf senescence at time k (CARBO(k)·PFL(k)) in proportion to the varietal characteristic for tillering (TR·G1). Leaf senescence is hastened in the presence of water, nitrogen, and temperature stresses. The conversion factor is 0.004 $m^2$ leaf area senescence per g of leaf senescence per plant. Thus, leaf senescence is modeled as follows:

$$PLAG(k) = 0.004 \cdot CARBO(k) \cdot PFL(k) \cdot TR \cdot G1 \cdot$$

$$(2 - \min[SWDF2(k), NDEF2(k), SLFT(k)])$$

Since PLAG(k) is negative, leaf area (PLA(k)) and leaf area index (LAI(k)) at time k are correspondingly reduced.

$$PLA(k) = PLA(k-1) + PLAG(k)$$

$$LAI(k) = PLA(k)$$

PFC(k) is also starting to decline linearly with thermal time by a slope of 0.00215 per degree-day but bounded on the left by zero. PFP(k) is increasing monotonically. That is,

$$PFC(k) = PFC(k-1) - 0.00215 \cdot DTT(k)$$

$$PFP(k) = 1 - PFR(k) - PFL(k) - PFC(k)$$

As in ISTAGE 1, PFL(k) is adjusted in favor of PFR(k) whenever there is a water deficit or nitrogen deficiency.

Daily root growth (GRORT(k)), leaf growth (GROLF(k)), stem growth (GROSTM(k)), panicle growth (PAWT(k)), single panicle growth (PNWT(k)), root weight (RTWT(k)), leaf weight (LFWT(k)), stem weight (STMWT(k)), panicle weight (PPAWT(k)), single panicle weight (PERPAWT(k)), stover weight (STOVWT(k)), biomass (BIOMAS(k)), and total plant weight (PLTWT(k)) at time k are updated, as in ISTAGE 3. That is,

$$GRORT(k) = CARBO(k) \cdot PFR(k)$$

$$GROLF(k) = CARBO(k) \cdot PFL(k)$$

$$GROSTM(k) = CARBO(k) \cdot PFC(k)$$

$$PAWT(k) = CARBO(k) \cdot PFP(k)$$

$$PNWT(k) = 0.00095 \cdot DTT(k)$$

$$RTWT(k) = RTWT(k-1) + GRORT(k)$$

$$LFWT(k) = LFWT(k-1) + GROLF(k)$$

$$STMWT(k) = STMWT(k-1) + GROSTM(k)$$

$$PPAWT(k) = PPAWT(k-1) + PAWT(k)$$

$$PERPAWT(k) = PERPAWT(k-1) + PNWT(k)$$

$$STOVWT(k) = LFWT(k) + STMWT(k)$$

$$BIOMAS(k) = LFWT(k) + STMWT(k) + PPAWT(k)$$

$$PLTWT(k) = BIOMAS(k) + RTWT(k)$$

Beginning at this stage until maturity, the leaves stop growing, that is,

$$TI(k) = 0.$$

**End of Grain Filling Stage (ISTAGE 5)**

The end of grain filling stage covers the period of grain filling. The duration, in degree-days, is 95 percent of the genetic coefficient P5.

This stage is characterized by grain growth, leaf senescence, and the rate of root growth being equal to the rate of root senescence. The latter event is represented as

$$PFR(k)=0.$$

During this stage, there is a translocation of assimilates from both the leaves and the stem to the panicles where the grains are growing. PFL(k) and PFC(k) continue to decrease as a function of thermal time while PFP(k) continues to increase. The translocation from both the leaves and the stem trigger an equivalent amount of senescence in those organs as will be demonstrated by the reduction of their respective weights.

$$PFL(k) = PFL(k-1) - 0.7 \cdot 0.0009 \cdot DTT(k)$$

$$PFC(k) = PFC(k-1) - 0.3 \cdot 0.0009 \cdot DTT(k)$$

$$PFP(k) = PFP(k-1) + 0.0009 \cdot DTT(k)$$

Daily root growth (GRORT(k)), leaf growth (GROLF(k)), stem growth (GROSTM(k)), panicle growth (PAWT(k)), single panicle growth (PNWT(k)), root weight (RTWT(k)), leaf weight (LFWT(k)), stem weight (STMWT(k)), panicle weight (PPAWT(k)), single panicle weight (PERPAWT(k)), stover weight (STOVWT(k)), biomass (BIOMAS(k)), and total plant weight (PLTWT(k)) at time k are updated, as in ISTAGE 4. That is,

$$GRORT(k) = CARBO(k) \cdot PFR(k)$$

$$GROLF(k) = CARBO(k) \cdot PFL(k)$$

$$GROSTM(k) = CARBO(k) \cdot PFC(k)$$

$$PAWT(k) = CARBO(k) \cdot PFP(k)$$

$$PNWT(k) = 0.00095 \cdot DTT(k)$$

$$RTWT(k) = RTWT(k-1) + GRORT(k)$$

$$LFWT(k) = LFWT(k-1) + GROLF(k)$$

$$STMWT(k) = STMWT(k-1) + GROSTM(k)$$

$$PPAWT(k) = PPAWT(k-1) + PAWT(k)$$

$$PERPAWT(k) = PERPAWT(k-1) + PNWT(k)$$

$$STOVWT(k) = LFWT(k) + STMWT(k)$$

$$BIOMAS(k) = LFWT(k) + STMWT(k) + PPAWT(k)$$

$$PLTWT(k) = BIOMAS(k) + RTWT(k)$$

A single grain-growth concept is introduced during this stage. The rate of grain growth is a linear function of thermal time with a slope of 0.000083 per degree-day. This single grain size will be used to estimate the number of grains $m^{-2}$ during harvest. Grain growth at time k (GROGRN(k)) and grain weight at time k (GRNWT(k)) are calculated as follows:

$$GROGRN(k) = 0.000083 \cdot DTT(k)$$

$$GRNWT(k) = GRNWT(k-1) + GROGRN(k)$$

During this growth stage, the nitrogen concentration in the panicle and grain are estimated. The estimation process is part

of the nitrogen transformation and uptake, which are outlined by Jones et al. (1986).

**Physiological Maturity Stage (ISTAGE 6)**

The duration of physiological maturity is the time required to complete P5 or when DTT(k) is less than or equal to zero. The latter condition allows for maturity even with insufficient thermal time accumulation due to low temperatures. When P5 is completed, the grains are harvested. At harvest time, $k = k_h$.

Panicle number $m^{-2}$ at harvest ($PNO(k_h)$) is calculated from the total plant panicle weight ($PPAWT(k_h)$) divided by the weight of one panicle ($PERPAWT(k_h)$).

$$PNO(k_h) = \frac{PPAWT(k_h)}{PERPAWT(k_h)}$$

Grain number $m^{-2}$ at harvest ($GRAIN(k_h)$) is calculated from 90 percent of $PPAWT(k_h)$, divided by a single grain weight in g per grain ($GRNWT(k_h)$), and multiplied by the percentage of grain filling (FERTILE).

$$GRAIN(k_h) = \frac{PPAWT(k_h) \cdot 0.9}{GRNWT(k_h)} \cdot FERTILE$$

The total weight of straw at harvest ($PSTRAW(k_h)$) is the sum of the total stover weight ($STOVWT(k_h)$) and 10 percent of the panicle weight ($PPAWT(k_h)$).

$$PSTRAW(k_h) = STOVWT(k_h) + (PPAWT(k_h) \cdot 0.1)$$

Panicle-straw ratio at harvest ($PSRATIO(k_h)$) is the ratio of the total panicle weight to the total straw.

$$PSRATIO(k_h) = \frac{PPAWT(k_h)}{PSTRAW(k_h)}$$

Dry grain yield ($DYIELD(k_h)$) is calculated as the product of the grain number ($GRAIN(k_h)$) and single grain weight ($GRNWT(k_h)$), adjusted to t $ha^{-1}$ by multiplying with 0.01.

$$DYIELD(k_h) = GRAIN(k_h) \cdot GRNWT(k_h) \cdot 0.01$$

Commercial grain ($YIELD(k_h)$) is dry grain yield adjusted to 14 percent moisture.

$$YIELD(k_h) = \frac{DYIELD(k_h)}{0.86}$$

## CHAPTER VI. THE ANALYTICAL STRUCTURE OF THE MULTICRITERIA OPTIMIZATION PROCEDURE

The multicriteria optimization procedure is a two-objective function resource-allocation technique. It uses the Monte Carlo search method to explore the space of decision variables, $\bar{u}(k)$, for feasibility. While the Pareto optimization procedure is conducted to identify a set of optimal, noninferior solutions, the ideal vector of objective functions is also generated. From the set of Pareto optimal solutions, the min-max optimization procedure is used to identify the best compromise solution considering the two criteria simultaneously and on equal terms of importance.

The general analytical structure of the algorithms of the Monte Carlo search method, the generation of the ideal vector, the Pareto optimization, and the min-max optimization used here were developed by A. Osyczka (1984). The analytical structures were modified, when necessary, to incorporate the simulation model and to fit the peculiar structure of the problem. Hence, the definitions and the basic structure of the equations were taken from Osyczka's book.

The multicriteria optimization problem is formulated as follows: find a vector of input decision variables, $\bar{u}(k)$, which satisfies constraints and optimizes a vector of objective functions, $\bar{f}(\bar{u})$. That is,

Find $\bar{u}^*$ such that

$$\bar{f}(\bar{u}^*) = \text{opt } \bar{f}(\bar{u}) \tag{6.1}$$

subject to:

$$g_m(\bar{u}) \geq 0 \qquad m = 1,2, \ldots, M \tag{6.2}$$

where $\bar{u}(k) = [u_1(k),\ldots,u_n(k)]^T$ is a vector of decision variables defined in n-dimensional Euclidean space of variables $E^n$, where $n = 3$. The three decision variables are: $u_1(k)$ = day of the year for planting; $u_2(k)$ = amount of nitrogen fertilizer, in kg N $ha^{-1}$; and, $u_3(k)$ = plant population, in plants $m^{-2}$. All three decision variables are input signals of the Kronecker delta sequence at $k = 0$. Hence, $\bar{u}(k)$ is $\bar{u}(0)$ at $k = 0$. The vector $\bar{u}(0)$ will be hereinafter represented as $\bar{u}$, $u_1(k)$ will be

written as $u_1$, $u_2(k)$ as $u_2$, and $u_3(k)$ as $u_3$. The variable k will be redefined as will be seen next. $\bar{f}(\bar{u})=[f_1(\bar{u}),\ldots,f_k(\bar{u})]^T$ is a vector function defined in k-dimensional Euclidean space of objectives $E^k$, where k = 2, and which are nonlinear functions of the variables $u_1$, $u_2$, and $u_3$. This vector function represents the criteria that will be considered in the optimization. The two criteria or objective functions are to maximize profit ($f_1(\bar{u})$) and to minimize production risk ($f_2(\bar{u})$) as a function of $\bar{u}$.

The inequality constraints $g_m(\bar{u})$ given by equation (6.2) define the feasible region U and represent the restriction imposed on the decision variables, $\bar{u}$. $g_m(\bar{u})$ are linear and nonlinear functions of the variables $u_1$, $u_2$, and $u_3$. Any point $\bar{u} \in U$ defines a feasible solution, and the vector function $\bar{f}(\bar{u})$ maps the set U in the set F, which represents all possible values of the objective functions.

The optimal solution (or set of optimal solutions) is denoted by $\bar{u}^*$. I = [1,2] is used to denote the set of indices for the two objective functions; i will be used as a generic index for any variable.

### The Monte Carlo Search Method

The Monte Carlo search method is an exploratory method used to randomly generate new values of the vector $\bar{u}$ by using the formula (Osyczka 1984:70-71):

$$u_i = u_i^a + \alpha_i(u_i^b - u_i^a) \qquad \text{for } i = 1,2,3 \tag{6.3}$$

where $u_i^a$ is the given lower limit for $u_i$, $u_i^b$ is the given upper limit for $u_i$, and $\alpha_i$ is a random number between zero and one. If $\lambda^a$ points of decision variables are desired to be evaluated, then the optimization procedure will generate $\lambda^a$ random numbers, one random number for each point. Equation (6.3) is used to obtain a new value of the decision variable $u_i$. Each generated point will be tested for constraint violation and discarded if it is not a feasible solution. If the point is in the feasible region, the simulation and optimization will proceed.

The random number generator is taken from the weather generator component of the CERES crop models.

### Pareto Optimization

As Osyczka (1984) presented it, Pareto optimization is based on the contact theorem which says that given a negative cone in $E^k$ which is the set

$$C^- = \{\bar{f} \in E^k \mid \bar{f} \leq 0\},$$

a vector $\bar{f}$ is a Pareto optimal solution for the multicriteria optimization problem if and only if

$$(C^- + \bar{f}^*) \cap F = \{\bar{f}^*\}.$$

Then he defines a Pareto optimum as follows: a point $\bar{u}^* \in U$ is Pareto optimum if for every $\bar{u} \in U$ either,

$$\bigwedge_{i \in I} (f_i(\bar{u}) = f_i(\bar{u}^*)) \tag{6.4}$$

or, there is at least one $i \in I$ such that

$$f_i(\bar{u}) > f_i(\bar{u}^*). \tag{6.5}$$

To demonstrate the Pareto optimization concept, Osyczka's illustration is presented for $n = 3$ and $k = 2$ (1984:66). Consider two solutions $\bar{u}^{(1)}$ and $\bar{u}^{(2)}$ for which there may be two specific cases

$$(1) \quad (C^- + \bar{f}(\bar{u}^{(1)})) \subset (C^- + \bar{f}(\bar{u}^{(2)})) \tag{6.6}$$

$$(2) \quad (C^- + \bar{f}(\bar{u}^{(1)})) \supset (C^- + \bar{f}(\bar{u}^{(2)})) \tag{6.7}$$

The following are defined:

$\bar{u}^{(\lambda)} = [u_1^{(\lambda)}, u_2^{(\lambda)}, u_3^{(\lambda)}]^T$ = any given point in U,

$\bar{f}(\bar{u}^{(\lambda)}) = [f(\bar{u}_1^{(\lambda)}), f(\bar{u}_2^{(\lambda)})]^T$ = vector of two objective functions for the point $\bar{u}^{(\lambda)}$

$\bar{u}_j^p = [u_{1j}^p, u_{2j}^p, u_{3j}^p]^T$ = the jth Pareto optimal solution,

$\bar{f}_j^p = [f_{1j}^p, f_{2j}^p]^T$ = vector of objective functions for the jth Pareto optimal solution.

The problem is to choose from any given set of solutions $\Lambda = \{1,2,\ldots,\lambda,\ldots,\lambda^a\}$, the set of Pareto optimal solutions

$J = \{1,2,\ldots,j,\ldots,j^a\}$.

Let $\bar{u}^{(\lambda)}$ be a vector of new solution to be considered. If in the set of Pareto optimal solutions there is a solution $\bar{u}_j{}^p$ such that it

1. satisfies equation (6.6) then $\bar{u}^{(\lambda)}$ is substituted for $\bar{u}_j{}^p$, or
2. satisfies equation (6.7) then $\bar{u}^{(\lambda)}$ is discarded.

If none of the solutions from the set of Pareto optimal solutions satisfies either equations (6.6) or (6.7), then $\bar{u}^{(\lambda)}$ becomes a new Pareto optimal solution.

This intuitively means that the point $\bar{u}^*$ is chosen as the optimum if no criterion can be improved without worsening the other criterion. A set of these optimal, noninferior solutions is generated to form a Pareto optimal curve.

**Min-max Optimization**

Min-max optimization uses the information of the optimum values of each objective function when solved separately. These values form the ideal vector of objective functions. The vector of objective functions for each point in the Pareto optimal curve is compared with the ideal vector. Relative deviations are calculated and the best solution is the one whose objective functions are as close as possible to their separately attainable minima.

Following Osyczka's outline (1984:32-33), the min-max optimization concept is presented as follows:

Consider the ith objective function for which the relative deviation can be calculated from the following methods:

$$z_i'(\bar{u}) = \frac{\left| f_i(\bar{u}) - f_i^0 \right|}{\left| f_i^0 \right|} \tag{6.8}$$

$$z_i''(\bar{u}) = \frac{\left| f_i(\bar{u}) - f_i^0 \right|}{\left| f_i(\bar{u}) \right|} \tag{6.9}$$

For equations (6.8) and (6.9) to be valid we have to assume that for every $i \in I$ and for every $\bar{u} \in U$, $f_i{}^0 \neq 0$ and $f_i(\bar{u}) \neq 0$.

Let $\bar{z}(\bar{u}) = [z_1(\bar{u}), z_2(\bar{u})]^T$ be a vector of relative increments which are defined in $E^2$. The components of the vector $\bar{z}(\bar{u})$ will be evaluated from the formula

$$\bigwedge_{i \in I} (z_i(\bar{u}) = \max(z_i'(\bar{u}), z_i''(\bar{u}))) \tag{6.10}$$

Then the min-max optimum is defined as follows:

A point $\bar{u}^* \in U$ is min-max optimal, if for every $\bar{u} \in U$ the following recurrence formula (6.11) is satisfied:

Step 1

$$\nu_1(\bar{u}^*) = \min_{u \in U} \max_{i \in I} (z_i(\bar{u}))$$

and then $I_1 = \{i_1\}$, where $i_1$ is the index for which the value of $z_i(\bar{u})$ is maximal.

If there is a set of solutions $U_1 \subset U$ which satisfies Step 1, then

Step 2

$$\nu_2(\bar{u}^*) = \min_{u \in U_1} \max_{\substack{i \in I \\ i \notin I_1}} (z_i(\bar{u}))$$

and then $I_2 = \{i_1, i_2\}$, where $i_2$ is the index for which the value of $z_i(\bar{u})$ in this step is maximal. _____ (6.11)

**Function Minimization**

For the sake of convenience, all the objective functions will be minimized, so the first objective function, to maximize profit, will be converted into a form which will allow for its minimization. This is done by employing the identity

$$\max f_1(\bar{u}) = \min(-f_1(\bar{u})) \tag{6.12}$$

Now, the first objective function is to minimize the negative function of profit.

In the same way, the inequality constraints of the form

$$g_m(\bar{u}) \leq 0 \qquad m = 1,2,\ldots,M$$

can be multiplied with -1 to convert them to the form

$$-g_m(\bar{u}) \geq 0 \qquad m = 1,2,\ldots,M$$

if necessary.

**The Analytical Representation of the Objective Functions**

The purpose of SMOT is to predict grain yield and correspondingly estimate profit and production risk, under a highly stochastic agricultural environment. Profit will be calculated from the expected value of grain yield, which is its mean. Production risk will be quantitatively expressed through a measure of the dispersion or variability from the mean, known as the standard deviation. The probability that a grain yield of one cropping season is within ± 1 standard deviation is 0.682. To illustrate the concept, an example is presented. Suppose a certain production strategy is expected to yield 5 t $ha^{-1}$ of grain with a standard deviation of ± 0.5 t $ha^{-1}$. The probability that the actual yield will be from 4.5 to 5.5 t $ha^{-1}$ (± 1 standard deviation) is 0.682. That is, for every 100 trials, 68 of those trials will yield between 4.5 and 5.5 t $ha^{-1}$. Compare this data with a second production strategy which is expected to yield 6 t $ha^{-1}$ with a standard deviation of ± 2.0 t $ha^{-1}$, and which is likely more costly. The probability of the actual yield being within the ± 1 standard deviation is still 0.682. However, the actual yield could be from 4 to 8 t $ha^{-1}$. The first production strategy has a smaller dispersion or variability (± 0.5 t $ha^{-1}$) compared to the second production strategy which has a wider dispersion or variability (± 2.0 t $ha^{-1}$). Thus, a larger value of the standard deviation corresponds to a more risky operation.

The probability distribution of the occurrence of grain yield must be known in order to find the maximum likelihood estimators of its mean and standard deviation. A goodness-of-fit test with two parameters (mean and variance) unknown, as outlined by Larsen and Marx (1981), was used to test the hypothesis ($H_0$) that rice grain yield can be described by a normal probability distribution with mean, $\mu$, and variance, $\sigma^2$.

Since there was no available actual yield data for a period long enough to be useful in the goodness-of-fit test, the simulation model was run for 25 years using actual weather conditions. The simulated grain-yield data were used in the goodness-of-fit test. The hypothesis testing showed that grain yield (y) is normally distributed, that is,

$$y_1, y_2, \ldots, y_{NCYCLE}$$

has $N(\mu, \sigma^2)$ distribution, where NCYCLE is the sample size. This probability distribution is described as follows:

$$p_Y(y) = \frac{1}{\sqrt{2\pi}\,\sigma} e^{-(\frac{1}{2})[(y-\mu)/\sigma]^2}, \qquad 0 < y < \infty \tag{6.13}$$

The maximum likelihood estimators for the mean, $\mu$, and variance, $\sigma^2$, are $\hat{\mu}$ and $\hat{\sigma}^2$, respectively (Larsen and Marx 1981:269-271):

$$\hat{\mu} = \frac{1}{NCYCLE} \sum_{i=1}^{NCYCLE} y_i \tag{6.14}$$

$$\hat{\sigma}^2 = \frac{1}{NCYCLE} \sum_{i=1}^{NCYCLE} (y_i - \hat{\mu})^2 \tag{6.15}$$

Larsen and Marx indicated that $\hat{\mu}$, the maximum likelihood estimator for $\mu$, is unbiased, efficient, and consistent. If $\sigma^2$ is known, $\hat{\mu}$ is sufficient. However, while $\hat{\sigma}^2$, the maximum likelihood estimator for $\sigma^2$, is consistent, and sufficient if $\mu$ is known, the estimator is biased; specifically, it tends to underestimate $\sigma^2$.

In practice, $\sigma^2$ is estimated by the sample variance, $s^2$, which can be expressed as follows:

$$s^2 = \frac{NCYCLE \cdot \sum_{i=1}^{NCYCLE} y_i^2 - (\sum_{i=1}^{NCYCLE} y_i)^2}{NCYCLE\ (NCYCLE - 1)} \tag{6.16}$$

Therefore, profit ($f_1(\bar{u})$) and risk ($f_2(\bar{u})$) is mathematically represented as follows:

$$f_1(\bar{u}) = PRICE \cdot \hat{\mu} - TOTAL\ COST \tag{6.17}$$

$$f_2(\bar{u}) = s \tag{6.18}$$

where

PRICE = market price of grain per ton (\$ $t^{-1}$),
TOTAL COST = total cost of production per hectare (\$ $ha^{-1}$)
s = standard deviation which measures variability from the mean yield (t $ha^{-1}$)

## The Economic Scenario of the Rice Farm

For an application of SMOT, the economic scenario is patterned after a rice farm in Laguna, Philippines, except that the dollar (\$) sign is used in the monetary value instead of the

Philippine peso sign. The farm could be briefly outlined as follows (Capule and Herdt 1983):

- the farmer is renting the land at \$699 $ha^{-1}$;
- land preparation, \$200 $ha^{-1}$;
- cost of seeds, \$80 $ha^{-1}$;
- hired labor for land preparation and weed control, \$606 $ha^{-1}$;
- complete pest (except weeds) control, \$133 $ha^{-1}$;
- weed control, \$385 $ha^{-1}$;
- cost of maintenance, \$156 $ha^{-1}$;
- opportunity cost of owned capital, \$215 $ha^{-1}$;
- imputed value of family labor, \$221 $ha^{-1}$;
- cost of nitrogen fertilizer, \$70 per 50 kg bag;
- no irrigation;
- hired labor for harvesting, \$148 $t^{-1}$;
- the farmer has at most \$1400 $ha^{-1}$ to spend for fertilizer;
- effective farm price of grain, \$1020 $t^{-1}$;
- the allowable limit of fertilizer is 900 kg nitrogen as urea in 1 ha of land area.

# CHAPTER VII. THE ALGORITHM OF THE SIMULATION-MULTICRITERIA OPTIMIZATION TECHNIQUE

The algorithm of SMOT has nine modules: the initialization module, the Monte Carlo search module, the constraint function module, the simulation module, the objective function module, the ideal vector module, the Pareto optimization module, the min-max optimization module, and the print module. Each module is made up of one or more subroutines.

The general algorithm of SMOT is outlined as follows:

A. Initialization Module

1. Set IPAR = 1, IWRITE = 1
2. Read n, $\lambda^a$, IPARCRV, NCYCLE, $u_1^a$, $u_1^b$, $u_2^a$, $u_2^b$, $u_3^a$, $u_3^b$ from subroutine LIMITS.
3. Set k = 2, $j^a = 1$, $f_i^0 = \infty$ and $f_{i1}^p = \infty$ for i = 1,2
4. Set $\lambda = 1$
5. If IWRITE = 1, read the initial values of the decision variables $\bar{u}^{(\lambda)}$, and other input data needed to run the CERES-Rice simulation model.

Do steps 6 through 15 for $\lambda = 1,2,\ldots,\lambda^a$

B. Simulation Module

6. Run the CERES-Rice simulation model NCYCLE times to generate the mean grain yield, $\hat{\mu}$.

C. Objective Function Module

7. Calculate $f_i(\bar{u}^{(\lambda)})$ for i = 1,2
8. Print $\lambda$, $\bar{u}^{(\lambda)}$, $\hat{\mu}$, $f_i(\bar{u}^{(\lambda)})$ for i = 1,2
9. Set IWRITE = 0

D. Ideal Vector Module

10. Replace $f_i^0$ by $f_i(\bar{u}^{(\lambda)})$ for every i for which $f_i(\bar{u}^{(\lambda)}) < f_i^0$.

E. Pareto Optimization Module

11. Call subroutine PARETO to check if the point $\bar{u}^{(\lambda)}$ is Pareto optimum.

12. If $\lambda < \lambda^a$ then $\lambda = \lambda + 1$ and go to 13, otherwise go to 16.

F. Monte Carlo Search Module

13. Call subroutine RANDOM to generate new values for $u_2^{(\lambda)}$ and $u_3^{(\lambda)}$.

G. Constraint Function Module

14. Check constraint functions for feasibility.

15. If the point $\bar{u}^{(\lambda)}$ is in the feasible region go to 6, otherwise go to 12.

Do step 16 for $j = 1,2,\ldots,j^a$

H. Min-max Optimization Module

16. Call subroutine MINMAX to check if the point $\bar{u}_j^P$ is the min-max optimum.

I. Print Module

17. Print $\bar{u}_j^P$ and $\bar{f}_j^P$ for $j = 1,2,\ldots,j^a$ and $\bar{u}^*$, $\lambda^*$, $\bar{f}(\bar{u}^*)$, $\bar{z}(\bar{u}^*)$.

Do steps 18,19 if IPARCRV > 1.

18. If IPAR < IPARCRV then IPAR = IPAR+1 and go to 19, otherwise end.

19. Call subroutine RANDOM to generate a new value for $u_1^{(\lambda)}$. Go to 3.

The algorithm of subroutine PARETO is as follows:

1. Read k, n, $j^a$, $\bar{u}^{(\lambda)}$, $\bar{f}(\bar{u}^{(\lambda)})$, and $\hat{\mu}$.

2. Set $j = 1$
3. If for every $i \in I$ we have $f_i(\bar{u}^{(\lambda)}) < f_{ij}^p$ then substitute $\bar{u}_j^p = \bar{u}^{(\lambda)}$, $\bar{f}_j^p = \bar{f}(\bar{u}^{(\lambda)})$, and $\hat{\mu}_j^p = \hat{\mu}$, and go to 7, otherwise go to 4.
4. If for every $i \in I$ we have $f_i(\bar{u}^{(\lambda)}) > f_{ij}^p$ then go to 8, otherwise go to 5.
5. Set $j = j + 1$
6. If $j > j^a$ then $j^a = j^a + 1$ and $\bar{u}_{j^a}^p = \bar{u}^{(\lambda)}$, $\bar{f}_{j^a}^p = \bar{f}(\bar{u}^{(\lambda)})$, and $\hat{\mu}_j^p = \hat{\mu}$, and go to 8, otherwise go to 3.
7. If $j < j^a$ then $j = j + 1$, and go to 3.
8. Return

The algorithm of subroutine MINMAX is outlined as follows:

1. Read $k$, $n$, $j$, $j^a$, $\bar{f}^0$, $\bar{u}_j^p$, $\bar{f}_j^p$, and $\hat{\mu}_j^p$ for $j = 1,2,\ldots,j^a$
2. Evaluate the vector $\bar{z}(\bar{u}_j^p)$ using formula (6.10) (subroutine MAX).
3. If $\bar{z}(\bar{u}_j^p) = 0$, then retain this solution as the optimun since there is no better solution, and go to 5, otherwise go to 4.
4. Find the maximal values of all the steps of formula (6.11) for the point $\bar{u}_j^p$.
5. Return

The algorithm of subroutine RANDOM is as follows:

1. Read $u_1^a$, $u_1^b$, $u_2^a$, $u_2^b$, $u_3^a$, $u_3^b$
2. Generate random number $\alpha_i$ (subroutine RANDN).
3. Generate the point $\bar{u}^{(\lambda)}$ following formula (6.3).
4. Return

A flowchart of the SMOT algorithm is presented in Figure 7.1.

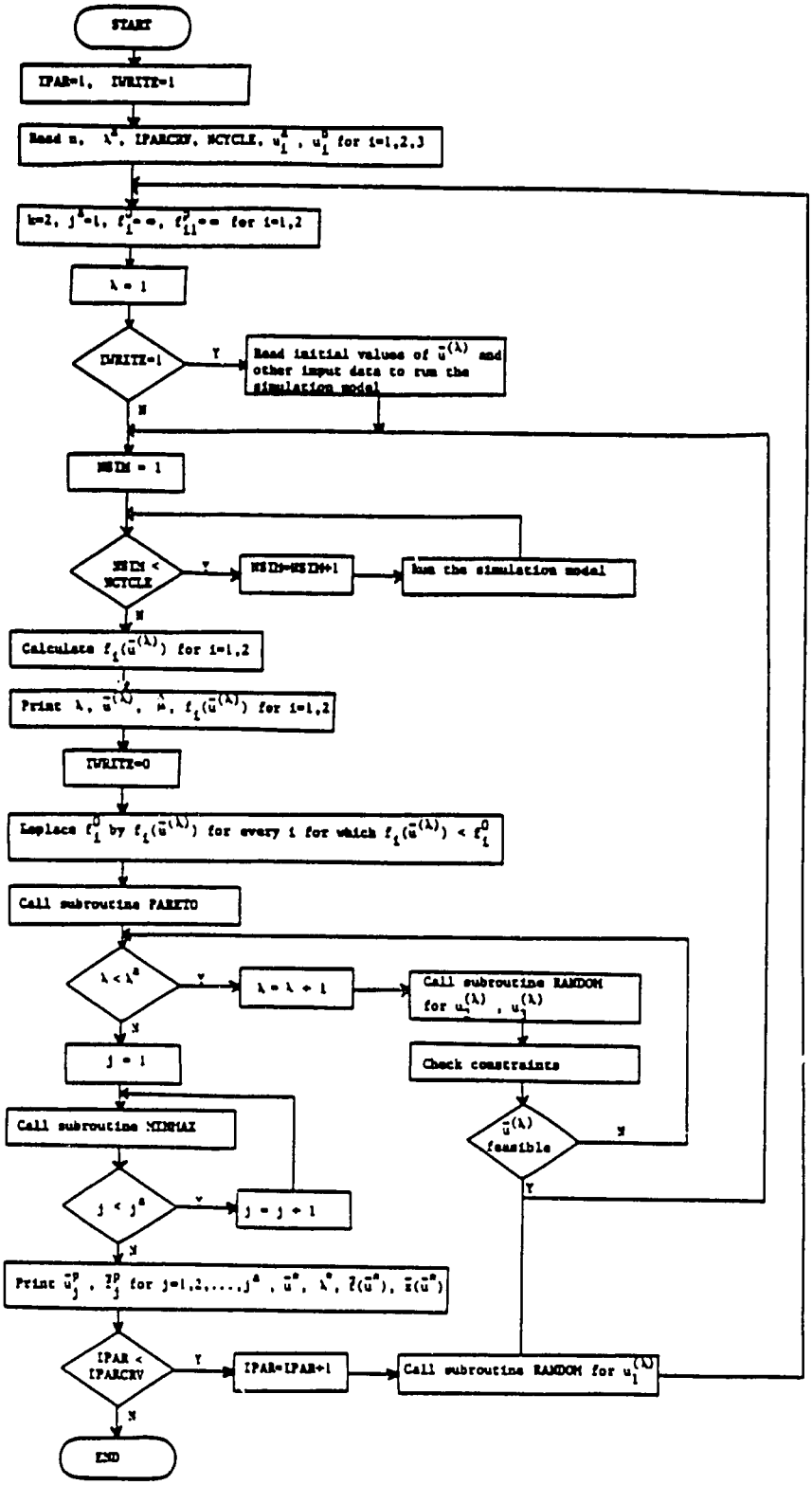


Figure 7.1. Flowchart of the simulation-multicriteria optimization technique (SMOT).

# CHAPTER VIII. DISCUSSION OF RESULTS

Two computer software packages have been developed as output of this research. These are the CERES-Rice simulation model and, with the model providing the foundation, the simulation-multicriteria optimization technique (SMOT). SMOT is a decision support system to evaluate profit and weather-related production risk for use by agricultural research scientists, extension workers, farmers, and policymakers involved in rice production under upland condition.

## The CERES-Rice Simulation Model

The CERES-Rice simulation model is a growth simulation model for upland conditions. It is designed to predict the growth components and yield of different rice varieties under the tropical and subtropical agroclimatic environments. The simulation model is programmed in Fortran 77 and set up to run interactively in any IBM-compatible microcomputer with at least 256 K bytes of random access memory (RAM). In an IBM-compatible microcomputer with 640 K bytes RAM, simulation time of one cropping season takes about 25 seconds. In the Hewlett Packard (HP) 9000 minicomputer system, the user time is between 9.3 to 9.9 seconds. For instructions on how to run the simulation model, a user documentation has been developed.

Model validation is based on observed field-measured data, whenever available, and on intuitive knowledge of experts, whenever data is lacking. The validation covers the phenology, growth and partitioning, leaf area index, and grain yield under water and nitrogen constraints.

Table 8.1 presents a comparison between the predicted (P, model) and the observed (O, field-measured) phenological occurrence, days after sowing (DAS), of three upland rice varieties, namely: "IR43," "UPLRI5," and "UPLRI7." The data were the result of a series of experiments for drought tolerance conducted at the upland experimental farm of IRRI, Los Baños, Philippines, during the period 1983-1984 (unpublished data obtained from IRRI). Actual weather data, collected from the site, were used in the simulation. Some of the soil parameters were estimated due to lack of information. The sowing dates were based on actual data. For each simulation, plant population was estimated to be 400 plants $m^{-2}$, and 60 kg N $ha^{-1}$ of fertilizer were applied as basal. The three phenological

Table 8.1. Comparison between predicted and observed phenological occurrence of three rice varieties, days after sowing (DAS).

| Variety Name | Sowing Date (1983) | Emergence P | Emergence O | Heading P | Heading O | Maturity P | Maturity O |
|---|---|---|---|---|---|---|---|
| "IR43" | May 26 | 4 | 8 | 99 | 97 | 128 | 125 |
| | Jun 30 | 4 | 6 | 96 | 99 | 127 | 134 |
| | Jul 8 | 4 | 4 | 97 | 99 | 128 | 127 |
| | Aug 4 | 4 | 4 | 95 | 100 | 127 | 123 |
| | Aug 28 | 4 | 4 | 94 | 100 | 127 | 127 |
| | Nov 10 | 4 | 6 | 98 | 93 | 129 | 134 |
| | (Average) | 4 | 5 | 97 | 98 | 127 | 128 |
| "UPLRI5" | Jun 20 | 4 | 4 | 98 | 95 | 121 | 119 |
| | Jun 30 | 4 | 6 | 98 | 92 | 120 | 116 |
| | Jul 8 | 4 | 4 | 97 | 95 | 120 | 120 |
| | Aug 4 | 4 | 4 | 94 | 100 | 118 | 123 |
| | Aug 28 | 4 | 4 | 93 | 93 | 117 | 116 |
| | Nov 10 | 4 | 6 | 96 | 91 | 119 | 125 |
| | (Average) | 4 | 5 | 96 | 94 | 119 | 120 |
| "UPLRI7" | May 26 | 4 | 8 | 92 | 91 | 119 | 116 |
| | Jun 20 | 4 | 4 | 89 | 88 | 117 | 112 |
| | Jun 30 | 4 | 6 | 88 | 91 | 116 | 116 |
| | Jul 8 | 4 | 4 | 88 | 89 | 117 | 119 |
| | Aug 4 | 4 | 4 | 86 | 99 | 115 | 123 |
| | Aug 28 | 4 | 4 | 84 | 93 | 115 | 116 |
| | (Average) | 4 | 5 | 88 | 92 | 117 | 117 |

events being compared are the time of emergence, heading, and physiological maturity. The comparison showed that from an average of six experiments, the predicted time of emergence was one day less than the observed for the three varieties. However, the predicted time of heading was one day earlier for "IR43," two days later for "UPLRI5," and four days earlier for "UPLRI7," compared with the observed data. The predicted occurrence for physiological maturity was only a day earlier than the observed for "IR43" and "UPLRI5" while about the same, on the average, for "UPLRI7."

A rice simulation model that is able to predict the phenological occurrence of the crop will provide good opportunities for a rice farmer to plan out and optimize the farm operations. Some farmers may want to apply fertilizer and/or irrigate just before heading. A good prediction on the physiological maturity will also allow the farmer to plan for harvesting and marketing. In the Philippines and other Asian countries where harvesting and marketing are done mostly by hand with the help of hired labor, advanced planning will ensure early contracts for hired labor and, hence, harvesting operation and marketing transportation may proceed on schedule. Other farmers may want to plant cash crops following rice to make use of the residual fertilizer and soil moisture. An evaluation of the maturity duration of the different varieties within the climatic area will give the farmer insight as to the kind of rice variety appropriate for the season in order to maximize the cropping pattern.

The next set of comparisons between predicted and observed rice growth is on variety "IR36." The data were from a Ph.D. dissertation by Chinchest (1981) on the effects of water regimes and amount of nitrogen on the growth of some selected rice varieties. The experiment was replicated four times and conducted at the IRRI experimental upland farm during the 1980 dry season. Actual weather data for the duration of the experiment, collected from the site, were used in the simulation run. Some of the soil parameters needed in the model were estimated. The simulation inputs include sowing date, plant population, fertilizer application, and irrigation levels, according to actual data.

Table 8.2 presents the result of the phenological comparison. The observed data were extracted from Chinchest's schematic diagram of phenology for five varieties. Model predictions regarding the time of occurrence for floral initiation and heading were a day earlier while the occcurrence for maturity was two days earlier compared to the observed time of occurrence.

Table 8.2. Comparison between predicted and observed phenological occurrence of "IR36" variety (Sowing Date: 9 January 1980).

| Phenological stage | Predicted Date | Observed Date |
|---|---|---|
| Floral Initiation | 27 February 1980 | 28 February 1980 |
| Heading or Flowering | 29 March 1980 | 30 March 1980 |
| Maturity | 26 April 1980 | 28 April 1980 |

Using more of Chinchest's experimental results, comparisons between the predicted output of the simulation model and the observed data were done on the growth components of "IR36" with four nitrogen treatments (0, 30, 60, and 120 kg N $ha^{-1}$) and two irrigation levels (about 810 and 795 mm of water). A biomass comparison, from four sampling dates on the four nitrogen treatments and irrigation of about 795 mm water, was conducted. The predicted and observed values are presented in Table 8.3. From an average of four sampling intervals, the comparison showed 12.6 percent, 18.1 percent, 21.2 percent, and 21.0 percent difference in biomass between the predicted and observed for 0, 30, 60, and 120 kg N $ha^{-1}$, respectively. The simulation model tends to underpredict biomass at all sampling intervals as demonstrated graphically in Figures 8.1, 8.2, 8.3, and 8.4 (0, 30, 60, and 120 kg N $ha^{-1}$, respectively).

Table 8.4 shows a comparison on the straw weight at harvest on the four fertilizer treatments and two irrigation levels, 810 mm (W1) and 795 mm (W2) of water. From an average of four nitrogen treatments, the difference in straw weight between predicted and observed is 3.1 percent for W1 and 4.7 percent for W2.

Table 8.5 is a rearrangement of the entries in Table 8.4 in order to demonstrate the effect of nitrogen treatments on the prediction of straw. It shows that the simulation model is able to predict consistently better at fertilizer treatments 0, 30, and 60 kg N $ha^{-1}$ (2.2, 2.7, and 3.8 percent difference, respectively) than at the 120 kg N $ha^{-1}$ treatment (7.0 percent difference).

Comparison between predicted and observed grain yield, at 14 percent moisture content, on the four nitrogen treatments (0, 30, 60, and 120 kg N $ha^{-1}$), and two irrigation levels (W1 and W2) is shown in Table 8.6. From an average of four nitrogen treatments, the difference in yield is 8.8 percent for W1 and 8.6 percent for W2.

Table 8.3. Predicted and observed biomass of "IR36" variety at four treatments of nitrogen fertilizer on four sampling intervals (795 mm water applied).

| Nitrogen Treatment (kg N $ha^{-1}$) | Sampling Interval (DAS) | Predicted ($g\ m^{-2}$) | Observed ($g\ m^{-2}$) | Percent Difference (%) |
|---|---|---|---|---|
| 0 | 57 | 202. | 228. | 11.4 |
| | 69 | 343. | 349. | 1.7 |
| | 89 | 604. | 829. | 27.1 |
| | 106 | 850. | 946. | 10.1 |
| (Average) | | | | (12.6) |
| 30 | 57 | 268. | 318. | 15.7 |
| | 69 | 427. | 501. | 14.8 |
| | 89 | 722. | 983. | 26.6 |
| | 106 | 1009. | 1192. | 15.3 |
| (Average) | | | | (18.1) |
| 60 | 57 | 319. | 366. | 12.8 |
| | 69 | 496. | 548. | 9.5 |
| | 89 | 821. | 1233. | 33.4 |
| | 106 | 1145. | 1614. | 29.1 |
| Average) | | | | (21.2) |
| 120 | 57 | 381. | 390. | 2.3 |
| | 69 | 589. | 793. | 25.7 |
| | 89 | 963. | 1302. | 26.0 |
| | 106 | 1342. | 1920. | 30.1 |
| (Average) | | | | (21.0) |

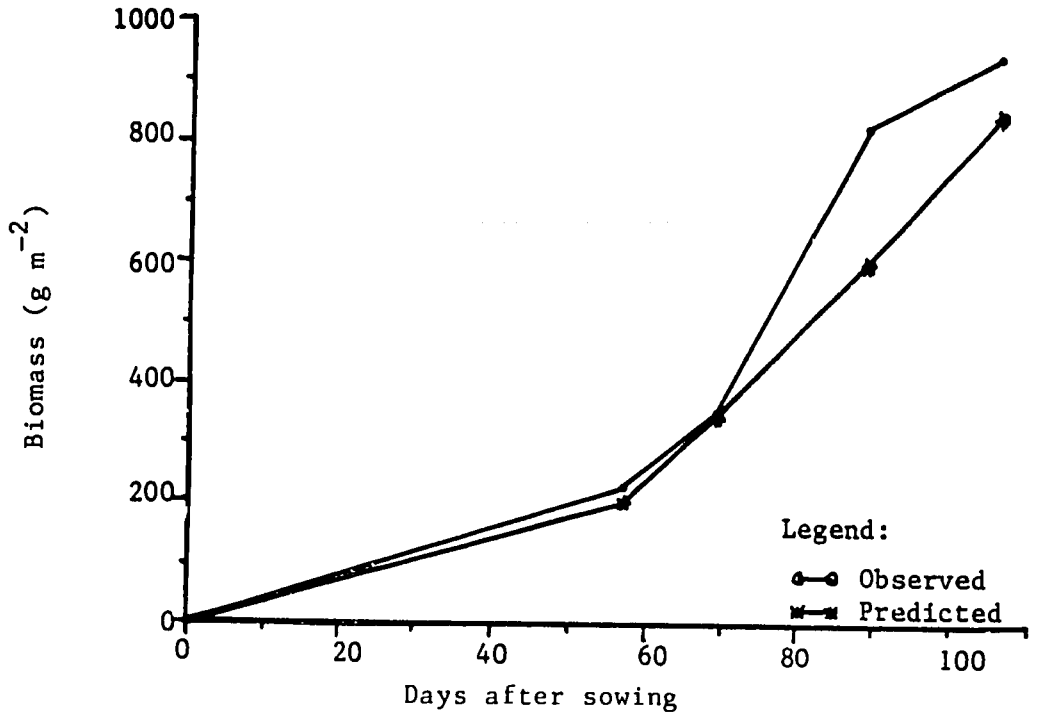


Figure 8.1. Comparison between predicted and observed biomass of "IR36" variety with 0 N.

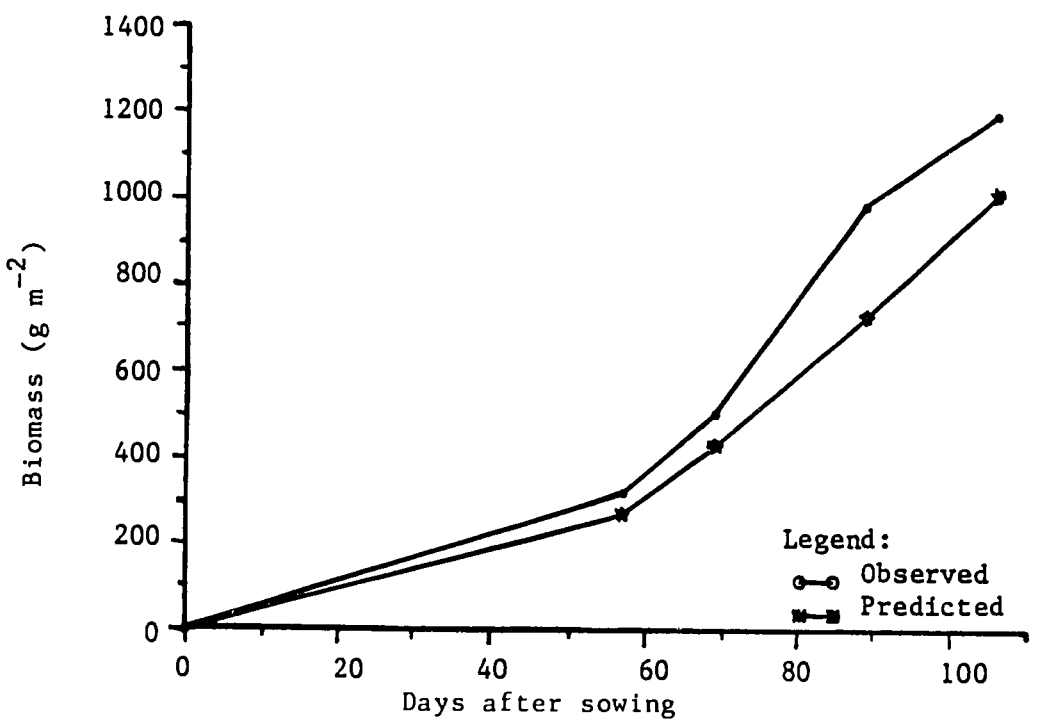


Figure 8.2. Comparison between predicted and observed biomass of "IR36" variety with 30 kg N ha$^{-1}$.

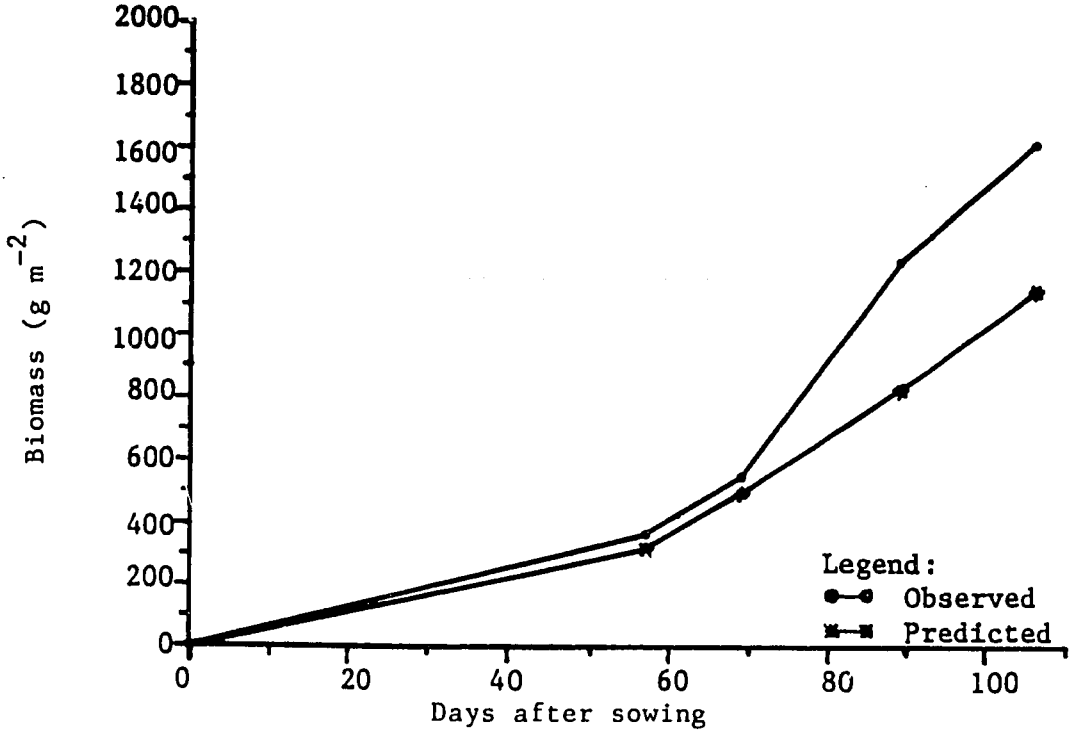


Figure 8.3. Comparison between predicted and observed biomass of "IR36" variety with 60 kg N ha$^{-1}$.

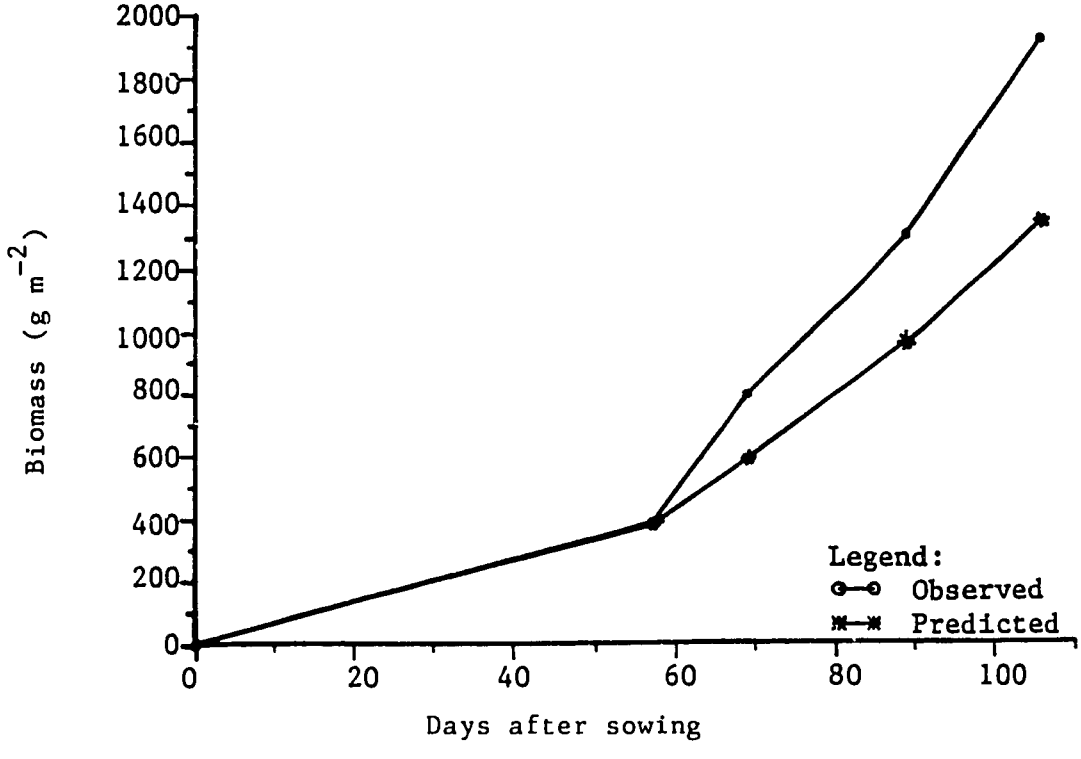


Figure 8.4. Comparison between predicted and observed biomass of "IR36" variety with 120 kg N ha$^{-1}$.

Table 8.4. Predicted and observed straw weight at harvest of "IR36" variety at two irrigation levels and four nitrogen treatments.

| Irrigation Level (mm) | Nitrogen Treatment (kg N $ha^{-1}$) | Predicted (g $m^{-2}$) | Observed (g $m^{-2}$) | Percent Difference (%) |
|---|---|---|---|---|
| 810 mm (W1) | 0 | 419. | 405. | 3.4 |
| | 30 | 512. | 523. | 2.1 |
| | 60 | 589. | 564. | 4.4 |
| | 120 | 700. | 683. | 2.5 |
| (Average) | | | | (3.1) |
| 795 mm (W2) | 0 | 416. | 420. | 1.0 |
| | 30 | 506. | 490. | 3.3 |
| | 60 | 581. | 600. | 3.2 |
| | 120 | 683. | 613. | 11.4 |
| (Average) | | | | (4.7) |

Table 8.5. Predicted and observed straw weight at harvest of "IR36" variety at four nitrogen treatments and two irrigation levels.

| Nitrogen Treatment (kg N $ha^{-1}$) | Irrigation Level (mm) | Predicted (g $m^{-2}$) | Observed (g $m^{-2}$) | Percent Difference (%) |
|---|---|---|---|---|
| 0 | 810 | 419. | 405. | 3.4 |
| | 795 | 416. | 420. | 1.0 |
| (Average) | | | | (2.2) |
| 30 | 810 | 512. | 523. | 2.1 |
| | 795 | 506. | 490. | 3.3 |
| (Average) | | | | (2.7) |
| 60 | 810 | 589. | 564. | 4.4 |
| | 795 | 581. | 600. | 3.2 |
| (Average) | | | | (3.8) |
| 120 | 810 | 700. | 683. | 2.5 |
| | 795 | 683. | 613. | 11.4 |
| (Average) | | | | (7.0) |

Table 8.6. Grain yield of "IR36" variety at two irrigation levels and four nitrogen treatments.

| Irrigation Level (mm) | Nitrogen Treatment (kg N $ha^{-1}$) | Predicted ($g\ m^{-2}$) | Observed ($g\ m^{-2}$) | Percent Difference (%) |
|---|---|---|---|---|
| 810 mm (W1) | 0 | 4.3 | 4.6 | 6.5 |
| | 30 | 5.0 | 5.6 | 10.7 |
| | 60 | 5.6 | 6.7 | 16.4 |
| | 120 | 6.6 | 6.7 | 1.5 |
| (Average) | | | | (8.8) |
| 795 mm (W2) | 0 | 4.3 | 4.6 | 6.5 |
| | 30 | 4.9 | 5.3 | 7.5 |
| | 60 | 5.5 | 6.9 | 20.3 |
| | 120 | 6.5 | 6.5 | 0.0 |
| (Average) | | | | (8.6) |

The entries of Table 8.6 were rearranged and presented in Table 8.7 in order to show the effect of nitrogen treatments on the prediction of yield. Table 8.7 shows that grain yield prediction is best at 120 kg N $ha^{-1}$ treatment (0.8 percent difference); prediction is poorest at 60 kg N $ha^{-1}$ treatment (18.4 percent difference).

The predicted leaf area index (LAI) on the four fertilizer treatments and 795 mm water irrigation for seven sampling dates is shown in Table 8.8. The graphical illustration of the LAI curve is shown in Figure 8.5.

To provide an approximate comparison, the observed LAI data of "IR36" sown on 6 November 1984 with 100 kg N $ha^{-1}$ in flooded condition at the IRRI experimental farm is presented in column six of Table 8.9 (unpublished data obtained from IRRI). The corresponding LAI curve is presented in Figure 8.6. The maximum observed LAI is 4.6 at 100 kg N $ha^{-1}$, while the maximum predicted LAI at 60 kg N $ha^{-1}$ is 4.9 (Table 8.8). Both maxima occurred 80 days after sowing.

To evaluate growth and partitioning, the predicted results of root weight, leaf weight, stem weight, and panicle weight of seven sampling dates on the four nitrogen treatments are presented in Tables 8.10, 8.11, 8.12, and 8.13 for 0, 30, 60, and 120 kg N $ha^{-1}$, respectively. For graphical illustration, the plant parts with 0 N and 120 kg N $ha^{-1}$ are shown in Figures 8.7 and 8.8, respectively.

Table 8.7. Grain yield of "IR36" variety at four nitrogen treatments and two irrigation levels.

| Nitrogen Treatment (kg N $ha^{-1}$) | Irrigation Level (mm) | Predicted ($g\ m^{-2}$) | Observed ($g\ m^{-2}$) | Percent Difference (%) |
|---|---|---|---|---|
| 0 | 810 | 4.3 | 4.6 | 6.5 |
| | 795 | 4.3 | 4.6 | 6.5 |
| (Average) | | | | (6.5) |
| 30 | 810 | 5.0 | 5.6 | 10.7 |
| | 795 | 4.9 | 5.3 | 7.5 |
| (Average) | | | | (9.1) |
| 60 | 810 | 5.6 | 6.7 | 16.4 |
| | 795 | 5.5 | 6.9 | 20.3 |
| (Average) | | | | (18.4) |
| 120 | 810 | 6.6 | 6.7 | 1.5 |
| | 795 | 6.5 | 6.5 | 0.0 |
| (Average) | | | | (0.8) |

Table 8.8. Predicted LAI of "IR36" variety on seven sampling intervals, days after sowing (DAS).

| DAS | 0 N | 30 kg N $ha^{-1}$ | 60 kg N $ha^{-1}$ | 120 kg N $ha^{-1}$ |
|---|---|---|---|---|
| 4 | 0. | 0. | 0. | 0. |
| 35 | 0.9 | 1.6 | 2.0 | 2.2 |
| 49 | 2.1 | 3.0 | 3.7 | 4.4 |
| 80 | 2.9 | 4.0 | 4.9 | 5.9 |
| 89 | 2.7 | 3.8 | 4.7 | 5.7 |
| 107 | 1.9 | 2.8 | 3.5 | 4.4 |
| 108 | 1.9 | 2.8 | 3.5 | 4.4 |

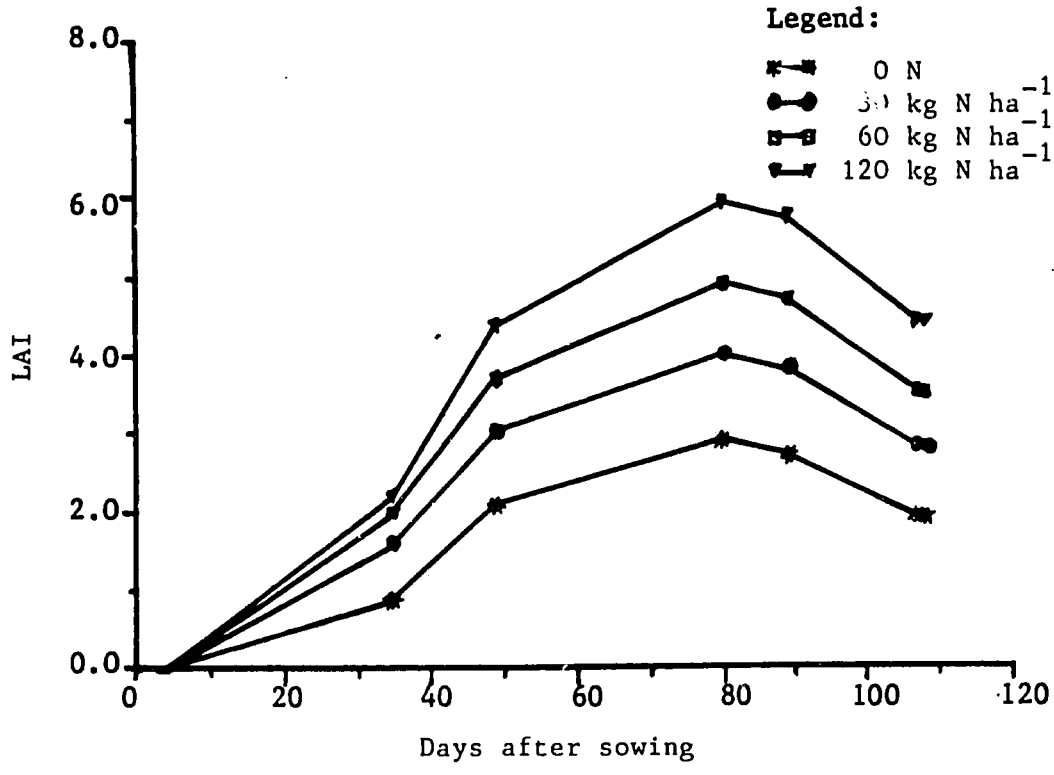


Figure 8.5. Leaf area index (LAI) of "IR36" variety with 0, 30, 60, and 120 kg N $ha^{-1}$.

Table 8.9. Root weight, leaf weight, stem weight, panicle weight, and LAI OF "IR36" variety on nine sampling intervals, days after sowing (Sown on 6 November 1984, with 100 kg N $ha^{-1}$ in flooded condition, IRRI, Philippines).

| DAS | Root Weight ($g\ m^{-2}$) | Leaf Weight ($g\ m^{-2}$) | Stem Weight ($g\ m^{-2}$) | Panicle Weight ($g\ m^{-2}$) | LAI |
|---|---|---|---|---|---|
| 30 | 4.0 | 4.8 | 3.6 | 0. | 0.1 |
| 40 | 9.8 | 11.4 | 9.4 | 0. | 0.3 |
| 50 | 19.8 | 44.2 | 34.3 | 9.8 | 1.2 |
| 60 | 53.5 | 107.6 | 94.7 | 25.5 | 2.9 |
| 70 | 82.0 | 173.3 | 214.3 | 46.9 | 4.3 |
| 80 | 73.0 | 195.7 | 341.0 | 60.9 | 4.6 |
| 90 | 93.1 | 193.4 | 537.9 | 82.4 | 4.6 |
| 100 | 99.7 | 178.5 | 302.9 | 591.4 | 3.7 |
| 110 | 105.3 | 162.3 | 242.0 | 652.6 | 3.4 |

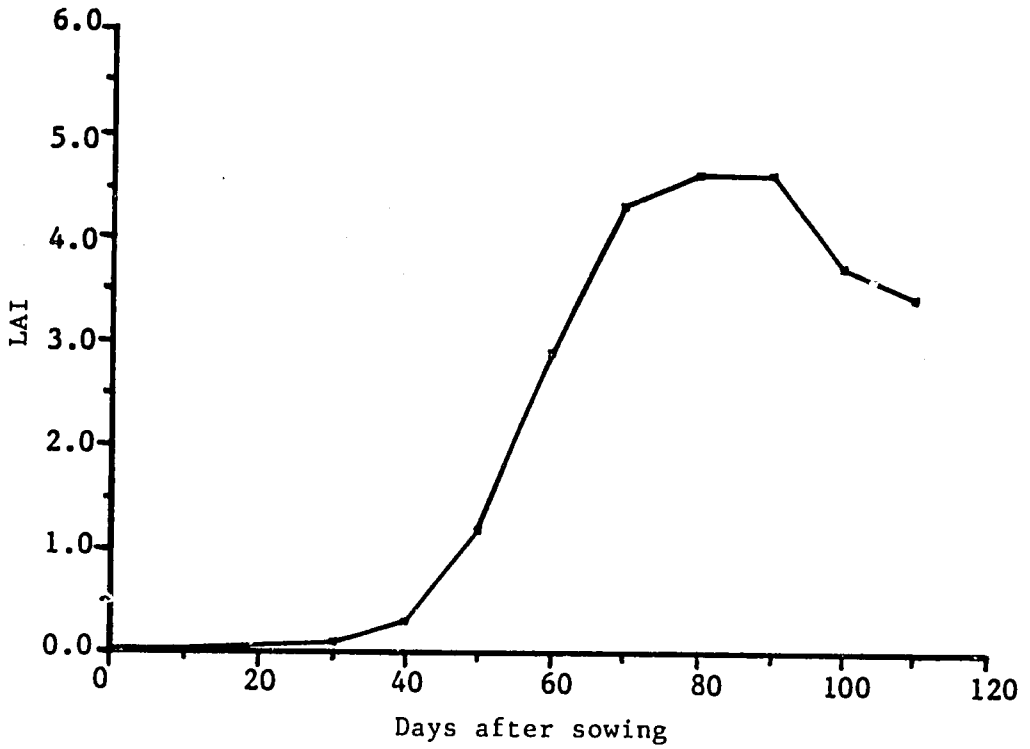


Figure 8.6. Observed LAI of "IR36" variety sown on 6 November 1984 in flooded condition with 100 kg N $ha^{-1}$.

Table 8.10. Predicted root weight, leaf weight, stem weight, and panicle weight of "IR36" variety on seven sampling intervals, days after sowing (DAS), with 0 kg N.

| DAS | Phenological Stage | Root Weight ($g\ m^{-2}$) | Leaf Weight ($g\ m^{-2}$) | Stem Weight ($g\ m^{-2}$) | Panicle Weight ($g\ m^{-2}$) |
|---|---|---|---|---|---|
| 4 | Emergence | 0.0 | 0.1 | 0.0 | 0.0 |
| 35 | End Juvenile Stage | 32.6 | 49.7 | 0.4 | 0.0 |
| 49 | Floral Initiation | 103.4 | 110.3 | 24.0 | 0.0 |
| 80 | Heading | 180.8 | 150.3 | 220.0 | 92.5 |
| 89 | Start Grain Fill | 187.6 | 144.3 | 291.7 | 168.4 |
| 107 | End Grain Fill | 171.4 | 92.7 | 274.2 | 491.0 |
| 108 | Physiological Maturity | 171.4 | 92.7 | 274.2 | 491.0 |

Table 8.11. Predicted root weight, leaf weight, stem weight, and panicle weight of "IR36" variety on seven sampling intervals, days after sowing (DAS), with 30 kg N $ha^{-1}$.

| DAS | Phenological Stage | Root Weight ($g\ m^{-2}$) | Leaf Weight ($g\ m^{-2}$) | Stem Weight ($g\ m^{-2}$) | Panicle Weight ($g\ m^{-2}$) |
|---|---|---|---|---|---|
| 4 | Emergence | 0.0 | 0.1 | 0.0 | 0.0 |
| 35 | End Juvenile Stage | 45.8 | 82.8 | 0.7 | 0.0 |
| 49 | Floral Initiation | 135.4 | 159.4 | 30.4 | 0.0 |
| 80 | Heading | 222.6 | 205.0 | 252.5 | 104.7 |
| 89 | Start Grain Fill | 229.9 | 197.9 | 333.3 | 190.4 |
| 107 | End Grain Fill | 210.1 | 136.7 | 312.8 | 568.2 |
| 108 | Physiological Maturity | 210.1 | 136.7 | 312.8 | 568.2 |

Table 8.12. Predicted root weight, leaf weight, stem weight, and panicle weight of "IR36" variety on seven sampling intervals, days after sowing (DAS), with 60 kg N $ha^{-1}$.

| DAS | Phenological Stage | Root Weight ($g\ m^{-2}$) | Leaf Weight ($g\ m^{-2}$) | Stem Weight ($g\ m^{-2}$) | Panicle Weight ($g\ m^{-2}$) |
|---|---|---|---|---|---|
| 4 | Emergence | 0.0 | 0.1 | 0.0 | 0.0 |
| 35 | End Juvenile Stage | 49.8 | 103.5 | 0.8 | 0.0 |
| 49 | Floral Initiation | 148.6 | 195.1 | 34.9 | 0.0 |
| 80 | Heading | 242.6 | 248.4 | 281.0 | 116.0 |
| 89 | Start Grain Fill | 251.1 | 240.1 | 370.1 | 210.6 |
| 107 | End Grain Fill | 229.5 | 170.0 | 346.9 | 638.9 |
| 108 | Physiological Maturity | 229.5 | 170.0 | 346.9 | 638.9 |

Table 8.13. Predicted root weight, leaf weight, stem weight, and panicle weight of "IR36" variety on seven sampling intervals, days after sowing (DAS), with 120 kg N $ha^{-1}$.

| DAS | Phenological Stage | Root Weight ($g\ m^{-2}$) | Leaf Weight ($g\ m^{-2}$) | Stem Weight ($g\ m^{-2}$) | Panicle Weight ($g\ m^{-2}$) |
|---|---|---|---|---|---|
| 4 | Emergence | 0.0 | 0.1 | 0.0 | 0.0 |
| 35 | End Juvenile Stage | 48.5 | 114.3 | 0.9 | 0.0 |
| 49 | Floral Initiation | 153.3 | 231.9 | 41.0 | 0.0 |
| 80 | Heading | 254.8 | 302.1 | 325.9 | 134.3 |
| 89 | Start Grain Fill | 266.2 | 291.5 | 428.7 | 243.2 |
| 107 | End Grain Fill | 243.2 | 207.7 | 400.9 | 746.8 |
| 108 | Physiological Maturity | 243.2 | 207.7 | 400.9 | 746.8 |

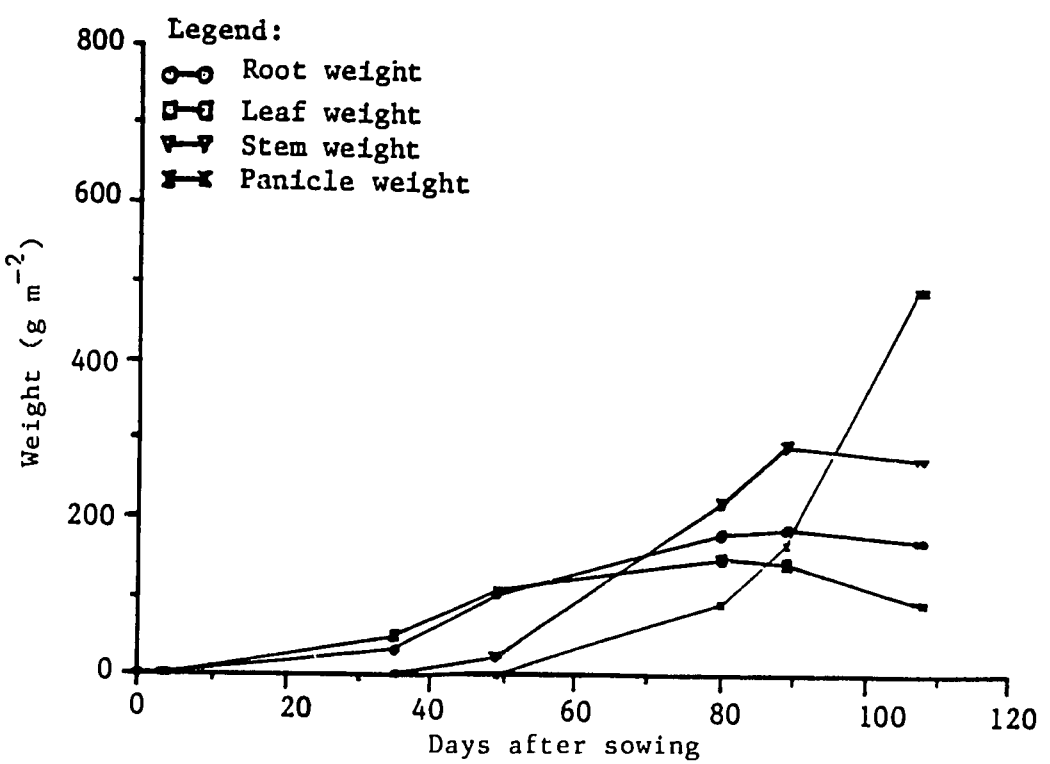


Figure 8.7. Predicted root weight, leaf weight, stem weight, and panicle weight of "IR36" variety with 0 N.

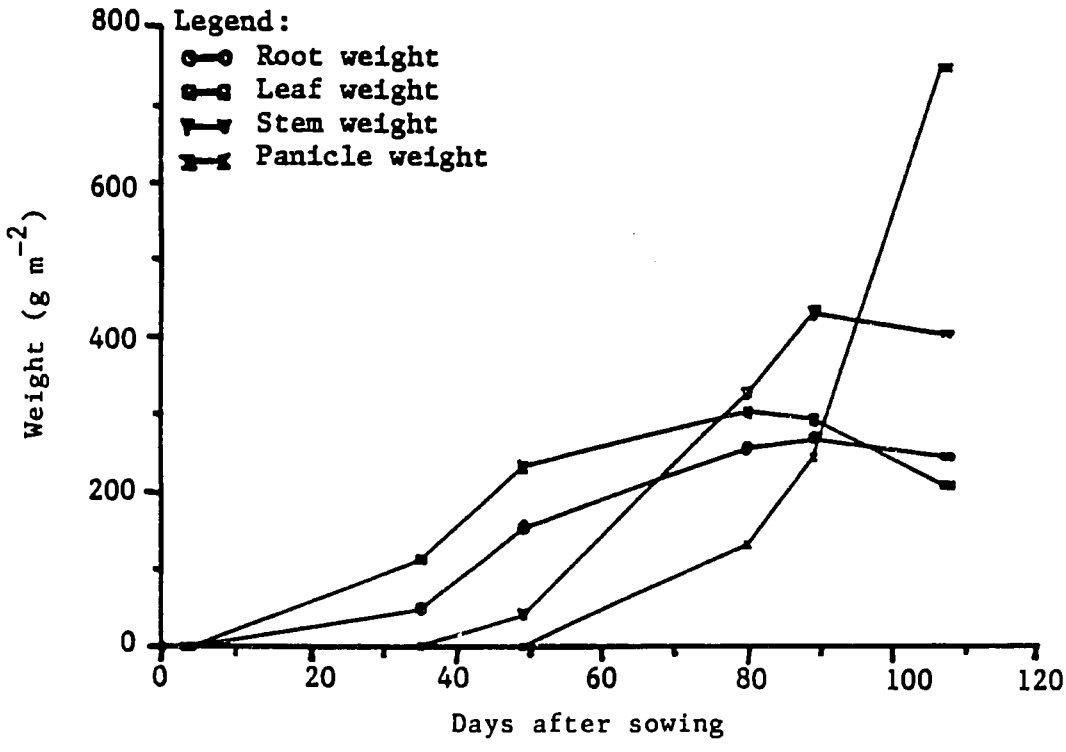


Figure 8.8. Predicted root weight, leaf weight, stem weight, and panicle weight of "IR36" variety with 120 kg N $ha^{-1}$.

For an approximate comparison, the observed data on root weight, leaf weight, stem weight, and panicle weight of "IR36" variety sown on 6 November 1984 in flooded conditions are presented in Table 8.9. Figure 8.9 illustrates graphically these plant parts.

The CERES-Rice simulation model will provide insights for rice physiologists and agronomists regarding the response mechanisms of the crop to various climates. It will also be useful in evaluating the economic farm plans. A more extensive discussion on the economics of rice production will be covered in the next section.

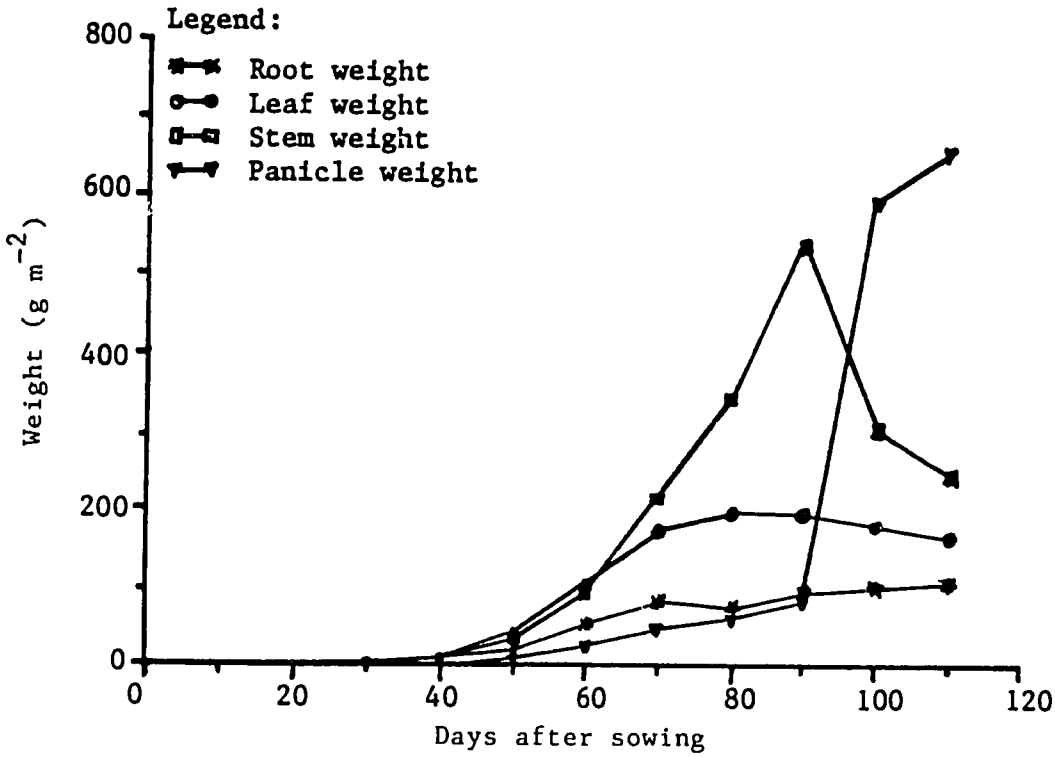


Figure 8.9. Observed plant parts of "IR36" variety sown on 6 November 1984 in flooded condition with 100 kg N $ha^{-1}$.

**The Simulation-Multicriteria Optimization Technique (SMOT)**

To demonstrate the capability of SMOT, it was implemented three times in a farm environment representative of the Philippines (refer to the section on The Economic Scenario of the Rice Farm). SMOT, however, can be reparameterized to fit the different agricultural environments in the tropics and subtropics. The first implementation had the following conditions: $u_1 = 171$ (20 June), $u_2$ and $u_3$ varying randomly; the second implementation had $u_1 = 171$ (20 June), $u_2$ varying randomly, and $u_3 = 400$ plants $m^{-2}$; and, the third implementation had $u_1 = 244$ (1 September), $u_2$ and $u_3$ varying randomly.

For each $u_1$, SMOT is run 200 times to generate 200 new points of $u_2$ and $u_3$. Every feasible combination of $u_1$, $u_2$, and $u_3$ represents a point $\bar{u} \in U$. Thus, a maximum of 200 $\bar{u}$ points are generated. Let every point $\bar{u} \in U$ be called a production strategy. Each point $\bar{u} \in U$ goes through 25 simulations of the rice model (with actual weather data collected from Los Baños, Philippines), and comprises one SMOT run. Hence, the maximum total number of iterations for each implementation is 5000 (200 x 25). For every 25 simulations, that is, one SMOT run, the user time in the HP 9000 minicomputer system is about 165 seconds, thus, the total user time for the 200 runs is estimated to be 33,000 seconds or 9 hours and 10 minutes. To reduce the execution time, SMOT can be run with less points and less iterations.

For each SMOT run, the mean yield ($\hat{\mu}$), profit ($f_1$), and sample standard deviation ($f_2$) are calculated. As indicated earlier, the sample standard deviation is used as a measure of risk: a low value of the standard deviation means a lower risk relative to a higher value which means a higher risk.

During the 200 SMOT runs, the set of Pareto optimal solutions is generated and the ideal solutions are identified. From the set of Pareto optimal solutions, the min-max optimum solution is determined.

SMOT output for the first implementation is presented in Table 8.14 and illustrated in Figure 8.10. Table 8.14 presents the ideal vector of objective functions, the set of Pareto optimal solutions, and the min-max optimum solution. Figure 8.10 shows the corresponding Pareto optimal curve and the min-max optimum point. In Figure 8.10, the vertical axis is profit (\$ $ha^{-1}$) and the horizontal axis is the sample standard deviation (t $ha^{-1}$) as a measure of risk. Each point in the Pareto optimal curve represents a set of production strategies including the sowing date ($u_1$), nitrogen fertilizer treatment ($u_2$), and plant population ($u_3$). The Pareto optimal curve shows that profit increases with risk. The curve then provides a

Table 8.14. Ideal vector of objective functions, Pareto optimal solutions, and min-max optimum solution for $u_1$ = 20 June, $u_2$ and $u_3$ varying.

A. The ideal vector of objective functions:

$f_1^0$ = \$3494.49 $ha^{-1}$

$f_2^0$ = 0.302 t $ha^{-1}$

B. The set of Pareto optimal solutions:

| $u_2$ | $u_3$ | yield | $f_1$ | $f_2$ |
|---|---|---|---|---|
| 0. | 400. | 3.16 | 61.42 | .302 |
| 498. | 792. | 7.33 | 2996.08 | 1.021 |
| 526. | 611. | 7.63 | 3191.91 | 1.060 |
| 463. | 541. | 7.69 | 3313.68 | 1.091 |
| 195. | 574. | 6.46 | 2662.32 | .966 |
| 544. | 333. | 7.84 | 3367.96 | 1.098 |
| 153. | 480. | 5.96 | 2225.57 | .882 |
| 399. | 434. | 7.74 | 3494.49 | 1.134 |
| 490. | 394. | 7.84 | 3439.37 | 1.109 |
| 111. | 530. | 5.24 | 1666.77 | .749 |
| 100. | 761. | 4.94 | 1473.72 | .708 |
| 120. | 256. | 5.38 | 1787.71 | .781 |
| 621. | 847. | 7.29 | 2751.00 | .996 |
| 62. | 436. | 4.37 | 971.67 | .574 |
| 631. | 411. | 7.92 | 3304.15 | 1.089 |
| 137. | 508. | 5.69 | 2058.25 | .834 |
| 136. | 744. | 5.54 | 1928.86 | .824 |
| 82. | 561. | 4.71 | 1269.66 | .645 |
| 613. | 499. | 7.85 | 3241.00 | 1.077 |
| 150. | 583. | 5.86 | 2201.54 | .869 |
| 102. | 639. | 5.04 | 1487.94 | .717 |
| 23. | 164. | 3.49 | 282.49 | .407 |
| 594. | 652. | 7.60 | 3090.10 | 1.042 |
| 12. | 770. | 3.25 | 68.09 | .356 |
| 179. | 888. | 6.01 | 2266.04 | .905 |
| 104. | 311. | 5.12 | 1563.28 | .729 |
| 172. | 665. | 6.11 | 2352.64 | .910 |
| 123. | 344. | 5.46 | 1858.83 | .794 |
| 203. | 500. | 6.62 | 2726.58 | .991 |
| 59. | 705. | 4.22 | 845.24 | .558 |
| 539. | 795. | 7.35 | 2942.21 | 1.013 |
| 571. | 595. | 7.68 | 3163.56 | 1.058 |
| 203. | 443. | 6.66 | 2763.21 | .997 |
| 490. | 394. | 7.84 | 3439.37 | 1.109 |
| 563. | 829. | 7.30 | 2832.90 | 1.003 |
| 415. | 607. | 7.53 | 3243.11 | 1.087 |

Table 8.14 (cont'd.)

| $u_2$ | $u_3$ | yield | $f_1$ | $f_2$ |
|---|---|---|---|---|
| 441. | 761. | 7.33 | 3066.80 | 1.040 |
| 491. | 769. | 7.36 | 3023.54 | 1.028 |
| 93. | 173. | 4.87 | 1408.66 | .694 |
| 550. | 779. | 7.38 | 2968.53 | 1.016 |
| 529. | 810. | 7.32 | 2917.11 | 1.012 |
| 30. | 268. | 3.68 | 442.14 | .442 |
| 518. | 660. | 7.55 | 3119.84 | 1.049 |
| 13. | 728. | 3.28 | 92.30 | .360 |
| 523. | 435. | 7.89 | 3416.33 | 1.102 |
| 29. | 738. | 3.60 | 370.97 | .434 |
| 442. | 713. | 7.41 | 3132.38 | 1.052 |
| 472. | 736. | 7.40 | 3056.69 | 1.039 |
| 45. | 217. | 3.98 | 703.75 | .510 |
| 527. | 402. | 7.87 | 3399.84 | 1.100 |
| 487. | 751. | 7.39 | 3046.25 | 1.033 |
| 484. | 463. | 7.84 | 3437.63 | 1.106 |
| 107. | 268. | 5.16 | 1597.54 | .736 |
| 174. | 313. | 6.23 | 2460.17 | .938 |
| 485. | 872. | 7.19 | 2878.69 | 1.005 |
| 75. | 407. | 4.62 | 1189.65 | .622 |
| 186. | 461. | 6.44 | 2640.77 | .960 |
| 221. | 655. | 6.67 | 2768.19 | 1.000 |
| 49. | 517. | 4.08 | 793.04 | .520 |
| 67. | 258. | 4.43 | 1025.08 | .598 |
| 152. | 508. | 6.48 | 2676.35 | .967 |
| 125. | 297. | 5.48 | 1874.90 | .799 |
| 17. | 586. | 3.39 | 187.69 | .379 |
| 574. | 617. | 7.65 | 3133.53 | 1.052 |

C. The min-max optimum solution:

$u_1^* = 171$ (20 June) yield$^* = 4.94$ t ha$^{-1}$

$u_2^* = 100$ kg N ha$^{-1}$ $f_1^* = \$1473.72$ ha$^{-1}$

$u_3^* = 761$ plants m$^{-2}$ $f_2^* = 0.708$ t ha$^{-1}$

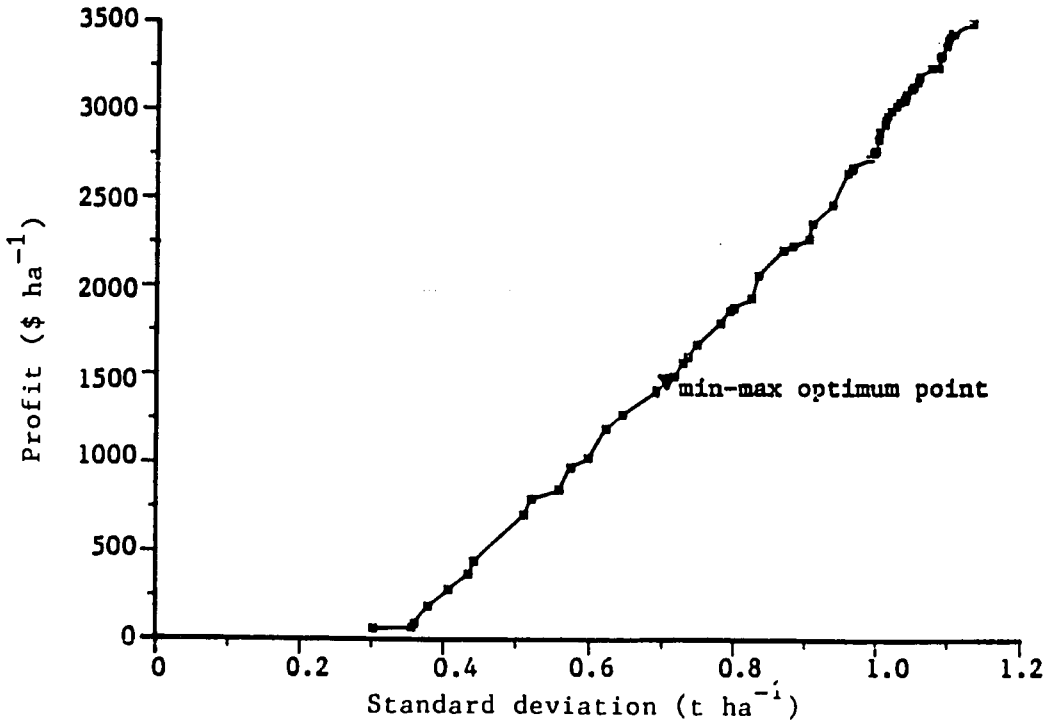


Figure 8.10. Pareto optimal curve and min-max optimum point for $u_1$ = 20 June, $u_2$ and $u_3$ varying.

range of feasible strategies, depending on the choice of profit and risk level. In this case, for example, the SMOT user who is risk-averse would probably choose a lower value of the sample standard deviation, with corresponding lower profit. The min-max optimum point represents the "best compromise" production strategy where both profit and risk are equally weighted. In this particular example, $\bar{u}^*$ (the min-max optimum solution) has the components: $u_1^*$ = 20 June, $u_2^*$ = 100 kg N ha$^{-1}$; $u_3^*$ = 761 plants m$^{-2}$. The corresponding grain yield is 4.94 t ha$^{-1}$, with a profit of \$1473.72 ha$^{-1}$ and a standard deviation of ± 0.708 t ha$^{-1}$.

The ideal vector of objective functions provides an estimate of the maximum profit ($f_1^0$) and minimum risk ($f_2^0$) if each objective function is separately considered. Their corresponding production strategies can be generated from the SMOT output. Table 8.14 shows that the maximum possible profit ($f_1^0$) is \$3494.49 ha$^{-1}$ but this profit level has the largest standard deviation (± 1.134 t ha$^{-1}$), equivalent to the highest point in the Pareto optimal curve of Figure 8.10. In the same manner, Table 8.14 also shows that the minimum possible risk ($f_2^0$) is ± 0.302 t ha$^{-1}$, which has the lowest profit (\$61.42

$ha^{-1}$), and is equivalent to the lowest point in the Pareto optimal curve of Figure 8.10.

In most rice production, the conventional plant population is 400 plants $m^{-2}$. SMOT was, therefore, run with a fixed plant population ($u_3$) of 400 plants $m^{-2}$ with the same planting date ($u_1$). The objective is to see how changes in nitrogen treatments with fixed plant population affect the shape of the Pareto optimal curve and the values of the min-max optimum solution. The ideal vector of objective functions, the set of Pareto optimal solutions, and the min-max optimum solution are presented in Table 8.15. The corresponding Pareto optimal curve and min-max optimum point are shown in Figure 8.11. The shape of the Pareto optimal curve in Figure 8.11 is smoother, although the slope is about the same, compared to that of Figure 8.10. This result is expected because $u_2$ is the only component of $\bar{u} \in U$ that varied randomly in the second implementation. The min-max optimum solution, $\bar{u}^*$, has the components: $u_1^*$ = 20 June, $u_2^*$ = 93 kg N $ha^{-1}$, and $u_3^*$ = 400 plants $m^{-2}$, with a mean yield of 4.95 t $ha^{-1}$, profit of \$1481.91 $ha^{-1}$, and sample standard deviation of ± 0.689 t $ha^{-1}$. This optimum solution shows a higher profit and lower standard deviation compared to the first implementation implying that the min-max strategy of the second implementation is better than the min-max strategy of the first implementation. The maximum profit ($f_1^0$) and the minimum risk ($f_2^0$), however, are about the same as the first implementation.

For the third implementation, the ideal vector of objective functions, the set of Pareto optimal solutions, and the min-max optimum solution are presented in Table 8.16 while the corresponding Pareto optimal curve and the min-max optimum point are illustrated in Figure 8.12. The Pareto optimal curve in Figure 8.12 is more "wiggly" compared to the Pareto optimal curve in Figure 8.10. The min-max optimum solution has the components: $u_1^*$ = 1 September, $u_2^*$ = 100 kg N $ha^{-1}$, and $u3^*$ = 761 plants $m^{-2}$, with a mean yield of 4.83 t $ha^{-1}$, profit of \$1374.12 $ha^{-1}$, and a standard deviation of ± 0.582 t $ha^{-1}$. Except for a difference in the value of $u_1^*$, the min-max optimum $u_2^*$ and $u_3^*$ for the first and third implementations have the same values. However, the mean yield, and, correspondingly, profit of the first implementation is higher than that of the third implementation. Their standard deviations, however, are inversely related to profit.

To provide more comparison between the Pareto optimal curves of the first and third implementations, Figure 8.10 and Figure 8.12 were drawn on the same x,y axes and illustrated in Figure 8.13. It demonstrates that the Pareto optimal curve of the first implementation (curve 1) is always to the right of the Pareto optimal curve of the third implementation (curve 2) until about the point (1.000, 2750). The position of curves 1 and 2

Table 8.15. Ideal vector of objective functions, Pareto optimal solutions, and min-max optimum solution for $u_1$ = 20 June, $u_2$ varying, $u_3$ = 400 plants $m^{-2}$.

A. The ideal vector of objective functions:

$f_1^0$ = \$3474.44 $ha^{-1}$

$f_2^0$ = 0.302 t $ha^{-1}$

B. The set of Pareto optimal solutions:

| $u_2$ | yield | $f_1$ | $f_2$ |
|---|---|---|---|
| 0. | 3.16 | 61.42 | .302 |
| 232. | 6.95 | 3011.83 | 1.056 |
| 697. | 7.93 | 3238.97 | 1.086 |
| 790. | 7.94 | 3105.74 | 1.084 |
| 735. | 7.93 | 3172.52 | 1.085 |
| 647. | 7.92 | 3301.45 | 1.088 |
| 848. | 7.94 | 3037.29 | 1.084 |
| 498. | 7.85 | 3449.08 | 1.107 |
| 157. | 6.03 | 2284.67 | .896 |
| 211. | 6.73 | 2824.97 | 1.018 |
| 399. | 7.72 | 3474.44 | 1.134 |
| 195. | 6.55 | 2734.82 | .983 |
| 550. | 7.89 | 3411.44 | 1.097 |
| 111. | 5.27 | 1693.38 | .755 |
| 100. | 5.08 | 1593.38 | .717 |
| 120. | 5.43 | 1831.05 | .785 |
| 150. | 5.92 | 2260.32 | .878 |
| 62. | 4.36 | 966.22 | .575 |
| 137. | 5.72 | 2080.42 | .840 |
| 136. | 5.70 | 2066.19 | .837 |
| 82. | 4.75 | 1304.92 | .648 |
| 23. | 3.54 | 322.74 | .407 |
| 226. | 6.89 | 2962.85 | 1.046 |
| 12. | 3.33 | 135.00 | .355 |
| 215. | 6.78 | 2862.83 | 1.026 |
| 594. | 7.91 | 3358.43 | 1.092 |
| 179. | 6.34 | 2556.99 | .949 |
| 108. | 5.22 | 1647.29 | .745 |
| 181. | 6.37 | 2581.14 | .955 |
| 123. | 5.48 | 1875.97 | .795 |
| 200. | 6.61 | 2785.95 | .993 |
| 59. | 4.30 | 913.88 | .564 |
| 213. | 6.75 | 2844.60 | 1.022 |
| 442. | 7.79 | 3465.82 | 1.122 |
| 162. | 6.11 | 2350.64 | .911 |
| 93. | 4.95 | 1481.91 | 1.097 |

Table 8.15 (cont'd.)

| $u_2$ | yield | $f_1$ | $f_2$ |
|---|---|---|---|
| 30. | 3.69 | 456.70 | .437 |
| 13. | 3.34 | 150.54 | .360 |
| 29. | 3.67 | 437.34 | .433 |
| 165. | 6.15 | 2387.97 | .918 |
| 45. | 4.01 | 735.57 | .507 |
| 209. | 6.71 | 2805.33 | 1.013 |
| 107. | 5.20 | 1631.93 | .742 |
| 174. | 6.28 | 2498.11 | .939 |
| 172. | 6.25 | 2473.83 | .934 |
| 75. | 4.61 | 1188.65 | .622 |
| 186. | 6.44 | 2636.92 | .966 |
| 227. | 6.90 | 2971.29 | 1.048 |
| 221. | 6.84 | 2918.30 | 1.038 |
| 231. | 6.94 | 3004.23 | 1.054 |
| 222. | 6.85 | 2927.71 | 1.040 |
| 10. | 3.29 | 103.74 | .346 |
| 49. | 4.10 | 807.57 | .523 |
| 67. | 4.46 | 1053.06 | .595 |
| 192. | 6.51 | 2702.20 | .977 |
| 125. | 5.52 | 1906.28 | .801 |
| 17. | 3.42 | 214.89 | .378 |

C. The min-max optimum solution:

$u_1^* = 171$ (20 June) yield* = 4.95 t $ha^{-1}$

$u_2^* = 93$ kg N $ha^{-1}$ $f_1^* = \$1481.91$ $ha^{-1}$

$u_3^* = 400$ plants $m^{-2}$ $f_2^* = 0.689$ t $ha^{-1}$

Table 8.16. Ideal vector of objective functions, Pareto optimal solutions, and min-max optimum solution for $u_1$ = 1 September, $u_2$ and $u_3$ varying.

A. The ideal vector of objective functions:

$f_1^0$ = \$3126.53 $ha^{-1}$

$f_2^0$ = 0.246 t $ha^{-1}$

B. The set of Pareto optimal solutions:

| $u_2$ | $u_3$ | yield | $f_1$ | $f_2$ |
|---|---|---|---|---|
| 0. | 400. | 3.07 | -15.81 | .246 |
| 316. | 513. | 7.06 | 2970.00 | 1.114 |
| 313. | 454. | 7.12 | 3025.78 | 1.124 |
| 150. | 583. | 5.69 | 2055.24 | .759 |
| 195. | 574. | 6.24 | 2467.26 | .869 |
| 399. | 434. | 7.32 | 3126.53 | 1.189 |
| 261. | 393. | 6.86 | 2871.07 | 1.056 |
| 329. | 578. | 7.01 | 2927.71 | 1.108 |
| 111. | 530. | 5.12 | 1561.51 | .643 |
| 100. | 761. | 4.83 | 1374.12 | .582 |
| 136. | 744. | 5.39 | 1794.18 | .702 |
| 153. | 480. | 5.79 | 2076.28 | .784 |
| 62. | 436. | 4.27 | 887.41 | .480 |
| 137. | 508. | 5.54 | 1929.93 | .736 |
| 82. | 561. | 4.61 | 1187.92 | .532 |
| 319. | 496. | 7.09 | 2997.05 | 1.121 |
| 155. | 722. | 5.67 | 1968.50 | .757 |
| 102. | 639. | 4.92 | 1388.01 | .599 |
| 29. | 738. | 3.51 | 292.40 | .355 |
| 203. | 500. | 6.39 | 2524.22 | .906 |
| 12. | 770. | 3.16 | -8.35 | .284 |
| 215. | 365. | 6.50 | 2621.61 | .958 |
| 179. | 888. | 5.81 | 2089.00 | .800 |
| 108. | 777. | 4.94 | 1406.35 | .611 |
| 172. | 665. | 5.92 | 2184.92 | .805 |
| 232. | 462. | 6.68 | 2778.49 | .977 |
| 59. | 705. | 4.13 | 765.88 | .450 |
| 203. | 443. | 6.43 | 2562.01 | .914 |
| 288. | 649. | 6.79 | 2803.41 | 1.051 |
| 273. | 512. | 6.89 | 2892.13 | 1.057 |
| 30. | 268. | 3.58 | 354.92 | .384 |
| 13. | 728. | 3.19 | 16.64 | .289 |
| 29. | 738. | 3.51 | 292.40 | .355 |
| 49. | 517. | 3.99 | 711.70 | .436 |
| 75. | 407. | 4.51 | 1100.68 | .525 |
| 355. | 413. | 7.23 | 3045.74 | 1.163 |

Table 8.16 (cont'd.)

| $u_2$ | $u_3$ | yield | $f_1$ | $f_2$ |
|---|---|---|---|---|
| 227. | 436. | 6.65 | 2753.33 | .971 |
| 319. | 560. | 7.01 | 2924.41 | 1.105 |
| 341. | 593. | 7.02 | 2934.89 | 1.113 |
| 315. | 432. | 7.13 | 3035.39 | 1.131 |
| 67. | 258. | 4.32 | 930.99 | .522 |
| 192. | 508. | 6.26 | 2486.76 | .876 |
| 104. | 311. | 5.00 | 1457.61 | .640 |
| 17. | 586. | 3.30 | 111.72 | .311 |

C. The min-max optimum solution:

$u_1^* = 244$ (1 September) yield* = 4.83 t $ha^{-1}$

$u_2^* = 100$ kg N $ha^{-1}$ $f_1^* = \$1374.12$ $ha^{-1}$

$u_3^* = 761$ plants $m^{-2}$ $f_2^* = 0.582$ t $ha^{-1}$

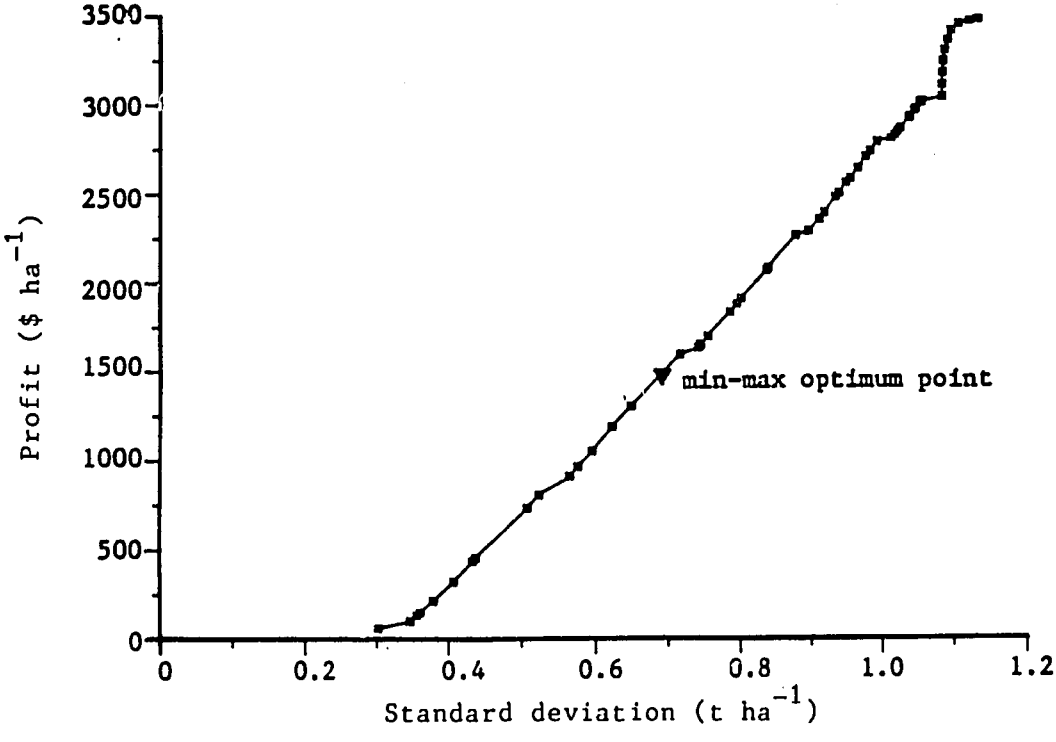


Figure 8.11. Pareto optimal curve and min-max optimum point for $u_1$ = 20 June, $u_2$ varying, and $u_3$ = 400 plants $m^{-2}$.

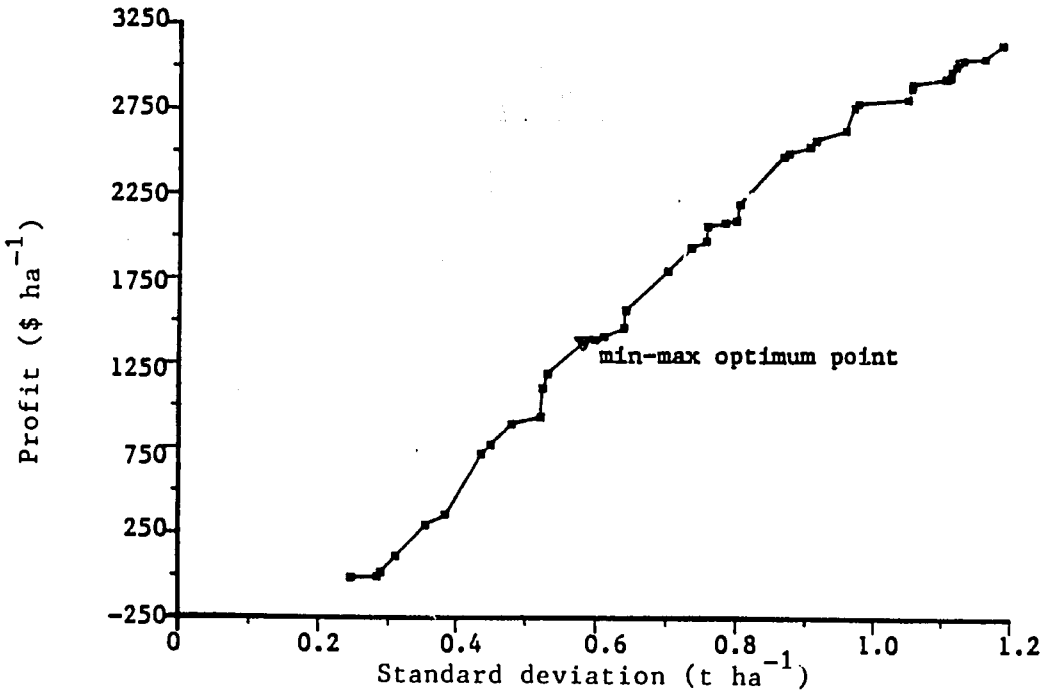


Figure 8.12. Pareto optimal curve and min-max optimum point for $u_1$ = 1 September, $u_2$ and $u_3$ varying.

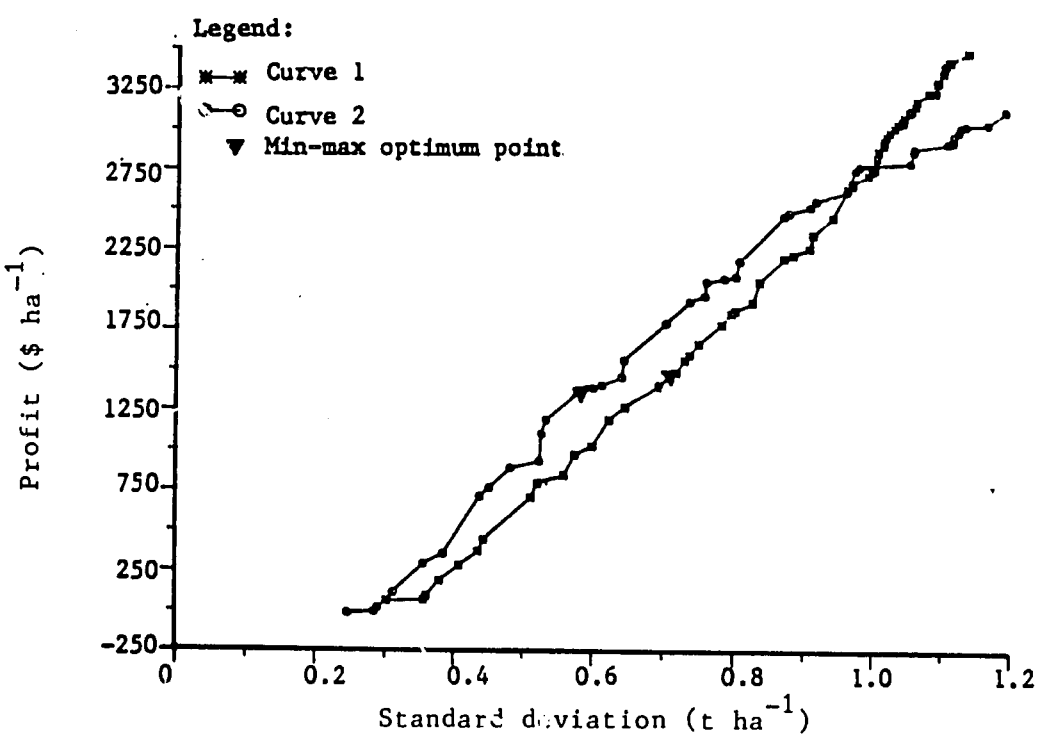


Figure 8.13. Pareto optimal curve and min-max optimum point for $u_1$ = 20 June (curve 1) and $u_1$ = 1 September (curve 2).

relative to each other shifted after this point, that is, curve 1 is now to the left of curve 2. This graph demonstrates that as long as the farmer chooses a point of risk less than ± 1.0 t $ha^{-1}$, the farmer is likely to have a higher profit along curve 2 than along curve 1. However, for a risk level higher than ± 1.0 t $ha^{-1}$, curve 1 will give more profit than curve 2. There is another way of looking at the graph in Figure 8.13. Note that, except for a difference in the sowing date ($u_1$), all other treatments corresponding to the min-max points of both curves 1 and 2 are the same. But the min-max point in curve 1 gives a higher profit (\$1473.72 $ha^{-1}$) than the min-max point in curve 2 (\$1374.12 $ha^{-1}$), although the standard deviation in curve 1 is higher (± 0.708 t $ha^{-1}$) than in curve 2 (± 0.582 t $ha^{-1}$). Tables 8.14 and 8.16 show that for the same treatments including fertilizer and plant population, rice sown on 20 June (curve 1) gives a higher profit than rice sown on 1 September (curve 2). Their corresponding standard deviations, however, are inversely related.

Tables 8.14 and 8.16 also reveal that the Pareto optimal curve is highly influenced by the amount of nitrogen fertilizer applied. The fertilizer level of the production strategies along the lower portion of the two curves (between ± 0.2 and 0.4 t $ha^{-1}$) range between 0 and 30 kg N $ha^{-1}$ while the fertilizer level around the top portion of the curves (above ± 1.0 t $ha^{-1}$) range between 260 and 630 kg N $ha^{-1}$. Thus, if fertilizer is not a constraint and the risk level is above 1.0, sowing on 20 June is a better strategy over sowing on 1 September.

To illustrate the concept of utilizing the standard deviation of a mean as a measure of risk, three representative points (lowest, highest, and min-max) from the Pareto optimal curve in Figure 8.10 were chosen for variability analysis. The mean ($\hat{\mu}$) and sample standard deviation (s) of each of the three points were fitted in a normal probability distribution function ($N(\hat{\mu}, s^2)$). Column 3 of Table 8.17 gives the calculated probability density values. The three normal curves are shown in Figure 8.14. In this graph, the horizontal axis represents mean yield, while the vertical axis represents the probability density. The normal curve to the left has a mean yield of 3.16 t $ha^{-1}$ (profit of \$61.42 $ha^{-1}$) and a sample standard deviation of ± 0.302 t $ha^{-1}$. The components of $\bar{u}$ are: $u_1$ = 20 June; $u_2$ = 0 kg N $ha^{-1}$; $u_3$ = 400 plants $m^{-2}$, equivalent to the strategy with the lowest risk. The normal curve to the right has a mean yield of 7.74 t $ha^{-1}$ (profit of \$3494.49 $ha^{-1}$) and a sample standard deviation of ± 1.134 t $ha^{-1}$. The components of $\bar{u}$ are: $u_1$ = 20 June; $u_2$ = 399 kg N $ha^{-1}$; $u_3$ = 434 plants $m^{-2}$, equivalent to the strategy with the highest risk. The normal curve at the middle has a mean yield of 4.94 t $ha^{-1}$ (profit of \$1473.72 $ha^{-1}$) and a sample standard deviation of ± 0.708 t $ha^{-1}$. The components of $\bar{u}$ are: $u_1$ = 20 June; $u_2$ = 100 kg N

Table 8.17. Grain yield, probability density, and profit.

| Description | Mean Yield (t $ha^{-1}$) | Probability Density | Profit ($ $ha^{-1}$) |
|---|---|---|---|
| $\hat{\mu}$ = 3.16, s = ± 0.302 (0 N, 400 plants $m^{-2}$) | 2.00 | 0.00 | -951.00 |
| | 2.20 | 0.01 | -776.60 |
| | 2.40 | 0.06 | -602.20 |
| | 2.60 | 0.24 | -427.80 |
| | 2.80 | 0.65 | -253.40 |
| | 3.00 | 1.15 | -79.00 |
| | 3.20 | 1.31 | 95.40 |
| | 3.40 | 0.96 | 269.80 |
| | 3.60 | 0.46 | 444.20 |
| | 3.80 | 0.14 | 618.60 |
| | 4.00 | 0.03 | 793.00 |
| | 4.20 | 0.00 | 967.40 |
| $\hat{\mu}$ = 4.94, s = ± 0.708 (100 kg N $ha^{-1}$, 761 plants $m^{-2}$) | 2.60 | 0.00 | -567.80 |
| | 2.80 | 0.01 | -393.40 |
| | 3.00 | 0.01 | -219.00 |
| | 3.20 | 0.03 | -44.60 |
| | 3.40 | 0.05 | 129.80 |
| | 3.60 | 0.09 | 304.20 |
| | 3.80 | 0.15 | 478.60 |
| | 4.00 | 0.23 | 653.00 |
| | 4.20 | 0.33 | 827.40 |
| | 4.40 | 0.42 | 1001.80 |
| | 4.60 | 0.50 | 1176.20 |
| | 4.80 | 0.55 | 1350.60 |
| | 5.00 | 0.56 | 1525.00 |
| | 5.20 | 0.53 | 1699.40 |
| | 5.40 | 0.46 | 1873.80 |
| | 5.60 | 0.36 | 2048.20 |
| | 5.80 | 0.27 | 2222.60 |
| | 6.00 | 0.18 | 2397.00 |
| | 6.20 | 0.12 | 2571.40 |
| | 6.40 | 0.07 | 2745.80 |
| | 6.60 | 0.04 | 2920.20 |
| | 6.80 | 0.02 | 3094.60 |
| | 7.00 | 0.01 | 3269.00 |
| | 7.20 | 0.00 | 3443.40 |

Table 8.17 (cont'd.)

| Description | Mean Yield ($t\ ha^{-1}$) | Probability Density | Profit ($\$\ ha^{-1}$) |
|---|---|---|---|
| $\hat{\mu}$ = 7.74, s = ± 1.134 (399 kg N $ha^{-1}$, 434 plants $m^{-2}$) | 4.40 | 0.00 | 511.80 |
| | 4.60 | 0.01 | 686.20 |
| | 4.80 | 0.01 | 860.60 |
| | 5.00 | 0.02 | 1035.00 |
| | 5.20 | 0.03 | 1209.40 |
| | 5.40 | 0.04 | 1383.80 |
| | 5.60 | 0.06 | 1558.20 |
| | 5.80 | 0.08 | 1732.60 |
| | 6.00 | 0.11 | 1907.00 |
| | 6.20 | 0.14 | 2081.40 |
| | 6.40 | 0.18 | 2255.80 |
| | 6.60 | 0.21 | 2430.20 |
| | 6.80 | 0.25 | 2604.60 |
| | 7.00 | 0.28 | 2779.00 |
| | 7.20 | 0.31 | 2953.40 |
| | 7.40 | 0.34 | 3127.80 |
| | 7.60 | 0.35 | 3302.20 |
| | 7.80 | 0.35 | 3476.60 |
| | 8.00 | 0.34 | 3651.00 |
| | 8.20 | 0.32 | 3825.40 |
| | 8.40 | 0.30 | 3999.80 |
| | 8.60 | 0.26 | 4174.20 |
| | 8.80 | 0.23 | 4348.60 |
| | 9.00 | 0.19 | 4523.00 |
| | 9.20 | 0.15 | 4697.40 |
| | 9.40 | 0.12 | 4871.80 |
| | 9.60 | 0.09 | 5046.20 |
| | 9.80 | 0.07 | 5220.60 |
| | 10.00 | 0.05 | 5395.00 |

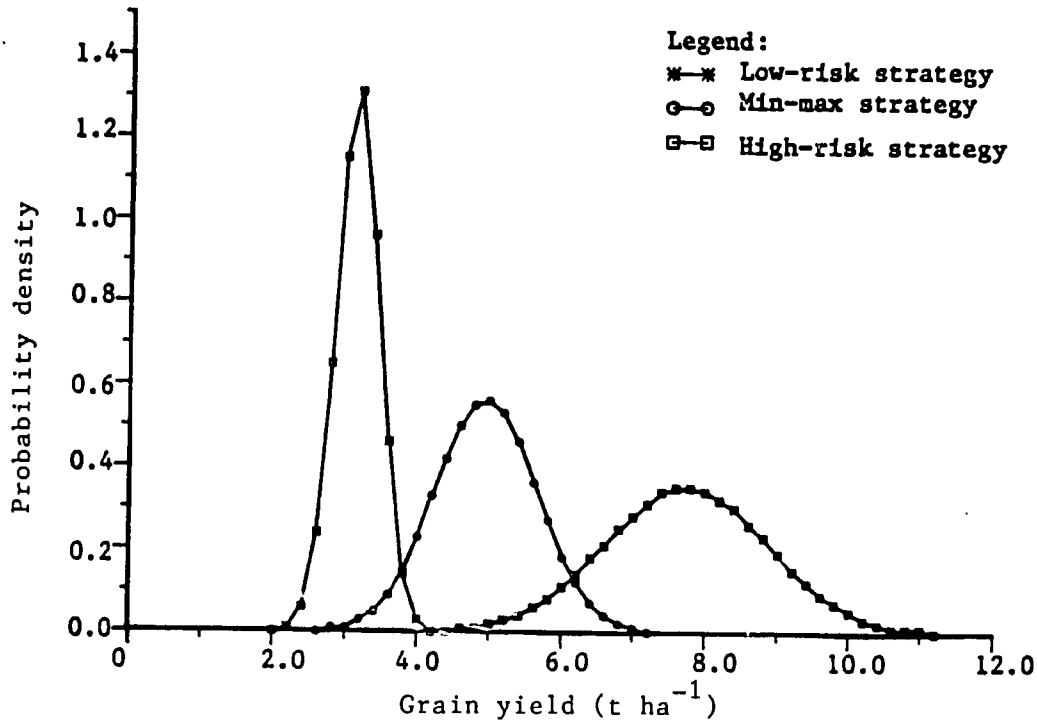


Figure 8.14. Normal curves of low-risk, min-max, and high-risk strategies.

ha$^{-1}$; $u_3$ = 761 plants m$^{-2}$, equivalent to the min-max optimum strategy. Figure 8.14 is a demonstration that associated with a larger mean yield is a wider dispersion or variability, or for this application, greater risk. It should be noted that the right tail of the low-risk normal curve ceases to have a positive probability density at the mean yield interval (from 4.2 to 4.4 t ha$^{-1}$) where the left tail of the high-risk normal curve starts to have a positive probability density. This interval is the "convergence interval" between the low-risk and high-risk strategies.

Extending the analysis to profit, each point on the normal curve corresponding to grain yield with positive probability density (Figure 8.14) was converted into profit (column 4 of Table 8.17). The three normal curves in Figure 8.14 are now represented by three profitlines in Figure 8.15, where the horizontal axis is mean yield and the vertical axis is profit. The low-risk strategy has the leftmost profitline and is consistently to the left, while the high-risk strategy has the rightmost profitline and is consistently to the right. The profitline of the min-max strategy is consistently at the middle. The low-risk profitline has its maximum at the point where the high-risk profitline has its minimum. The yield

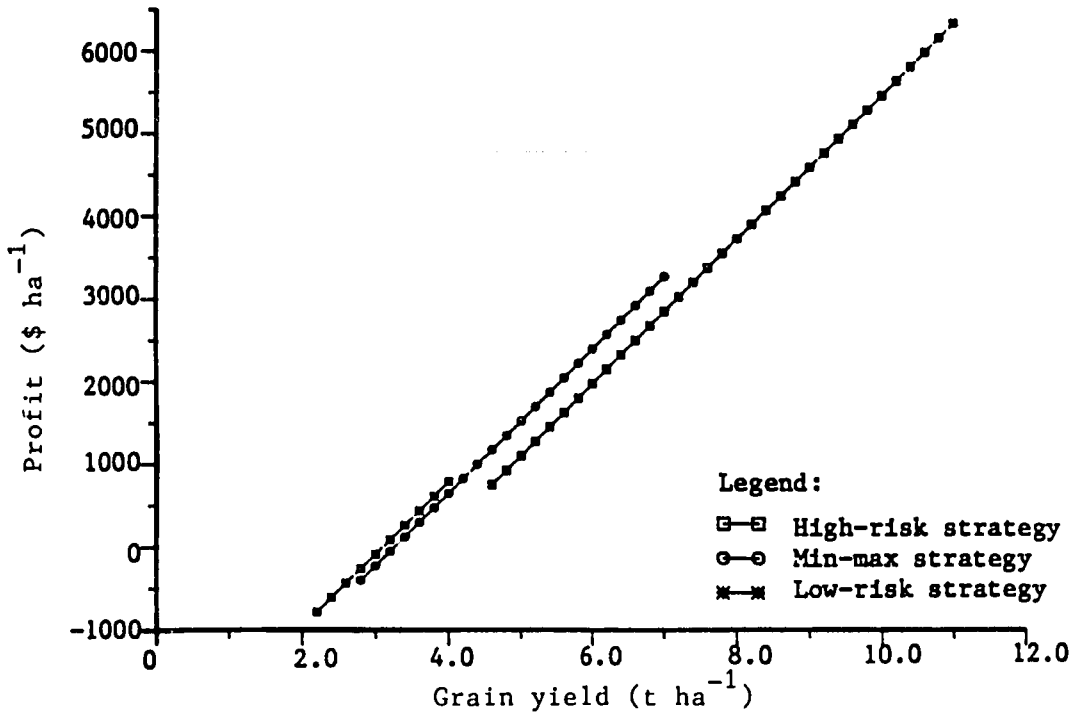


Figure 8.15. Profitlines of low-risk, min-max, and high-risk strategies.

interval between the two profit points is the convergence interval. Figure 8.15 shows that if the mean yield is between 3.4 and 4.0 t ha$^{-1}$, the low-risk strategy is more profitable than the min-max strategy. However, the low-risk strategy has only a maximum profit of \$793 ha$^{-1}$ and can lose as much as \$776.60 ha$^{-1}$ (as indicated by a negative profit), whereas the min-max strategy can have a maximum profit of \$3269 ha$^{-1}$ (maximum yield of 7.0 t ha$^{-1}$) with a possible loss of as much as \$393.80 ha$^{-1}$). If the yield is between 4.6 and 7.0 t ha$^{-1}$, the min-max strategy is more profitable than the high-risk strategy. However, the min-max strategy can only yield at most 7.0 t ha$^{-1}$, while the high-risk strategy can yield at most 10 t ha$^{-1}$ with a profit of as much as \$5395 ha$^{-1}$. If the yield is within the convergence interval, the min-max strategy provides for an alternative between the low-risk strategy and the high-risk strategy.

To further clarify the use of standard deviation as a measure of risk, Table 8.18 presents ± 1 standard deviation within the mean of the low-risk, high-risk, and min-max strategies so far discussed. The low-risk strategy is expected to yield 3.16 t ha$^{-1}$ with a standard deviation of ± 0.302 t ha$^{-1}$. The probability of the actual yield being between 2.86

Table 8.18. Within ± 1 standard deviation for low-risk, min-max, and high-risk strategies.

| Strategy | Yield Range (t $ha^{-1}$) | Profit Range ($ $ha^{-1}$) |
|---|---|---|
| Low-risk ($\hat{\mu}$=3.16, s=± 0.302) | 2.86-3.46 | -201.08 - 322.12 |
| Min-max ($\hat{\mu}$=4.94, s=± 0.708) | 4.23-5.65 | 853.56 - 2091.80 |
| High ($\hat{\mu}$=7.74, s=± 1.134) | 6.61-8.87 | 2508.92 - 4479.64 |

and 3.46 t $ha^{-1}$ is 0.682. However, the profit range is between $-201.08 and $322.12 $ha^{-1}$. Thus, the low-risk strategy has 0.682 probability of losing as much as $201.08 $ha^{-1}$ or gaining up to $322.12 $ha^{-1}$. The min-max strategy is expected to yield 4.94 t $ha^{-1}$ with a standard deviation of ± 0.708 t $ha^{-1}$. It has a 0.682 probability that the actual yield will be between 4.23 and 5.65 t $ha^{-1}$, with profit between $853.56 and $2091.80 $ha^{-1}$. In the same manner, the high-risk strategy is expected to yield 7.74 t $ha^{-1}$ with a standard deviation of ± 1.134 t $ha^{-1}$. It has a 0.682 probability that the actual yield will be between 6.61 and 8.87 t $ha^{-1}$, with profit between $2508.92 and $4479.64 $ha^{-1}$. These results, however, do not provide for an outright conclusion in favor of the high-profit/high-risk strategy because of high cost functions associated with it. The high-profit/high-risk strategy involves high inputs and, consequently, high cost. Capital and input availability are major constraints in developing countries. The possibilities of typhoons, pest infestation, and other natural catastrophies, which are assumed to have no destructive effect on the simulation, are major contributors to the risk factor. The market system, an assumed constant in the model, introduces additional uncertainty which needs to be reckoned with. These risks are in addition to an already high variability due to the stochastic weather conditions.

## CHAPTER IX. CONCLUSION

The needs analysis indicates that rice deficiency in many countries is due largely to low yields and that the agrotechnology exists for increasing yields commensurate with population growth. The primary barrier to the implementation of high-yielding agrotechnology is the economic environment of the farmer and the farmer's perception of profit and risk in this environment. Under present economic conditions, the farmer cannot, and does not, strive for maximum yields or maximum profit alone because the perceived risks are too high and the cost of inputs may be beyond reach. Both issues, profit and risk, must be dealt with simultaneously at policy levels as well as at the farm level to overcome the low-yield syndrome. The CERES-Rice simulation model and SMOT presented here are developed as computer software tools in support of analysis and strategic planning at both the policy and farm levels of organization.

The CERES-Rice simulation model is a first approximation to a practical and flexible computer software for simulating upland-rice production. The simulation software is intended as a tool in assessing the yield potential of alternative technologies from high-yielding countries to low-yielding countries, or from its site of origin to new locations within the tropical and subtropical regions of the world. The conventional research/demonstration method of transferring new rice varieties and management practices from one soil type and climate to another requires time, money, and careful field evaluation. In using the simulation model, the initial trial-and-error experimentation in selecting new varieties and management practices under a specific soil type and climatic environment can, to a degree, be done in the computer. Those varieties and management practices that look promising are the principal technologies to be tried in the field. This procedure is expected to reduce dramatically the cost, time, and risks involved in agrotechnology transfer.

SMOT is an initial attempt to develop a software package that quantifies the trade-offs between profit and risk of alternative rice technologies under farm conditions. SMOT is presented as a first generation decision support system for use by extension workers, researchers, and policymakers in the economic analysis of rice farms. Alternative production strategies can be tested through SMOT to help identify problems

and issues before they actually occur in the field.

As with all computer software packages, a note of caution is in order when using SMOT. SMOT will not and is not intended to eliminate all the uncertainties in decision making, nor is it intended to replace the vital role of the farmer or farm adviser or the policymaker in the decision-making process. It is not a decision-making instrument. SMOT will help to illuminate some of the process's dimensions. The value of SMOT in the decision-making process depends on the user's understanding of its strengths and limitations as well as on the user's attitude toward profit and risk. The attitude will be conditioned by the user's expectations of the performance of SMOT, the amount of information available at the time the choice of production strategy is made, and the user's access to the controllable inputs. SMOT should be viewed as a tool to increase the user's understanding of the rice production system performance, help quantify preferences, and improve overall decision-making ability.

## CHAPTER X. OTHER POSSIBLE APPLICATIONS OF SMOT

SMOT can be used for further economic analysis. The incorporation of nitrogen transformation subroutines for lowland, flooded conditions will increase the application of SMOT in paddy production.

SMOT can be applied to any of the CERES and other crop simulation models adapted by IBSNAT. At present, these include maize, wheat, and soybean; and when sufficiently validated, potato, sorghum, millet, barley, peanut, and dry beans.

SMOT is presently set up to handle two objective functions for easy plotting of the trade-off points in the x y plane. If necessary, more than two objective functions can be incorporated with minimum effort.

### Objective Function Pairs

The results of this research demonstrate that SMOT can be used to improve trade-off decision making between profit and stability of yield. However, due to farm size variations, individual preferences, and family needs, some farms may have other goals. Consumption-oriented farm families are concerned with food supply for the present as well as the future. They are not necessarily interested in selling the harvested grain for profit, but would rather store the excess after consumption for future use. In this situation, the objective function pair is to maximize yield and stability of yield. The major constraints, among other things, are the size and quality of the storage space. Generally, consumption-oriented farmers choose varieties that have good eating qualities and flavors. Access to and cost of the seed supply of these preferred varieties may also be constraints. Analytically, the objective function pair may be represented as follows:

$$\max f_1(u) = \text{maximize } \hat{\mu}$$

$$\min f_2(u) = \text{minimize } s$$

where $\hat{\mu}$ is the mean yield (t $ha^{-1}$) and s is the sample standard deviation (t $ha^{-1}$).

In most cases, profit remains a major goal coupled with other goals. For example, some farmers interested in profit are

indifferent to the variance (or standard deviation) as a measure of stability. They are interested in miminizing the risk of total failure in a given cropping season. Typhoon and pest infestation are major factors contributing to total failure. The addition of pest epidemic models and/or the incorporation of a mechanism to account for the probability distribution of the occurrence and destructive strength of these catastrophies over a cropping season becomes necessary. Analytically, the objective function pair can be represented as follows:

$$\max f_1(u) = \text{maximize profit}$$

$$\min f_2(u) = \text{minimize the frequency of } y_i \leq 0,$$

$$i = 1,\ldots,NCYCLE$$

where profit is as defined in the section on The Analytical Representation of the Objective Functions and $y_i$ is the grain yield of cropping season i.

In other cases, some farmers are interested in maximizing profitability and stability of income. In this case, the uncertainty of the market situation including the price of grain, cost of fertilizers and other inputs, interest rates, and other stochastic parameters need to be considered by SMOT. Stability of income implies minimization of total failure. Analytically, the objective of income stability can be written as follows:

$$\min f_2(u) = \text{minimize the frequency of } profit_i \leq c,$$

$$i = 1,\ldots,NCYCLE$$

where $profit_i$ is the profit of cropping season i and c is the minimum allowable profit.

Although profit continues to be a major objective, environmental degradation must also be a concern. A strategy to reduce environmental degradation from farm operations has to be developed in the context of profit. It would be difficult to convince farmers to reduce the application of nitrogen fertilizers, pesticides, or water because they also reduce profit. The economic advantage now is more than the perceived disadvantage of environmental degradation later. Some farmers or policymakers may be interested in minimizing nitrate leaching, runoff, or pesticide application to protect the water and soil resources and the air environment for the present as well as future generations if their families or constituencies would be able to survive economically at the present.

With regard to nitrate leaching, for example, SMOT can be

used to develop nitrogen fertilizer scheduling suited to the climatic and soil environment such that the amount of nitrates lost is below a certain minimum tolerable level without drastic reduction in profit. Figure 10.1 illustrates this concept. The vertical axis represents profit while the horizontal axis represents the amount of nitrates leached. Four curves are shown on the graph. Each point along the curve corresponds to a nitrogen fertilizer scheduling strategy. The first curve may reflect the amount of leaching during the Fall application; the second curve, that of the Spring application; and the third curve, that of the Spring-split application. However, all three strategies may be above the minimum allowable limit of nitrates in the soil. The fourth curve represents a SMOT-generated nitrogen fertilizer scheduling strategy where leaching can be minimized while improving profit. This example illustrates the capability of SMOT to deal with environmental issues quantitatively and simultaneously with profit.

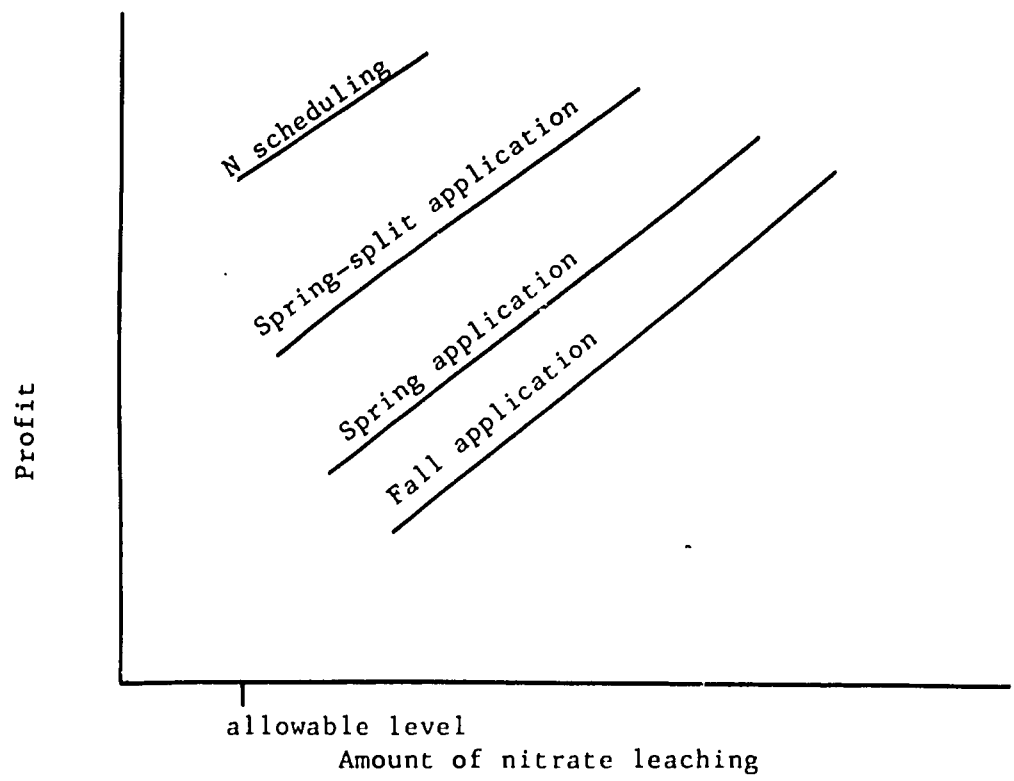


Figure 10.1. Pareto optimal curves for profit and nitrate leaching trade-off.

**Production Constraints**

Farmers try to optimize production under existing constraints. The farm production system is defined directly by resources and by social (Thornton and Dent 1987), institutional, and environmental constraints. Constraints on resources, such as the size and quality of storage, availability of seeds, and availability of cash, have been mentioned in the previous section on Objective Function Pairs. The section on The System Parameters in chapter III summarizes many of the constraints in farm operation, both in the framework of the individual farm and in the region or country.

Availability of labor is often a major resource constraint. Thornton and Dent (1987) indicated that in many locations, labor is highly seasonal. It may not be available during certain periods of time, or if available, it cannot be paid for. Availability of fertilizer, pesticides, and other inputs is another constraint. Because of the market situation, fertilizers, pesticides, or seeds may be either unavailable when needed or in short supply. Work animals or machinery may be unavailable during peak labor times.

Accessibility to credit is another constraint. Farmers often need a large amount of cash at certain times to secure the farm inputs. Its availability affects the type of management and operation on the farm. A good market facility is necessary for crop production. It supplies the farm inputs and manages the farm outputs. Accessibility to it is vital and will affect the technology and operation the farmer will employ on the farm. Credit and market are directly affected by inflation and interest rates, as well as by the local and international market situation as to demand and supply. The international market situation, though not directly felt by the farmer, is real just the same.

Crop production is also constrained by social norms. A market-oriented farmer needs to be sensitive to the preferences of consumers for certain varieties because of taste and eating quality. Some farmers have special preferences for certain farm practices. These social factors need to be considered in optimizing the farm operation.

Crop production also needs to account for institutional constraints created by the production policies of the government. Government price supports, input subsidies, and storage facilities affect the management and scale of production. The form of government also affects the type of technology allowed on the farm. Finally, the availability of technology is a major constraint in many localities.

Seasonality of rainfall poses a major environmental constraint to many subsistence farmers who depend on rain for irrigation. Solar radiation and air temperature as well as deficiencies in the soil nutrients are also possible constraints to production.

Another form of constraint is synchrony of farm input. Synchrony is necessary for optimum farm operation; if one item is not available, the other things may be useless. For example, labor, work animals or machinery, and cash may need to be available at the same time. Seeds, work animals, fertilizer, labor, and water supply may need to be packaged together and made available at the beginning of the cropping season. There are many inputs which need to be available singly or together at specific periods if production is to be successful and efficient.

The last constraint is the limitations of the simulation and of the optimization capabilities of SMOT. It is not a "do-it-all" software. It is, however, presented as first generation computer software to evaluate, quantitatively and simultaneously, profit and a limited class of risk issues in the context of a nonlinear, stochastic, continuous-time, time-varying, dynamic, and causal biological production system.

## LITERATURE CITED


Amir, I., U. Shamir, and R.S. Broughton. 1978. Monitoring and decision-making processes for operating agricultural production systems. Agricultural Systems 3:253-264.

Avery, D. 1985. U.S. dilemma: The global bad news is wrong. Science 230:408-412.

Baker, C.H., and R.B. Curry. 1976. Structure of agricultural simulators: A philisophical view. Agricultural Systems 1:201-218.

Barker, R., and R.W. Herdt, with B. Rose. 1985. The rice economy of Asia. Resources for the Future, Inc., Washington, D.C.

Bazaraa, M.S., and C.M. Shetty. 1979. Nonlinear programming theory and algorithms. John Wiley and Sons, New York.

Cadzow, J.A. 1973. Discrete-time systems. Prentice-Hall, Inc., Englewood Cliffs, New Jersey.

Capule, C.C., and R.W. Herdt. 1983. Economics of rice production. *In* University of the Philippines. Rice production manual, Philippines. Los Banos, Philippines.

Chang, T.T., and B.S. Vergara. 1975. Varietal diversity and morpho-agronomic characteristics of upland rice. *In* The International Rice Research Institute. Major research in upland rice. Los Banos, Philippines.

Chinchest, A. 1981. The effects of water regimes and nitrogen rates on the nitrogen uptake and growth of rice varieties. Ph.D. diss. Cornell University, New York.

Cirillo, R. 1979. The economics of Vilfredo Pareto. Frank Cass & Co. Ltd., New Jersey.

De Datta, S.K. 1981. Principles and practices of rice production. John Wiley and Sons, New York.

De Datta, S.K. 1975. Upland rice around the world. *In* The International Rice Research Institute. Major research in upland rice. Los Banos, Philippines.

De Datta, S.K., and R. Feuer. 1975. Soils on which upland rice is grown. *In* The International Rice Research Institute. Major research in upland rice. Los Banos, Philippines.

French, S., R. Hartley, L.C. Thomas, and D.J. White. 1983. Multi-objective decision making. Academic Press, New York.

Godwin, D.C., and P.L.G. Vlek. 1985. Simulation of nitrogen dynamics in wheat cropping systems. *In* W. Day and R.K. Atkin (ed.) Wheat growth and modelling. Plenum Press, New York.

International Rice Research Institute. 1963. Annual report for 1963. Los Banos, Philippines.

International Rice Research Institute. 1964. Annual report for

1964. Los Banos, Philippines.
International Rice Research Institute. 1965. Annual report for 1965. Los Banos, Philippines.
International Rice Research Institute. 1966. Annual report for 1966. Los Banos, Philippines.
International Rice Research Institute. 1967. Annual report for 1967. Los Banos, Philippines.
International Rice Research Institute. 1968. Annual report for 1968. Los Banos, Philippines.
International Rice Research Institute. 1969. Annual report for 1969. Los Banos, Philippines.
International Rice Research Institute. 1970. Annual report for 1970. Los Banos, Philippines.
International Rice Research Institute. 1971. Annual report for 1971. Los Banos, Philippines.
International Rice Research Institute. 1972. Annual report for 1972. Los Banos, Philippines.
International Rice Research Institute. 1973. Annual report for 1973. Los Banos, Philippines.
International Rice Research Institute. 1974. Annual report for 1974. Los Banos, Philippines.
Jones, C.A., J.T. Ritchie, J.R. Kiniry, and D.C. Godwin. 1986. Subroutine structure. *In* C.A. Jones and J.R. Kiniry (ed.) CERES-Maize: A simulation model of maize growth and development. Texas A&M University Press, Texas.
Larsen, R.J., and M.L. Marx. 1981. An introduction to mathematical statistics and its applications. Prentice-Hall, New Jersey.
Livingston, B.E., and F.W. Haasis. 1933. Relations of time and maintained temperature to germination percentage for a lot of rice seed. American Journal of Botany 20:596-615.
Michigan State University Agricultural Experiment Station. 1981. Michigan Science in Action. No.46.
Murayama, N. 1979. The importance of nitrogen for rice production. *In* The International Rice Research Institute. Nitrogen and rice. Los Banos, Philippines.
Osyczka, A. 1984. Multicriterion optimization in engineering with Fortran programs. John Wiley and Sons, New York.
Patnaik, S., and M.V. Rao. 1979. Sources of nitrogen for rice production. *In* The International Rice Research Institute. Nitrogen and rice. Los Banos, Philippines.
Ponnamperuma, F.N. 1975. Growth-limiting factors of aerobic soils. *In* The International Rice Research Institute. Major research in upland rice. Los Banos, Philippines.
Priestly, C.H.B., and R.J. Taylor. 1972. On the assessment of surface flux and evaporation using large-scale parameters. Monthly Weather Rev 100:81-92.
Ritchie, J.T. 1985. A user-oriented model of the soil water balance in wheat. *In* W. Day and R.K. Atkin (ed.) Wheat growth and modelling. Plenum Press, New York.
Ritchie, J.T., J.R. Kiniry, C.A. Jones, and P.T. Dyke. 1986.

Model inputs. *In* C.A. Jones and J.R. Kiniry (ed.) CERES-Maize: A simulation model of maize growth and development. Texas A&M University Press, Texas.

Ruttan, V. 1982. Agricultural research policy. University of Minnesota Press, Minnesota.

Sahal, D. 1980. Technical progress and policy. *In* D. Sahal (ed.) Research, development and technological innovation. Lexington Book, Massachusetts.

Shapiro, R.D. 1984. Optimization models for planning and allocation: text and cases in mathematical programming. John Wiley and Sons, New York.

Suzuki, M. 1983. Growth characteristics and dry matter production of rice plants in the warm region of Japan. JARQ 17(2):98-105.

Swaminathan, M.S. 1975. The Green Revolution can reach the small farmer. *In* S. Aziz (ed.) Hunger, politics and markets. New York University Press, New York.

Swisher, G.M. 1976. Introduction to linear systems analysis. Matrix Publishers, Oregon.

Tanaka, A., K. Kawano, and J. Yamaguchi. 1966. Photosynthesis, respiration and plant type of the tropical rice plant. International Rice Research Institute Technical Bull. 7.

Thornton, P.K., and J.B. Dent. 1987. IBSNAT crop models in a socio-economic whole farm framework. Agrotechnology Transfer No. 6.

Wortman, S., and R.W. Cummings. 1978. To feed this world. The Johns Hopkins University Press, Baltimore.

Yoshida, S. 1973. Effects of temperature on growth of the rice plant (*Oryza sativa L.*) in a controlled environment. Soil Sci. Plant Nutr. 19(4):299-310.

Yoshida, S. 1975. Factors that limit the growth and yields of upland rice. *In* The International Rice Research Institute. Major research in upland rice. Los Banos, Philippines.

Yoshida, S. 1981. Fundamentals of rice crop science. The International Rice Research Institute, Los Banos, Philippines.

Yoshida, S., and F.T. Parao. 1972. Performance of improved rice varieties in the tropics with special reference to tillering capacity. Expl. Agric. 8:203-212.